Comments from the Editor

We sincerely thank the Editor for taking such a commendable effort to allow us to clarify many points in the manuscript. We have taken utmost care in revising ALL the points raised by the editor. Action taken for each of the comment is elaborated here. We also indicate the relevant lines in the revised manuscript where the corrections are incorporated. A mark-up version also provides to easy locate the corrections made.

All comments are given in blue fonts and replies in black fonts.

I have read the revised version of your manuscript and based on that I find that major revisions are needed for the following reasons.

In its present form, the manuscript is still difficulty understandable for a general reader not experienced with the type of models used for OCMIP. Since the beginning, I was wondering why the compensation depth is not dynamically computed by the model then I had to read Najjar and Orr, 1992 to understand the approach. Therefore, I suggest that you clarify since the beginning the general approach of OCMIP modeling e.g. a simple biological model with a reduced number of state variables without an explicit representation of chlorophyll like in mechanistic models because …). It can be done briefly already in the introduction and then clearly in the methods section.

After reading the above comment, we read the manuscript with this view point in mind and agree with the Editor that some clarification in the introduction will indeed help the general audience who are not familiar to OCMIP-II protocols. To answer the question, 'Why the OCMIP-II by default did not include Chl-a dependent light module for biological modeling' can be answered as follows. OCMIP-II is designed for global simulations of carbon cycle for very long time scales by a family of models under a common protocol. The models were generally coarse in resolutions both horizontally and vertically. The intention was to 'inter-compare' the models run under a common protocol. The detailed light penetration and satellite Chl-a dependent modeling of biological production are more suitable in fine resolution models with more vertical levels such as the one used in the present study. Moreover, the implementation of Chl-a modules also would bring additional computational load in those days computing (late 1990s). Although all these details are not necessary in our paper, by respecting the Editor's view, we have added few sentences in the Introduction (see lines 113 - 117 of revised manuscript).

“However, Zc was held constant in time and space in OCMIP-II models (Najjar and Orr, 1998; Matsumoto et al., 2008) because the OCMIP-II protocol takes the minimalistic approach to biology and simplifies the model calculations with a very limited set of state variables suitable for long term simulations when casted in coarse resolution models (Orr et al., 2005)”.

In addition to the general approach, I also find that the description of the model is insufficient. The information provided does not allow to understand the approach (even the basics). I would start the material and methods section, by informing the reader on the structure of the biogeochemical model (a scheme would be helpful), listing the state variables and interactions between them, mentioning that these variables are transported by a 3D physics. For instance, a synthesis of section 7 of the paper by Najjar and Orrr, 1992 would really help the general reader to understand the modelling approach (see also my detailed comments below).

ALL these have been carefully rectified in the revised manuscript. The detailed reply below locates them with line-numbers.

I still have concerns about the definition of the compensation depth made in the manuscript and how it translates in terms of model formulation and validation. You decided to define the compensation depth as the depth at which the community respiration equals photosynthesis but then after I noted some confusions that need to be clarified :

1) you mention that at the compensation depth, phytoplankton production is zero, which is not true (lines 112-115),
2) in the model formulation, you consider that below Zc, there is no biological production (Jprod=0),
3) model estimations of biological production are compared with vertically integrated primary production over the euphotic zone as proposed by Behrenfeld and Falkowski (1997). It would be helpful finally that you clearly define as early as possible the biological production (most of the time it is photosynthesis which is not the case here).

These three points raised by the Editor are extremely valuable and we are grateful to the Editor for pointing that out. The paper, in the present form, was not clear enough for general as well as expert readers. The usage of “phytoplankton production” confuses the reader in this context. In the OCMIP-II, the definition says that ‘at the compensation depth, the photosynthesis is equal to total community respiration’. The phytoplankton production is not zero in this case but it represents a balance between phytoplankton production and community respiration. Therefore we have revised the manuscript relevant sections as follows.

"In this protocol, the community compensation depth (hereinafter Zc) is defined as the depth at which photosynthesis equals entire community respiration and the irradiance at which this balance is achieved is the compensation irradiance (E_{com}). Note that Zc is clearly different from the conventional euphotic zone depth (Morel, 1988). At Zc, the Net Community Production is zero, i. e., when the Net Primary Production (NPP) balances the community respiration and above Zc the NPP exceeds the community respiration and the ecosystem will grow (Smetacek and Passow, 1990; Gattuso et al., 2006; Sarmiento and Gruber, 2006; Regaudix-de-Gioux and Duarte, 2010; Marra et al., 2014)".

We have also removed the wording of 'negative growth' and irradiance which might have added to the confusion.

For the comparison of satellite NPP with the model export production, we first converted the satellite NPP into Export production by scaling with an e-ratio. The suitable e-ratio was taken from available observations and literature for the Arabian Sea. We admit that the confusion might have risen from the Figure labeling as 'Biological Production', which has been corrected to 'Export and New Production' in the revised manuscript.

Point by Point Reply to the comments:

1. Abstract: Lines 27-28: "Utilizing the principle of minimum solar radiation for the production zone..." What is the principle of minimum solar radiation?

In the revised version it is corrected as "Utilizing the criteria of surface Chl-a based attenuation of solar radiation and the minimum solar radiation required for production, we have proposed a new parameterization for a spatially and temporally varying 'compensation depth' which captures the seasonality in the production zone reasonably well." Please refer to lines 27 – 30 in the revised manuscript. Thank you for noticing this wording issue.

2. Lines 112-115: I do not agree that if the irradiance is less than Ecom, phytoplankton growth will be negative and hence phytoplankton will decline due to respiration. This would be true if Ecom represents the irradiance at which photosynthesis equals autotrophic respiration. I would like that you clarify that point. Besides, clarify what you mean by "the growth will be negative". Growth of? (line 113).

We partially agree that the statement written perhaps was not clear, so it is rewritten in simple words with more clarity. And, the revised lines are consistent with Smetacek and Passow, 1990;

Gattuso et al., 2006; Sarmiento and Gruber, 2006; Regaudix-de-Gioux and Duarte, 2010; Marra et al., 2014. Please see lines 106 – 113 in the revised manuscript.

The corrected statement is as follows:

"In this protocol, the community compensation depth (hereinafter Zc) is defined as the depth at which photosynthesis equals entire community respiration and the irradiance at which this balance is achieved is the compensation irradiance (E_{com}). Note that Zc is clearly different from the conventional euphotic zone depth (Morel, 1988). At Zc, the Net Community Production is zero, i. e., when the Net Primary Production (NPP) balances the community respiration and above Zc the NPP exceeds the community respiration and the ecosystem will grow (Smetacek and Passow, 1990; Gattuso et al., 2006; Sarmiento and Gruber, 2006; Regaudix-de-Gioux and Duarte, 2010; Marra et al., 2014)."

3. Line 116: please define what you mean by "oceanic production zone".

Corrected as "production zone". OCMIP –II protocol clearly refers to the region above the community compensation depth as the production zone where the model protocol allows production and the region below the compensation depth as the consumption zone (please see Najjar and Orr, 1998, page-10, para-4). Here we refer to the same as "production zone". Please refer to lines 112 – 114.

4. Line 121: please avoid parentheses insides parentheses.

Corrected accordingly. Kindly see lines 121-123 in the revised manuscript.

5. Line 127: please define "optimum" solar radiation? What do you mean by optimum? How variable will be the surface light? And which data do you use? Please specify

Thank you for pointing out the wording issue. Corrected as "production as a function of solar radiation and Chl-a availability." The data for shortwave radiation, which is scaled to PAR as 55% of the total shortwave, is taken from the same atmospheric forcing as used for the GFDL Re-analysis (Chang et al., 2012). Please refer to lines 124 -127 in the revised manuscript.

6. Lines 127-129: This sentence is not clear and needs to be reformulated. First a reference is needed for justifying the choice of 10 W/m2 for the value of the compensation

irradiance. Then, the second part of the sentence "…and calculated its depth…" needs to be reformulated. Do you mean that " a spatially and temporally varying compensation depth is estimated from a vertical light profile taking into account the shading effect using a typical? Chlorophyll profile. Please specify how the chlorophyll profile varies in space and time?

As in the replies to the comments of reviewer-2 in the first round revision and also incorporated in the first revised version of the manuscript, our justification for the choice of 10 Wm^{-2} is based on following references.

1. The observations show that the primary production reduces rapidly to 20% or less of the surface value below the threshold of 10 Wm^{-2} (Parsons et. al., 1984, Ryther, 1956).
2. Higher ocean temperature (those in tropics) enhances the respiration rates resulting in high compensation irradiance (Parsons et. al., 1984, Ryther, 1956, Lopez-Urrutia et al., 2006, Regaudie-de-Gioux and Duarte, 2010).
3. The Table-1 of Regaudie-de-Gioux and Duarte (2010) infers that the 0.4±0.2 mole photon/m^2/day in case of the Arabian Sea which is close to 10 Wm^{-2}.

Therefore this choice is amply justified with reference to existing literature. The citation for chlorophyll data (SeaWiFS) is given in the Acknowledgement. We have not presented any figures for chlorophyll because that has been included in several of the previous papers (Wiggert et al., 2005; Levy et. al., 2007; Prakash et al., 2012; Resplandy et al., 2009). It may also be noted that the combination of Chl-a and SSW attenuation through Chl-a mimic a varying Zc which has the inherent property of Chl-a variation and therefore our Figure 3 in the revised manuscript is more meaningful in this context.

In order to answer the Editor's comment here we show the seasonal mean map of chlorophyll variability.

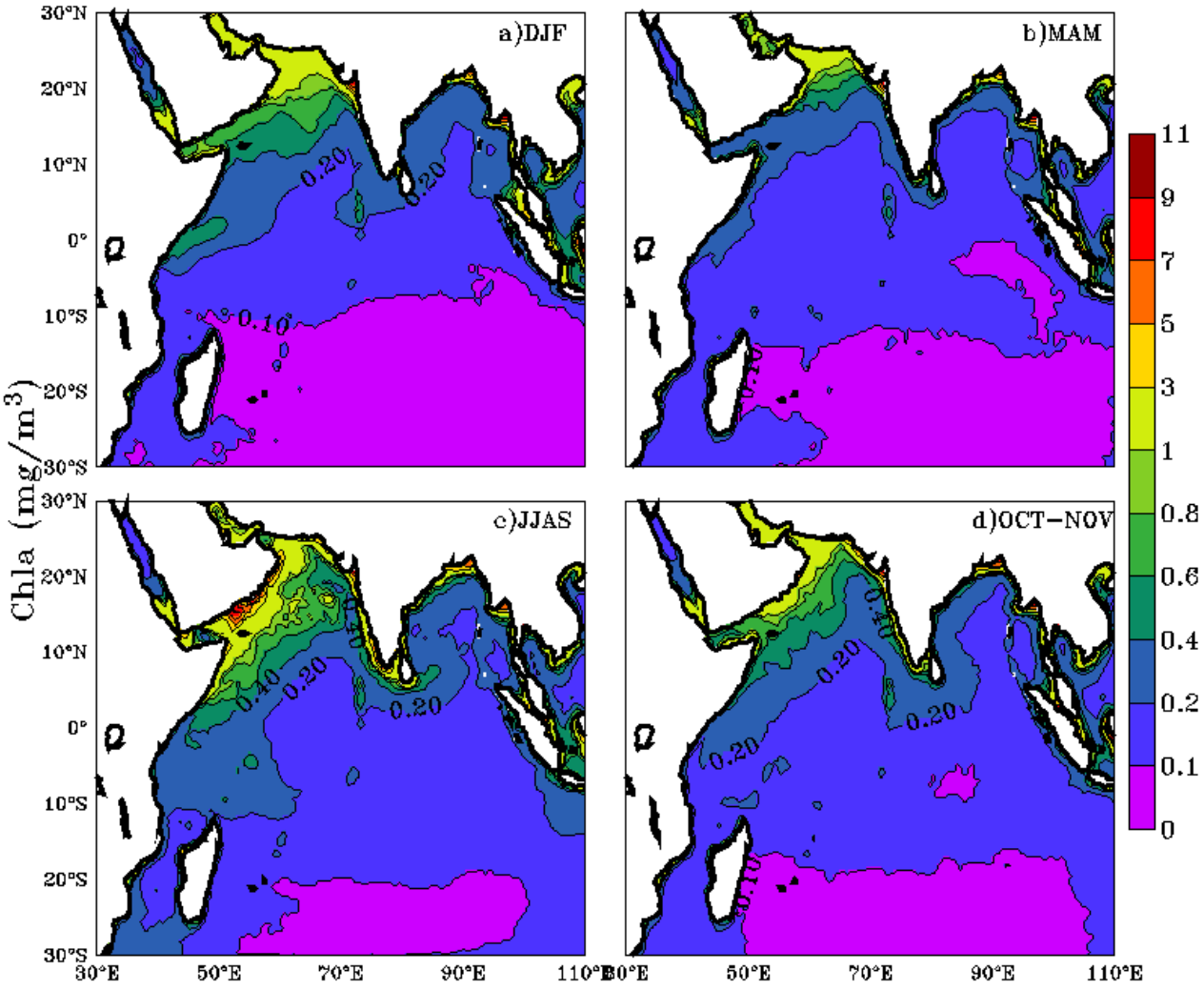

Figure 1. Seasonal mean map of Chlorophyll-a variability over the Indian Ocean from SeaWiFS data.

7. Line 141: please clarify what do you mean by "positive" effect? Better representation?

'Positive' effect means a better representation saying that the variable compensation depth has a significant impact on both solubility as well as the biological pump. This has been revised as "the improvements due to the effect of a variable Zc". Please refer to lines 140 – 143 in the revised manuscript.

8. Line 161: why “respectively”?

Corrected accordingly. Please refer to lines 160-161.

9. Lines 163-179: Please specify that all the details that you are giving concern the biogeochemical model and if the model is solved on the same grid as the physical model. At the beginning I thought that it was for the physics and was wondering why all these details are given since you did not run the physics but rather force it from another simulation.

Yes, the BGC model is implemented on the same grid as the physical model. As per your suggestions, a detailed description of the biogeochemical model design is provided in the Model, data and methods section and more details in Appendix A.

10. Lines 180 -: Conversely, I would like to have further specifications on the biogeochemical modeling approach since the OCMIP-II protocol is not known by everybody. I think that the description of the approach that you gave at lines 181-183 is not enough for understanding the methodology and in particular, how it differs from “classic” biogeochemical modelling approach. You mention a restoration to ocean biology (which biology) and appropriate biogeochemical parameterization. Please give more details and give a reference with the methods is described because as it is, this is not enough to understand what is done.

We do agree with the editor that some more details may clarify the scenario. Please refer to section 2.2 of revised manuscript as well as Appendix A.

The “restoration biology” is a terminology common to OCMIP-II protocol meaning that the biological production is calculated as a restoration of model PO_4 to observational PO_4 from the World Ocean Atlas. See equation (2) in the manuscript (Najjar et al., 1992; Najjar and Orr, 1998).

11. Line 184: what is the first order carbon cycle?

This word has been removed for avoiding confusion.

12. Line 185: “explicit ecosystem models” please specify. I guess that it is the classic modeling approach but as said before, due to the lack of details we cannot understand how you approach differ from this “explicit” approach. Do you mean models that explicitly solve the light profile? Your model is also explicit for certain variables.

As the editor pointed out “explicit ecosystem models” is indeed classical ecosystem models with multiple compartments of NPZD. Our model is rather a “nutrient restoration approach of OCMIP-II” (Najjar et. al., 1992, Anderson and Sarmiento, 1995, Najjar and Orr, 1998). The advantage of this approach is basically ensuring the correct spatial and temporal distribution of surface nutrients, which is necessary for modeling the correct spatial and temporal distribution of surface ocean pCO_2 and air-sea CO_2 transfer.

13. Line 191: phosphorus and not phosphate

Corrected accordingly. Thank you for pointing this out.

14. Line 202: Since as far as I understood you did not run the physics? If yes, I would move what concerns the physics to this section and leaves to the model section what concerns the biology. Besides, you mention that you use ocean reanalysis products, is it for the physics only or do you use them for restoring the biology? For the remaining of the manuscript, I guess that this reanalysis is only used for the physics and so I do not see why we need to describe twice. Please clarify

Yes, we use ocean reanalysis only for physics. Ocean Tracer Transport Model (OTTM) is an offline model which uses reanalysis data from a parent model (here GFDL – MOM) to drive the physics. However in the biogeochemical model the nutrient restoration approach (Najjar et al., 1992, Anderson and Sarmiento, 1995) is achieved using Phosphate observational data (World Ocean Atlas: WOA; Garcia et. al., 2014) not with reanalysis data (For biogeochemical model details please refer Section 2.2 and Appendix A of the revised manuscript).

The repeated sentence is removed and corrected as per your suggestion.

Please refer line 217-218 in the revised manuscript.

15. Lines 208-210: Please reformulate. The initial conditions for PO4 and O2 were taken from World Ocean Atlas (Garcia et al., 2014) while for DIC and ALK data from the Global Ocean Data Analysis Project (GLODAP; Key et al., 2004) are taken. What about

DOP? Oxygen is not listed as a state variable in the appendix so why do you need to initialize it? You mention a list of data for validation like satellite estimated NPP, how do you link with model?

Dissolved Organic Phosphorous is initialized with a constant value of 0.02 μmol kg^{-1}. Oxygen is removed from listing. Please refer to lines 225 – 227 in the revised manuscript.

Satellite-derived Net Primary Production (NPP) data were taken from Sea-viewing Wide Field of view Sensor (SeaWiFS) Chl-a product, calculated using Vertically Generalized Production Model (VGPM: Behrenfeld and Falkowski, 1997). The NPP data is approximated to export production EP = NPP * e-ratio, here the value of e-ratio for the Indian Ocean upwelling zones is adapted as 0.37 as per Sarmiento and Gruber, 2006; Laws et al., 2000; Falkowski et al., 2003 and then compared with the OTTM model export production profiles (See Model, Data and Methods for details).

16. Line 219: please add a reference.

A reference is added. Please see line 235 in the revised manuscript.

17. Line225-227: Please reformulate. " This includes anthropogenic increase…" what represent "This" this is not clear what includes anthropogenic DIC?

Restated as "Since the study is focused only on bias correction to the seasonal cycle with a variable Zc, a model climatology of carbon cycle has been constructed from 1990 to 2010, which includes the anthropogenic increase of oceanic DIC in the climatological calculation and is comparable with the Takahashi et al. (2009) observations."

The time period of 1990 – 2010 is taken for climatology since the Takahashi observations are available from 1990 onwards. This is a better way to validate the model against Takahashi observations.

Please refer to line 240 – 243 of the revised manuscript.

18. Lines 228-229: please clarify the aim of these sensitivity experiments directly (you want to remove the effect of upwelling). . You remove the seasonal cycle form the physics and only impose that from Zc? (we understand afterwards reading the results section).

The aim of conducting these sensitivity experiments is to understand how much a varZc parameterization in the biogeochemical model is successful in capturing the upwelling related pCO2 and CO2 fluxes even though the seasonal cycle in physics of upwelling mechanisms is removed when compared with a constZc simulation. By removing the seasonal cycle in currents we are suppressing the Ekman divergence over the upwelling region. Similarly, by suppressing the seasonal cycle in the temperature we are removing the cooling effect due to upwelling in the solubility pump and quantifying how much the model seasonality is improved due to varZc parameterization alone.

Please refer to lines 246 – 250 in the revised manuscript.

19. Line 265-266: "the model permits 100 % relative photosynthesis for radiation above 50 W/M2" what do you mean by relative photosynthesis? from equations given in the appendix, no term related to photosynthesis is presented. Do you mean Jprod is not null when the irradiance is above 50W/m2(so when Z Line 268-269: clarify the link between phot inhibition and phosphate availability as it is not clear how the availability of phosphate can be linked as a general rule with photo inhibition.

The editor is right that we do not have any explicit term to calculate the photosynthesis alone. However, in order to compare our model production of organic phosphorous to the curve of Ryther et al., we have merely scaled our total production to "relative photosynthesis", which is, according to Ryther et al., (1956) is an index between 0 and 1 indicating the strength of production estimated as Pl/Pmax,where Pl is the photosynthesis at each intensity (of light) of different species and Pmax is the maximum photosynthesis observed in the same control experiment. The curve between relative photosynthesis and light intensity shows the relation between photosynthetic activity and light in marine phytoplankton. Since our method relates the biological production to a function of light (limitation) by Chl-a attenuation, it is the best curve to cross-compare our results. Therefore we also scaled our total biological production within Zc into relative values between 0-1 by P_l/P_{max}. In our case, P_l is taken as the individual grid cell biological component of organic phosphorus production and P_{max} is the maximum production available in the domain at any given instant. All the grid points align similarly to the curve of Ryther et al., (1956) which is quite encouraging.

We have included the above steps into the Appendix B of the manuscript.

The relation between photo-inhibition and phosphate availability can be explained by taking an example of a gyre region. Indian Ocean gyre is an oligotrophic region where the continuous downwelling water at the gyre centre does not allow the nutrients to come up into the production zone (above Zc). Due to the absence of chlorophyll over this region, solar radiation penetrates deeper (approximately Zc=60m see figure 3 in the revised manuscript). But the production of organic phosphorus (J_{prod}) in the model is allowed at radiation values above 50 W m^{-2}. Since

there are no sufficient new nutrients above the Zc over this region, the production of organic phosphorus is limited. Thus the limited availability of phosphate for these gyre regions above the Zc will indirectly represent photoinhibition (eventhough solar radiation is available).

20. Lines 235-238: this part is not clear. What does "x" represent and reformulate.

A smoothing technique with linear interpolation ($u = u(1 - x) + \bar{u}x$) is applied to the offline-data in order to blend the annual mean fields ($\bar{u}$) provided to the selected region with the rest of the domain (u) to reduce the sudden transition at the boundaries. Here x represents an index which varies between 0 and 1 within a distance of 10^0 from the boundaries of the region of interest to the rest of the model domain.

Reformulated as per your suggestion. Please refer to lines 252 – 256 in the revised manuscript.

21. Line 241: compensation depth is already previously defined. Once defined, Zc should be used throughout the manuscript.

Corrected throughout the manuscript.

22. Line 252: Same remark as for Zc for varZc

Corrected accordingly.

23. Line 262: the average relative photosynthesis needs to be defined and details on how it is computed need to be provided.

Kindly refer to the reply to comment 19. Please refer to Appendix B in the revised manuscript.

24. Line 272-273: Please reformulate, this sentence is heavy. Consider for instance: "The value of Zc estimated from equation… shows marked seasonal and spatial variability (Figure 3). ..
An equation stating clearly how Zc is estimated would help.

Zc is calculated as defined in section 2.5, lines 268 -271 in the revised manuscript.

25. Line 275: "..and deepens up to 45 m from March to May due to the increase in the surface solar radiation".

Corrected accordingly. Please refer to lines 291 – 295 in the revised manuscript.

26. Line 278: Zc and not "the Zc "

Corrected accordingly. Please refer to line 290 - 296 in the revised manuscript.

27. Line 281: Please replace compensation depth by Zc and do it through the manuscript for consistency.

Revised throughout the manuscript.

28. Line 282: Zc and not "the Zc"

Corrected accordingly. Please refer to lines 299 – 301 in the revised manuscript.

29. Lines 283-286: Please explain how these factors can affect the penetration of light. If it is through chlorophyll, this is taken into account since in your profile you use a chlorophyll profile from the observation. Turbidity? Please clarify the link or remove.

This sentence is removed.

30. Line 299: Please clarify what does mean "optimum" here. Surface value? If yes this is not optimum.

We have removed the word "optimum" here. Please refer to lines 313 - 316 in the revised manuscript.

31. Line 299-300: reference to Parsons et al 1984 is for the parameterization used for Zc? If Yes you do not need to remind it here again (better to do in the description of the equation above) because it is confusing as we can wonder whether this reference to Parson concerns the fact that the production zone is never larger than 75m.

The citation has been removed. Please see lines 313 – 316 of the revised manuscript

32. Line 300-301: "The consequence of this on the seasonality …". The consequence of What? A varying Zc? Or a Zc limited to 75m?

Reformulated as "The relevance of varZc in the seasonality of the modeled carbon cycle is illustrated as follows." Please refer to lines 315 – 316 in the revised manuscript.

33. Lines 306-307: How pCO2 is derived from your model state variables? Give a reference in the modeling section.

A detailed derivation of pCO_2 from model state variables are provided at the end of this report (See Section A) and the equation for the calculation of pCO_2 is provided in Model, data, and Methods section 2.2 in the revised manuscript. (See the equation 7 in the revised manuscript).

34. Line 316: please explain how the new production is estimated from the model? Jprod converted into carbon? This is confusing because at line 702-703, it is mentioned: " the biological production in the model Jprod is calculated using equation A1" then lines 730-731: "… the rate of change of phosphate which represents biological production in the model …". However, the rate of phosphate change (see eq A3) also incorporates some remineralization of DOP and hence is not only linked to "primary production". As far as I know new production, is the production based on "new nutrients" (and not remineralized nutrients).

This was a technical error while writing the appendix. The first term in the R.H.S of Equation A18 is the rate of change of phosphate resulting from photosynthesis and respiration in the model (i.e., J_{po4} in this case) multiplied by the carbon to phosphorous Redfield ratio ($R_{C:P}$ = 117:1) and J_{Ca} represents the calcite formation in the model (see Equation A8 & A16). This has been corrected in the manuscript (see lines 754-759).

The vertically integrated new production (g C m^{-2} yr^{-1}) in the model is calculated as per Najjar et al., (1992) as follows.

$$New\ production = -\int_{zc}^{0} J_{prod}\ dz$$

(Najjar et al., 1992)

Please refer to the Biogeochemical model section 2.2 in the revised manuscript.

35. Line 378: Please explain how the export production is estimated from satellite estimated vertically integrated production over the euphotic zone and how this can compare with the model estimated production over the compensation depth.

By the relation,

$$e\ ratio = \frac{Export\ \ Production}{Primary\ \ Production}$$

$$Export\ Production = Primary\ Production * e\ ratio$$

Here the value of primary production is used from the satellite-derived Net Primary Production (NPP) and e- ratio, which is the ratio of export production to the primary production is taken as 0.37 (Sarmiento and Gruber, 2006, Laws et al., 2000, Falkowski et al. 2003). Thus the export production is computed from the satellite-derived NPP data.

However, in the model, the export production is calculated as

$$Export\ production, EP = (1-\sigma)\int_{0}^{Z_c} J_{prod}\ dz$$

Where σ = 0.67 is the fraction of nutrients transferring to dissolved organic phosphorous and J_{prod} represents the production of organic phosphorous (Yamanaka and Tajika, 1997; Najjar and Orr, 1998; Oka et. al., 2011)

This has been added in section 2.2 of the revised manuscript.

36. Line 375: what do you mean by "new biological parameterization"? Are they related to the model that you described in the appendix? Or is it the use of varZc? In that last case

please mention the use of varZc as this is how it is referred in the text. I find that using biological parameterization is confusing.

As per your suggestion, the sentence is reformulated as "The improvements shown by the use of varZc in the simulation of CO_2 flux and pCO_2 can be elicited by further analysis of the model biological production." Please refer to lines 390 – 391 of the revised manuscript.

37. Line 363: fails or simulations

Corrected accordingly. Please refer to line 378 in the revised manuscript.

38. Line 380 simulations or has

Corrected accordingly. Please refer to line 395 in the revised manuscript.

39. Line 408: please explain how Fig 8d shows that the simulated export production is consistent with satellite data.

Thank you for pointing out the error. Corrected to Figure 7b. Please refer to line 421 in the revised manuscript.

40. Line 410-411: Tables 1-4 summarize

Corrected accordingly. Please refer to line 425 in the revised manuscript.

41. Line 413 strengthened

Corrected accordingly. Please see line 427 in the revised manuscript.

42. Lines 570-571: please explain how temperature affects your biological model? For appendix this is not explained.

The sensitivity of temperature is assessed for the carbon cycle but NOT for biology. The varZc alters the DIC gradients and impact the carbon cycle. The dynamic effects are also cross-checked along with temperature effect.

Temperature sensitivity of the carbon cycle comes into play during the estimation of pCO_2. Takahashi et al. (1993) provide a useful relationship that summarizes the temperature sensitivity of pCO_2 in a closed system.

$$\frac{1}{pCO_2}\frac{\partial pCO_2}{\partial T} = \frac{\partial lnpCO_2}{\partial T} \approx 0.0423^o C^{-1}$$

For example, if we take a water parcel with an initial pCO_2 of 300 µatm at 20°C and with a salinity of 35, a one-degree warming increases pCO_2 by approximately 13 µatm, whereas a salinity increase of 1 results in a pCO_2 increase of 9 µatm.

Thus the effect of seasonal changes in SST on pCO_2 is estimated simply by multiplying the observed seasonal SST changes, ΔSST by

$$\Delta\, pCO_2|_{thermal} \approx pCO_2 . 0.0423^o C^{-1} . \Delta\, SST$$

For the estimation of model pCO_2, the solubility constant K_o, and dissociation constants K_1, K_2 are computed by using the temperature and salinity relations. This will indirectly affect the pCO_2 seasonal cycle in the biogeochemical model. (See section A given below)

43. Appendix: the description that is made is insufficient. Please provide the evolution equations for each of your state variables (i.e. DIC, ALK, PO4, DOP, O2?).

As per your suggestions, a detailed model description is provided in Model, Data and Methods (see Section 2.2) and Appendix A. Please refer to the revised manuscript.

Also, see the end of this report (Section B)

44. Line 701: As far as I understand, JDOP, JPO4 represents the balance between sources and sinks while Jprod and JCa represent biogeochemical flows with respectively production and calcification, so J is not always the balance between sink and sources.

Corrected accordingly. Please refer to lines 727 – 729 in the revised manuscript.

45. Line 703: please define precisely what is meant by biological production.

Corrected as “the production of organic phosphorous in the model.” Please refer to lines 729-730 of the revised manuscript.

46. Line 706: please clarify in equation A1 that when the phosphate concentration is lower than the climatology, there is no production.

Clarified according to your suggestion. Please refer to lines 731 - 733 in the revised manuscript.

47. Line 707: “a fixed fraction of production” rather than “ a fixed fraction of phosphate”, “a source for DOP”

Corrected accordingly. Please refer to lines 734 – 737 in the revised manuscript.

48. Line 708: phosphorus

Corrected accordingly.

49. Line 709: remaining is (1-sigma) Jprod and not kappa*[DOP, Kappa*[DOP] is remineralization.

Corrected accordingly.

50. Line 728: What does phi represent? In the main text, eq 1 states that phi represents the production/destruction term? In the appendix, we are told that J is the production/destruction term and here what does phi represent?

Thank you for pointing out this error. In the main text phi is replaced with F. and restaed as

“J represents any sink or source due to the internal consumption or production of the tracer. F represents the emission or absorption of fluxes at the ocean surface.” (See section 2.2 in the revised manuscript)

51. Line 732: the value of Rc:p is inconsistent: here Rc:P equals 117 while at line 720 this ratio equals 106.

Corrected as $R_{C:P}$ = 117. Please refer to line 746 in the revised manuscript.

52. Line 733: Phi needs to be defined. At line 171, phi is defined as a source/sink term. Now J is used to define that term.

Kindly refer to the reply to comment 50.

53. Figure 3: Seasonal maps of the compensation depth estimated from equation (give the number of the equation) … …Please explain what is the blue rectangle in Figure 3a.

We could not locate the “blue rectangle” in figure 3.

54. Table 4: I guess that it is model derived values and not satellite derived values

Corrected accordingly.

Section A: Derivation of pCO_2 from model state variables.

In general, ocean carbon cycle models derive pCO_2 based on two approaches (1) Specifying DIC and ALK and then calculating pCO_2 (2) Specifying pCO_2 and ALK and computing DIC. In OCMIP –II model protocol pCO_2 is derived by specifying DIC and ALK. The details are given below.

The reactions which take place when carbon dioxide dissolves in water can be represented by the following series:

$$CO_2 + H_2O \overset{K_0}{\leftrightarrow} H_2CO_3^* \quad (1)$$

$$H_2CO_3^* \overset{K_1}{\leftrightarrow} H^+ + HCO_3^- \quad (2)$$

$$HCO_3^- \overset{K_2}{\leftrightarrow} H^+ + CO_3^{2-} \quad (3)$$

$$H_2O \overset{K_w}{\leftrightarrow} H^+ + OH^- \quad (4)$$

$$H_3BO_3 + H_2O \overset{K_B}{\leftrightarrow} H^+ + B(OH)_4^- \quad (5)$$

Where K_0, K_1, K_2, K_w, K_B are the equilibrium constants for dissociations respectively, which are given as below:

$$K_0 = \frac{[H_2CO_3^*]}{pCO_2} \quad (6)$$

$$K_1 = \frac{[H^+][HCO_3^-]}{[H_2CO_3^*]} \quad (7)$$

$$K_2 = \frac{[H^+][CO_3^{2-}]}{HCO_3^-} \quad (8)$$

$$K_w = [H^+][OH^-] \quad (9)$$

$$K_B = \frac{[H^+][B(OH)_4^-]}{[H_3BO_3]} \quad (10)$$

From the concentration definition,

$$DIC = [H_2CO_3^*] + [HCO_3^-] + [CO_3^{2-}] \quad (11)$$

$$ALK = [HCO_3^-] + 2[CO_3^{2-}] + [OH^-] - [H^+] + [B(OH)_4^-] \quad (12)$$

$$TB = [B(OH)_4^-] + [H_3BO_3] = c.S \quad (13)$$

Neglecting the minor contribution of other weak bases to alkalinity (ALK; Dickson and Goyet, 1994) and rewriting the equation for ALK in terms of the known parameters DIC and TB and then by solving the resulting equation for unknown $[H^+]$, pCO_2 can be calculated as

$$pCO_2 = \frac{[DIC]}{K_0}\frac{[H^+]^2}{[H^+]^2 + K_1[H^+] + K_1K_2} \qquad (14)$$

Where $[H^+]$ is calculated using Newton-Raphson iterative method (Press et. al., 1996, Najjar and Orr, 1998), [DIC] is calculated using equation (11) and the value of equilibrium constants are derived from temperature and salinity dependent equation as given below.

The solubility of CO_2 (mol kg^{-1} atm^{-1}):

$$\ln K_0 = -60.2409 + 93.4517\left(\frac{100}{T}\right) + 23.3585\ln\left(\frac{T}{100}\right) + S\left(0.023517 - 0.023656\left(\frac{T}{100}\right) + 0.0047036\left(\frac{T}{100}\right)^2\right) \qquad (15)$$

(Weiss, 1974)

The dissociation constant of carbonic acid (mol kg^{-1}):

$$-\log K_1 = -62.008 + \frac{3670.7}{T} + 9.7944\ln(T) - 0.0118S + 0.000116S^2 \qquad (16)$$

$$-\log K_2 = 4.777 + \frac{1394.7}{T} - 0.0184S + 0.000118S^2 \qquad (17)$$

(Mehrbach et al., 1973, Dickson and Millero, 1987)

The dissociation constant of water K_w (mol kg^{-1})

$$-\ln K_w = 148.96502 + \frac{-13847.26}{T} - 23.6521\ln(T) + S^{\frac{1}{2}}\left(-5.977 + \frac{118.67}{T} + 1.0495\ln(T)\right) - 0.01615S \qquad (18)$$

(Millero, 1995)

The dissociation constant of boric acid K_B [(mol kg^{-1})^2]

$$-\ln K_B = \frac{1}{T}\left(-8966.9 - 2890.53\,S^{0.5} - 77.942\,S + 1.728\,S^{1.5} - 0.0996\,S^2\right)148.0248 + 137.1942\,S^{0.5} + 1.62142\,S + 0.053105\,S^{0.5}\,T + \ln(T)\left(-24.4344 - 25.085\,S^{0.5} - 0.2474\,S\right) \qquad (19)$$

(Dickson, 1990)

Where T is the temperature in [K] and S is the salinity on the practical salinity scale.

The total boron equation (μmol kg^{-1}; Uppström, 1974):

$$TB = 1.185\ S \qquad (20)$$

Thus using equation (14) pCO_2 is calculated in the biogeochemical model (Najjar and Orr, 1998; Sarmiento and Gruber, 2006).

Section B

Biogeochemical model

The biogeochemical model used in the study is based on the OCMIP – II protocol as stated above. The main motivation of OCMIP–II model design is to simulate the ocean carbon cycle with a nutrient restoration approach to ocean primary production. The present version of the model has five prognostic variables coupled with the circulation field, viz., inorganic phosphate (PO_4^{3-}), dissolved organic phosphorus (DOP), oxygen (O_2), dissolved inorganic carbon (DIC) and alkalinity (ALK). In order to retrieve the accurate spatial and temporal distribution of CO_2 flux and pCO_2, the model uses a "nutrient restoring" approach (Najjar et al., 1992; Anderson and Sarmiento, 1995) for primary production. The basic currency for primary production in the model is phosphorous because of the availability of a more extensive database and to eliminate the complexities associated with nitrogen fixation and denitrification.

Air-sea CO_2 flux in the model is estimated by,

$$F = K_w\ \Delta\ pCO_2 \qquad (2)$$

where K_w is gas transfer velocity and $\Delta\ pCO_2$ is the difference in partial pressure of carbon dioxide between the ocean and atmosphere.

pCO_2 is calculated in the model by using DIC and ALK and is given by,

$$pCO_2 = \frac{[DIC]}{K_0}\frac{[H^+]^2}{[H^+]^2 + K_1[H^+] + K_1K_2} \quad (3)$$

Where $[H^+]$ is calculated using Newton-Raphson iterative method (Press et. al., 1996, Najjar and Orr, 1998). K_0 is the solubility constant of CO_2 and K_1, K_2 are the dissociation constant for carbonic acid respectively (Sarmiento and Gruber, 2006, Weiss, 1974, Mehrbach et al., 1973, Dickson and Millero, 1987, Najjar and Orr, 1998).

The conservation equations of the model variables are given below as

$$\frac{d[PO_4]}{dt} = L([PO_4]) + J_bPO_4 \quad (4)$$

$$\frac{d[DOP]}{dt} = L([DOP]) + J_bDOP \quad (5)$$

$$\frac{dDIC}{dt} = L([DIC]) + J_bDIC + J_gDIC + J_vDIC \quad (6)$$

$$\frac{d[ALK]}{dt} = L([ALK]) + J_bALK + J_vALK \quad (7)$$

Where L is the 3D transport operator, which represents the effects due to advection, diffusion and convection. [] or square brackets indicate the concentrations in mol m^{-3}. J_bPO_4, J_bDOP, J_bDIC, J_bALK is the biological source/sink terms and J_vDIC, J_vALK are the virtual source-sink terms representing the changes in surface DIC and ALK, respectively, due to evaporation and precipitation. J_vDIC is the source-sink term due to air-sea exchange of CO_2.

The production of organic phosphorus in the model using the nutrient restoring approach is given by

$$J_{prod} = \frac{1}{\tau}([PO_4] - [PO_4]^*) \quad (9)$$

$$[PO_4] > [PO_4]^* \; ; Z < Zc$$

$$J_{prod} = 0 \qquad (10)$$

$$[PO_4] \leq [PO_4]^* \; ; Z > Zc$$

Where $[PO_4]^*$ is the observed phosphate concentration and τ =30 days is the restoration time scale.

The vertically integrated new production (g C m^{-2} yr^{-1}) in the model is defined as

$$New\ production = -\int_{zc}^{0} J_{prod}\ dz \qquad (11)$$

The export production (g C m^{-2} yr^{-1}) in the model is calculated as given below

$$Export\ production = (1-\sigma) \int_{0}^{zc} J_{prod}\ dz \qquad (12)$$

The detailed biogeochemical dynamics implemented in the model and the calculations of solubility and biological pump are provided in Appendix-A. The design and validation of the physical model are reported by Valsala et al., (2008, 2010) and biogeochemical design by Najjar and Orr (1998).

References

Anderson, L. A. and J. L. Sarmiento: Global ocean phosphate and oxygen simulations, Global Biogeochem.cycles, 9, 621 – 636.

Behrenfeld, M. J., Falkowski. P. G.: Photosynthetic rates derived from satellite-based chlorophyll concentration, Limnol. Oceanogr., 42, 1 – 20, doi: 10.4319/lo.1997.42.1.0001, 1997.

Chang, Y. S., Zhang. S., Rosati. A., Delworth. T., Stern. W. F.: An assessment of oceanic variability for 1960-2010 from the GFDL ensemble coupled data assimilation, Clim. Dyn., 40, 775 – 803, doi: 10.1007/s00382-012-1412-2, 2012.

Dickson, A. G. (1990), Thermodynamics of the dissociation of boric acid in synthetic seawater from 273.15 to 318.15K, Deep-Sea Res., 37, 755 – 766.

Dickson, A. G., and F. J. Millero (1987), A comparison of the equilibrium constants for the dissociation of carbonic acid in seawater media, Deep-Sea Res., 34, 1733 – 1743.

Falkowski, P. G., E. A. Laws, R. T. Barber, and J. W. Murray: phytoplankton and their role in the primary, new and export production, In: Fasham M.J.R (eds) Ocean Biogeochemistry, Global Change – The IGBP series (closed). Springer, Berlin, Heidelberg, doi:https://doi.org/10.1007/978-3-642-55844-3_5, 2003.

Garcia, H. E., R. A. Locarnini, T. P. Boyer, J. I. Antonov, O.K. Baranova, M.M. Zweng, J.R. Reagan, D.R. Johnson.: World Ocean Atlas 2013, Volume 4: Dissolved Inorganic Nutrients (phosphate, nitrate, silicate), S. Levitus, Ed., A. Mishonov Technical Ed.; NOAA Atlas NESDIS 76, 25 pp, 2014.

Gattuso, J. P., B. Gentili, C. M. Duarte, J. A. Kleypas, J. J. Middelburg, and D. Antoine.: Light availability in the coastal ocean: Impact on the distribution of benthic photosynthetic organisms and their contribution to primary production, Biogeosciences, 3, 489 – 513, doi:10.5194/bg-3-489-2006, 2006.

Laws, E. A., P. G. Falkowski, W.O. Smith, Jr., H. Ducklow and J. J. McCarthy: Temperature effects on export production in the open ocean, Global Biogeochem. Cycles, 14, 1231 – 1246.

Levy, M., D. Shankar, J. M. Andre, S. S. C. Shenoi, F. Durand, and C. de Boyer Montegut: Basin wide seasonal evolution of the Indian Ocean's phytoplankton blooms, J. Geophys., 112, C12014, doi: 10.1029/2007JC004090, 2007.

Lopez-Urrutia, A., E. San Martin, R. P. Harris, and X. Irigoien.: Scaling the metabolic balance of the oceans, Proc. Natl. Acad. Sci. U.S.A., 103, 8739-8744,doi:10.1073/pnas.0601137103, 2006.

Marra, J. F., Veronica P. Lance, Robert D. Vaillancourt, Bruce R. Hargreaves.: Resolving the ocean's euphotic zone, Deep Sea. Res. pt. I., 83, 45 -50, doi:10.1016/j.dsr.2013.09.005, 2014.

Mehrbach, C., C. H. Culberson, J. E. Hawley, and R. M. Pytkowicz (1973), Measurement of the apparent dissociation constants of carbonic acid in seawater at atmospheric pressure, Limnol. Oceanogr., 18, 897 – 907.

Millero, F. J. (1995), Thermodynamics of the carbon dioxide system in the oceans, Geochim. Cosmochim. Acta, 59, 661 – 677.

Morel, A.: Optical modeling of the upper ocean in relation to its biogenous matter content (Case 1 Waters), J. Geophys. Res., 93, 10479-10, 768, doi: 10.1029/JC093iC09p10749, 1988.

Najjar, R. G., Orr, J. C.: Design of OCMIP-2 simulations of chlorofluorocarbons, the solubility pump and common biogeochemistry, http://www.ipsl.jussieu.fr/OCMIP/., 1998.

Najjar, R. G., Sarmiento, J. L., Toggweiler, J. R.: Downward transport and fate of organic matter in the ocean: simulations with a general circulation model, Global biogeochem. Cycles., 6, 45-76, doi:10.1029/91GB02718, 1992.

Orr, J. C., and co-authors.: Anthropogenic ocean acidification over the twenty-first century and its impact on calcifying organisms, Nature, 437, 681 – 686, doi:10.1038/nature04095, 2005.

Parsons, T. R., Takahashi, M., Habgrave, B.: In Biological Oceanographic Processes, 3rd ed., 330pp., Pergamon Press, New York, doi: 10.1002/iroh.19890740411, 1984.

Prakash, P., S. Prakash, H Rahaman, M. Ravichandran, and S. Nayak: Is the trend in chlorophyll-a in the Arabian Sea decreasing?, Geophys. Res. let., 39, L23605, doi:10.1029/2012GL054187.

Press, W. H., and others: Numerical Recipes in FORTRAN. Cambridge University Press, Cambridge, England.

Regaudie-de-Gioux, A., and C. M. Duarte.: Compensation irradiance for planktonic community metabolism in the ocean, Global Biogeochem. Cycles, 24, GB4013, doi:10.1029/2009GB003639, 2010.

Resplandy, L., J. Vialard, M. levy, O. Aumont and Y. Dandonneau: Seasonal and intraseasonal biogeochemical variability in the thermocline ridge of the southern tropical Indian Ocean. J. Geophys. Res., 114, C07024.

Ryther, J.: Photosynthesis in the ocean as function of light Intensity, Limnol. Oceanogr., vol 1, issue 1, doi: 10.4319/lo.1956.1.1.0061, 1956.

Sarmiento, J. L., and Gruber, N.: Ocean Biogeochemical Dynamics, Princeton University Press, New Jersey, 2006.

Smetacek, V., and Passow, U.: Spring bloom initiation and Sverdrup's critical depth model, Limnol. Oceanogr., 35, 228 – 234, doi: 10.4319/lo.1990.35.1.0228, 1990.

Takahashi, T., J. Olafsson, J. G. Goodard, D. W.. Chipman, and S.C. Sutherland: Seasonal variation of CO_2 and nutrients in the high latitudes surface oceans: A comparative study, Global Biogeochem. Cycles, 7, 843 – 878.

Takahashi, T., Sutherland, S. C., Wanninkhof, R., Sweeney, C., Feely, R. A., Chipman, D. W., Hales, B., Friederich, G., Chavez, F., Sabine, C., et al.: Climatological mean and decadal changes in surface ocean pCO_2 and net sea-air CO_2 flux over the global oceans. Deep Sea Res., Pt. II., 56, 554 – 557, doi:10.1016/j.dsr2.2008.12.009, 2009.

Uppström, L. (1974), The boron/chlorinity ratio of deep sea water from the Pacific Ocean, Deep-Sea Res., 21, 161-162.

Valsala, K. V., Maksyutov, S., Ikeda, M.: Design and Validation of an offline oceanic tracer transport model for a carbon cycle study, J. clim., 21, doi: 10.1175/2007JCLI2018.1, 2008.

Valsala, V., Maksyutov, S.: Simulation and assimilation of global **oc**ean pCO_2 and air-sea CO_2 fluxes using ship observations of surface ocean pCO_2 in a simplified biogeochemical model, Tellus., 62B, doi: 10.1111/j.1600-0889.2010.00495, 2010.

Weiss, R. F. (1974), Carbon dioxide in water and seawater: The solubility of a non-ideal gas, Mar. Chem., 2, 203-215.

Wiggert, J. D., Hood, R. R., Banse, K., Kindle, J. C.: Monsoon-driven biogeochemical processes in the Arabian Sea, Progr. Oceanogr., 65, 176-213, doi:10.1016/j.pocean.2005.03.008, 2005.

Yamanaka, Y., and E. Tajika: Role of dissolved organic matter in the marine biogeochemical cycle: studies using an ocean biogeochemical general circulation model. Global Biogeochem. Cycles, 11, 599 – 612, 1997.

Optimization of Biological Production for Indian Ocean upwelling zones: Part – I: Improving Biological Parameterization via a variable Compensation Depth

Mohanan Geethalekshmi Sreeush[1,2,*].

Vinu Valsala[1],

Sreenivas Pentakota[1],

Koneru Venkata Siva Rama Prasad[2],

Raghu Murtugudde[3]

[1]Indian Institute of Tropical Meteorology, Pune, India

[2]Department of Meteorology and Physical Oceanography, Andhra University, India

[3]ESSIC, University of Maryland, USA

(*Under revision BGD*)

*Corresponding author address:
Indian Institute of Tropical Meteorology,
Dr. Homibhabha Road, Pashan, Pune 411 008, India
E-Mail: sreeushmg@tropmet.res.in

Abstract

Biological modeling approach adopted by the Ocean Carbon Cycle Model Inter-comparison Project (OCMIP-II) provided amazingly simple but surprisingly accurate rendition of the annual mean carbon cycle for the global ocean. Nonetheless, OCMIP models are known to have seasonal biases which are typically attributed to their bulk parameterization of 'compensation depth'. Utilizing the ~~principle of minimum solar radiation for the production and its attenuation by the surface Chl-a~~ criteria of surface Chl-a based attenuation of solar radiation and the minimum solar radiation required for production, we have proposed a new parameterization for a spatially and temporally varying 'compensation depth' which captures the seasonality in the production zone reasonably well. This new parameterization is shown to improve the seasonality of CO_2 fluxes, surface ocean pCO_2, biological export and new production in the major upwelling zones of the Indian Ocean. The seasonally varying compensation depth enriches the nutrient concentration in the upper ocean yielding more faithful biological exports which in turn leads to an accurate seasonality in carbon cycle. The export production strengthens by ~70% over western Arabian S~~s~~ea during monsoon period and achieved a good balance between export and new production in the model. This underscores the importance of having a seasonal balance in model export and new production for a better representation of the seasonality of carbon cycle over upwelling regions. The study also implies that both the biological and solubility pumps play an important role in the Indian Ocean upwelling zones.

Keywords: Indian Ocean upwelling zones, Carbon cycle, Seasonal cycle - CO_2 flux and Oceanic pCO_2, Biogeochemical model parameterization, Export production - New production balance, Solubility and Biological pump.

1. Introduction

Indian Ocean is characterized by the unique seasonally reversing monsoon wind systems which act as the major physical drivers for the coastal and open ocean upwelling processes. The major upwelling systems in the Indian Ocean are (1) the western Arabian Sea (WAS; Ryther and Menzel, 1965; Smith et al., 2001; Sarma, 2004; Wiggert et al., 2005, 2006; Murtugudde et al., 2007; McCreary et al., 2009; Prasanna Kumar et al., 2010; Naqvi et al., 2010; Roxy et al., 2015) (2) the Sri Lanka Dome (SLD; Vinayachandran et al., 1998, 2004), (3) Java and Sumatra coasts (SC; Murtugudde et al., 1999; Susanto et al., 2001; Osawa et al., 2010; Xing et al., 2012) and (4) the Seychelles-Chagos thermocline ridge (SCTR; Murtugudde et al., 1999; Dilmahamod et al., 2016, Figure 1). The physical and biological processes and their variability over these key regions are inseparably tied to the strength of the monsoon winds and associated nutrient dynamics. The production and its variability over these coastal upwelling systems are a key concern for the fishing community, since they affect the day-to-day livelihood of the coastal populations (Harvell et al., 1999; Roxy et al., 2015; Praveen et al., 2016) and are important for the Indian Ocean rim countries due to their developing country status.

Arabian Sea is a highly productive coastal upwelling system characterized by phytoplankton blooms both in summer (Prasanna Kumar et al., 2001; Naqvi et al., 2003; Wiggert et al., 2005) and winter (Banse and McClain, 1986; Wiggert et al., 2000; Barber et al., 2001; Prasannakumar et al., 2001; Sarma, 2004). Arabian Sea is known for the second largest Tuna fishing region in the Indian Ocean (Lee et al., 2005). The Somali and Omani upwelling regions experience phytoplankton blooms that are prominent with Net Primary Production (NPP) exceeding 435 g C m^{-2} yr^{-1} (Liao et al., 2016). On the other hand productivity over the SLD (Vinayachandran and

Yamagata, 1998), in the sea of Sri Lanka is triggered by an open ocean Ekman suction with strong Chl-a blooms during the summer monsoon (Murtugudde et al., 1999; Vinayachandran et al., 2004). Similarly the SC upwelling is basically due to the strong alongshore winds and its variation is associated with impact of equatorial and coastal Kelvin waves (Murtugudde et al., 2000). The interannual variability associated with the Java-Sumatra coastal upwelling is strongly coupled with ENSO (El-Niño Southern Oscillation) through the Walker cell and Indonesian throughflow (Susanto et al., 2001; Valsala et al., 2011) and peaks in July through August with a potential new production of 0.1 Pg C yr^{-1} (Xing et al., 2012). The SCTR productivity has a large spatial and interannual variability. The warmer upper ocean condition associated with El Niño reduces the amplitude of subseasonal SST variability over the SCTR (Jung and Kirtman., 2016). The Chl-a concentration peaks in summer when the southeast trade winds induce mixing and initiate the upwelling of nutrient-rich water (Murtugudde et al., 1999; Wiggert et al., 2006; Vialard et al., 2009; Dilmahamod et al., 2016).

Understanding the biological production and variability in the upwelling systems is important because it gives us crucial information regarding marine ecosystem variability (Colwell, 1996; Harvell et al., 1999). The observations also provide vital insights into physical and biological interactions of the ecosystem (Naqvi et al., 2010) as well as the bio-physical feedbacks (Murtugudde et al., 2001) although limitations of sparse observations often force us to depend on models to examine the large spatio-temporal variability of the ecosystem (Valsala et al., 2013). Simple to inter-mediate complexity marine ecosystem models have been employed by several of the previous studies (Sarmiento et al., 2000; Orr et al., 2001; Matsumoto et al., 2008). However the representation of marine ecosystem with proper parameterizations in models has always been a daunting task. This is an impediment to the accurate representation of biological primary and

export productions in models (Friedrichs et al., 2006, 2007) and the issues also impact the modeling of upper trophics levels (Lehodey et al., 2010).

Biological production can be quantified with a better understanding of primary production which depends on water temperature, light and nutrient availability (Brock et al., 1993; Moisan et al., 2002) and this became the key reason for parameterizing the production in models as one or more combinations of these terms (Yamanaka et al., 2004). Any of these basic parameters can be tweaked to alter production in models. For example the availability of nutrients and light determines the phytoplankton growth (Eppely et al., 1972) or growth rate (Boyd et al., 2013). Stoichiometry and carbon-to-Chl-a ratios are other important factors to be considered in modeling (Christian et al., 2001, Wang et al., 2009) but we will not consider them in this study.

The Ocean Carbon cycle Model Intercomparison Project (OCMIP) greatly improved our understanding of global carbon cycle (Najjar and Orr, 1998). OCMIP-II further introduced a simple phosphate dependent production term in biological models for long term simulations of carbon cycle in response to anthropogenic climate change with an accurate annual mean state (Najjar and Orr, 1998; Orr et al., 2001; Doney et al., 2004). However, the OCMIP – II model simulations come with a penalty of ~~higher~~ strong seasonal biases when compared with observations (Orr et al., 2003). In this protocol, the community compensation depth (hereinafter Zc) is defined as the depth at which photosynthesis equals entire community respiration and the irradiance at which this balance is achieved is the compensation irradiance (E_{com}). ~~the light limitation is formulated as a bulk quantity with the notion that the minimum light irradiance at which phytoplankton photosynthesis is sufficient to balance the community respiration, E_{com}, is the compensation irradiance (Sarmiento and Gruber, 2006) and the depth at which the phytoplankton photosynthesis equals whole community respiration is the community~~

~~compensation depth (Smetacek and Passow, 1990; Gattuso et al., 2006; Sarmiento and Gruber, 2006; Regaudix-de-Gioux and Duarte, 2010; Marra et al., 2014).~~ Note that Zc is clearly different from the conventional euphotic zone depth (Morel, 1988). ~~If the irradiance is less than E_{com}, the growth will be negative, phytoplankton will decline through respiration. If the irradiance is larger than E_{com}, the planktonic photosynthesis will exceed the community respiration and production will increase (Parsons et al., 1984; Sarmiento and Gruber, 2006).~~ At Zc, the Net Community Production is Zero. i. e., when the Net Primary Production (NPP) balances the heterotrophic respiration (R_h) and above Zc the NPP exceeds the R_h and the ecosystem will grow (Smetacek and Passow, 1990; Gattuso et al., 2006; Sarmiento and Gruber, 2006; Regaudix-de-Gioux and Duarte, 2010; Marra et al., 2014). Therefore the region above Zc ~~compensation depth~~ represents the ~~oceanic~~ production zone in this modeling approach. However, Zc was held constant in time and space in OCMIP-II models (Najjar and Orr, 1998; Matsumoto et al., 2008) because the OCMIP-II protocol takes the minimalistic approach to biology and simplifies the model calculations with a very limited set of state variables suitable for long term simulations when casted in coarse resolution models (Orr et al., 2005). Though in reality Zc varies in space and time (Najjar and Keeling, 1997) just as the euphotic zone depth does as documented in ship measurements (Qasim, 1977, 1982). The variation in Zc ~~compensation depth~~ indicates the seasonality of the production zone itself.

Most of the biophysical models prescribe a constant value for Zc ~~compensation depth~~ e.g., Zc = 75m in OCMIP –II protocol (Najjar and Orr, 1998), Zc = 100m for Minnesota Earth System Model (Matsumoto et al., 2008). Depending on the latitude, Zc ~~compensation depth~~ varies between 50m and 100m in the real world (Najjar and Keeling, 1997). In our study we have attempted a novel biological parameterization scheme for spatially and temporally varying Zc

~~community compensation depth~~ in the OCMIP–II framework by representing the production as a function of ~~optimum~~ solar radiation (Parsons et al., 1984) and Chl-a availability. In this hypothesis, ~~the compensation irradiance is taken as 10 W m^{-2} and calculated its depth from a Chl-a attenuated solar radiation inorder to yield spatially and temporally varying Zc,~~ a spatially and temporally varying Zc is estimated from vertical attenuation of insolation through Chl-a profile and the depth at which this insolation reaches the compensation irradiance (chosen as 10 Wm^{-2}) is taken as Zc. ~~Phosphate~~ Phosphorous is the basic currency which limits biological production within this Zc ~~varying compensation depth.~~ This spatially and temporally varying Zc ~~compensation depth~~ represents the seasonality in the production zone which is lacking in OCMIP-II.

Regions of sustained upwelling like the eastern equatorial Pacific are well understood in terms of the role of upwelling in increasing the surface water pCO_2 to drive an outgassing of CO_2 into the atmosphere (Feely et al., 2001; Valsala et al., 2014). The Indian Ocean on the other hand only experiences seasonal upwelling which is relatively weak in the deep tropics but stronger off the coasts of Somalia and Oman and in the SLD (Valsala et al., 2013). The relative importance of the solubility vs. biological pump is not well understood. Our focus here on implementing seasonality in the Zc ~~compensation depth~~ of OCMIP models nonetheless leads to new insights on the impact of improved biological production on surface water pCO_2 and air-sea CO_2 fluxes. The largely the improvements due to ~~positive effects~~ of the variable Zc ~~compensation depth~~ over the Indian Ocean and the sensitivity experiments where upwelling is muted strongly imply that the biological pump may play as much of a role as the solubility pump in determining surface pCO_2 and CO_2 fluxes over the Indian Ocean.

159 The paper is organized as follows. Model, Data and Methods are detailed in Section 2.
160 The spatially inhomogeneous Zc derived out of the new parameterization and its impact in
161 simulated seasonality of biology and carbon cycle are detailed in Section 3. Further results and
162 discussion are followed in Section 4 and a conclusion is given in Section 5.

163

164 **2. Model, Data and Methods**

165 **2.1. Model**

166 The study utilizes the Offline Ocean Tracer Transport Model (OTTM; Valsala et al., 2008)
167 coupled with OCMIP biogeochemistry model (Najjar and Orr, 1998). OTTM does not compute
168 currents and stratifications (i.e., temperature and salinity) on its own. It is capable of accepting
169 any ocean model or data-assimilated product as physical drivers. The physical drivers prescribed
170 include 4-dimensional currents (u,v), temperature, salinity, and 3-dimensional mixed layer depth,
171 surface freshwater and heat fluxes, surface wind stress and sea surface height. The resolution of
172 the model setup is similar to the parent model from which it borrows the physical drivers. With
173 the given input of Geophysical Fluid Dynamics Laboratory (GFDL) reanalysis data, the zonal
174 and meridional resolutions are 1^{o} with 360 grid points longitudinally and 1^{o} at higher latitudes but
175 having a finer resolution of 0.8^{o} in the tropics, with 200 latitudinal grid points~~, respectively~~. The
176 model has 50 vertical levels with 10m increment in the upper 225m and stretched vertical levels
177 below 225m. The horizontal grids are formulated in spherical co-ordinates and vertical grids are
178 in z levels. The model employs a B-grid structure in which the velocities are resolved at corners
179 of the tracer grids. The model uses a centered-in-space and centered-in-time (CSCT) numerical
180 scheme along with an Asselin-Robert filter (Asselin, 1972) to control the ripples in CSCT.

The tracer concentration (C) evolves with time as

$$\frac{\partial C}{\partial t} + U.\nabla_H C + W\frac{\partial C}{\partial z} = \frac{\partial}{\partial z}K_z\frac{\partial}{\partial z}C + \nabla_H.(K_h\nabla_H C) + J + F \qquad (1)$$

where ∇_H is the horizontal gradient operator, U and W are the horizontal and vertical velocities respectively. K_z is the vertical mixing coefficient, and K_h is the two-dimensional diffusion tensor. J represents any sink or source due to the internal consumption or production of the tracer. F represents the emission or absorption of fluxes at the ocean surface. Here, the source and sink terms are provided through the biogeochemical model. Vertical mixing is resolved in the model using K- profile parameterization (KPP) (Large et al., 1994).

In addition to KPP, the model uses a background vertical diffusion reported by Bryan and Lewis (Bryan and Lewis, 1979). For horizontal mixing model incorporates Redi fluxes (Redi, 1982) and GM fluxes (Gent and Mcwilliams, 1990) which represent the eddy-induced variance in the mean tracer transport. A weak Laplacian diffusion is also included in the model for computational stability where sharp gradient in concentration occurs.

~~The biogeochemical model used in the study is based on the OCMIP – II protocol as stated above. The main motivation of OCMIP-II model design is to simulate the ocean carbon cycle with a restoration approach to ocean biology using appropriate biogeochemical parameterizations. The major advantage of the OCMIP – II protocol is (i) it reproduces the first order carbon cycle and the associated elemental cycles in the ocean reasonably well and (ii) it is much easier to implement and computationally efficient than the explicit ecosystem models. The present version of the model has five prognostic variables coupled with the circulation field, viz., inorganic phosphate (PO_4^{3-}), dissolved organic phosphorous (DOP), oxygen (O_2), dissolved inorganic carbon (DIC) and alkalinity (ALK). In order to retrieve the accurate spatial and~~

~~temporal distribution of CO_2 flux and pCO_2, the model uses a "nutrient restoring" approach (Najjar et al., 1992; Anderson and Sarmiento, 1995) for biological production. The basic currency for biological production in the model is phosphate because of the availability of a more extensive database and to eliminate the complexities associated with nitrogen fixation and denitrification. The biogeochemical dynamics implemented in the model and the calculations of solubility and biological pump are provided in Appendix A~~

~~The air – sea CO_2 flux in the model is estimated by,~~

~~$F = K_w \Delta pCO_2$ (2)~~

~~where K_w is gas transfer velocity and ΔpCO_2 is the difference in partial pressure of carbon dioxide between the ocean and atmosphere. The design and validation of the physical model is reported by Valsala et al., (2008, 2010) and biogeochemical design by Najjar and Orr (1998).~~

2.2.Biogeochemical model

The biogeochemical model used in the study is based on the OCMIP – II protocol as stated above. The main motivation of OCMIP–II protocol is to employ a minimalistic approach to simulate the ocean carbon cycle with a nutrient restoration approach to calculate the oceanic biological production (Najjar et al., 1992; Anderson and Sarmiento, 1995). The present version of the model has four prognostic variables coupled with the circulation field, viz., inorganic phosphate (PO_4^{3-}), dissolved organic phosphorus (DOP), dissolved inorganic carbon (DIC) and alkalinity (ALK). The basic currency for the biological model is phosphorous because of the availability of a more extensive phosphate database and to eliminate the complexities associated with nitrogen fixation and denitrification.

The production of organic phosphorus in the model using the nutrient restoring approach is given by

$$J_{prod} = \frac{1}{\tau}([PO_4] - [PO_4]^*) \quad (2)$$

$$[PO_4] > [PO_4]^* \; ; Z < Zc$$

$$J_{prod} = 0 \quad (3)$$

$$[PO_4] \leq [PO_4]^* ; Z > Zc$$

Where $[PO_4]^*$ is the observed phosphate concentration and τ=30 days is the restoration time scale (Najjar et. al., 1992).

The vertically integrated new production (g C m^{-2} yr^{-1}) in the model is defined as

$$New\ production = \int_{zc}^{0} -J_{prod}\ dz \quad (4)$$

The export production (g C m^{-2} yr^{-1}) in the model is calculated as given below

$$Export\ production = (1 - \sigma) \int_{0}^{zc} J_{prod}\ dz \quad (5)$$

Air-sea CO_2 flux in the model is estimated by,

$$F = K_w\ \Delta\ pCO_2 \quad (6)$$

where K_w is gas transfer velocity and $\Delta\ pCO_2$ is the difference in partial pressure of carbon dioxide between the ocean and atmosphere.

pCO_2 is calculated in the model by using DIC and ALK and is given by,

$$pCO_2 = \frac{[DIC]}{K_0}\frac{[H^+]^2}{[H^+]^2 + K_1[H^+] + K_1K_2} \quad (7)$$

Where $[H^+]$ is calculated using Newton-Raphson iterative method (Press et. al., 1996, Najjar and Orr, 1998). K_0 is the solubility constant of CO_2 and K_1, K_2 are the dissociation constant for carbonic acid respectively (Sarmiento and Gruber, 2006, Weiss, 1974, Mehrbach et al., 1973, Dickson and Millero, 1987, Najjar and Orr, 1998).

Details of all parameters in the biogeochemical model and calculations of solubility and biological pump are provided in Appendix-A. The design and validation of the physical model is reported by Valsala et al., (2008, 2010) and biogeochemical model by Najjar and Orr (1998).

2.3. Data

~~The present setup of the model uses ocean reanalysis products based on MOM-4 (Modular Ocean Model) developed by GFDL (Chang et al., 2012). Monthly data from 1961 to 2010 were utilized in the present study.~~ For validating the results observational datasets of CO_2 flux and pCO_2 were taken from Takahashi et al., (2009). Satellite-derived Net Primary Production (NPP) data were taken from Sea-viewing Wide Field of view sensor (SeaWiFS) Chl-a product, calculated using Vertically Generalized Production Model (VGPM) (Behrenfeld and Falkowski, 1997). The NPP data is approximated to export production (EP) by multiplying with an e-ratio (e = 0.37) representative for Indian Ocean upwelling zones (Sarmiento and Gruber, 2006, et al., 2000; Falkowski et al., 2003). The initial condition for PO_4 ~~and O_2 were~~ is taken from World Ocean Atlas (Garcia et al., 2014). Initial conditions for DIC and ALK were taken from the Global Ocean Data Analysis Project (GLODAP; Key et al., 2004) dataset. The

dissolved Organic Phosphorous (DOP) is initialized with a constant value of 0.02 μmol kg^{-1} (Najjar and Orr, 1998). The data sources and citations are provided in the Acknowledgement.

2.4. Methods

A spin-up for 50 years from the given initial conditions is performed with the climatological physical drivers. Because the initial conditions were provided from a mean state observed climatology this duration of spin-up is sufficient to reach statistical equilibrium in the upper 1000 m (Le Quere et al., 2000). Atmospheric pCO_2 has been set to a value from the 1950s in the spin-up run for calculating the air-sea CO_2 exchange. A seasonal cycle of atmospheric pCO_2 has been prescribed as in Keeling et. al., 1995.

After the spin-up, an interannual simulation for 50 years from 1961 to 2010 has been carried out with the corresponding observed atmospheric pCO_2 described in Keeling et al., (1995). The first five years of the interannual run were looped five times through the physical fields of 1961 repeatedly for a smooth merging of the spin-up restart to the interannual physical variables. Since the study is focused only on bias corrections to the seasonal cycle with a variable Zc, a model climatology for carbon cycle has been constructed from 1990 to 2010, which ~~This~~ includes the anthropogenic increase of oceanic DIC in the climatological calculation and is comparable with the Takahashi et al. (2009) observations.

Additional two sensitivity experiments have been performed separately by providing annual mean currents or temperatures as drivers over selected regions of the basin for segregating the role of varying Zc ~~compensation depth (varZc)~~ in improving the seasonality of carbon cycle and biological production. The aim of conducting these sensitivity experiments is

to understand how much a varZc parameterization is successful in capturing the upwelling episodes eventhough the seasonal cycle in physics is removed. The model driven with annual mean currents suppress the effect of upwelling by muting the Ekman divergence over the region of interest. On the other hand, the model forced with annual mean temperatures suppresses the cooling effect of upwelling. This will highlight the effect of new parameterization in simulating seasonality of carbon cycle and biological production. A smoothing technique with linear interpolation ($u = u(1-x) + \bar{u}x$) is applied to the offline-data in order to blend the annual mean fields ($\bar{u}$) provided to the selected region with the rest of the domain (u) to reduce the sudden transition at the boundaries. Here x represents an index which varies between 0 and 1 within a distance of 10^0 from the boundaries of the region of interest to the rest of the model domain.

2.5. Community compensation depth (Zc) parameterization

The OCMIP – II protocol separates the production and consumption zones by a depth termed as community compensation depth (Zc); the depth at which phytoplankton photosynthesis is large enough to balance the community respiration (i.e., both the autotrophic and heterotrophic respirations). At the Zc, the Net Community Production (NCP) is zero i.e., NCP = NPP - R_h = 0, where NPP is Net Primary Production (i.e. NPP = GPP – R_a), GPP is gross primary production, and R_h and Ra are the heterotrophic and autotrophic respirations, respectively (Smetacek and Passow, 1990; Najjar and Orr, 1998; Gattuso et al., 2006; Regaudix-de-Gioux and Duarte, 2010; Marra et al., 2014). The light intensity at Zc ~~compensation depth~~ is compensation irradiance (E_{com}), the irradiance at which the gross community primary production balances respiratory

carbon losses for the entire community (Gattuso et al., 2006; Regaudix-de-Gioux and Duarte, 2010). We define a spatially and temporally varying compensation depth (hereinafter varZc) as a depth where compensation irradiance (attenuated by surface Chl-a, Jerlov et al., 1976) reaches a minimum value of 10 W m^{-2}. In this way the varZc has both spatio-temporal variability of light as well as Chl-a. The Chl-a is given as monthly climatology as constructed from the satellite data. Observations show that the primary production reduces rapidly to 20% or less of the surface value below a threshold of 10 W m^{-2} (Parsons et al., 1984; Ryther, 1956; Sarmiento and Gruber, 2006). Moreover higher ocean temperature (those in the tropics) enhances the respiration rates resulting in high compensation irradiance (Parsons et al., 1984; Ryther, 1956; Lopez-Urrutia et al., 2006; Regaudix-de-Gioux and Duarte, 2010). A study by Regaudix-de-Gioux and Duarte (2010) reported the mean value of compensation irradiance of Arabian Sea as 0.4 ± 0.2 mol photon m^{-2} day^{-1} which is close to 10 W m^{-2} day^{-1}.

Figure 2 compares the scatter of average relative photosynthesis within varZc as a function of solar radiation for the Indian Ocean. This encapsulate the corresponding curve from the observations for the major phytoplankton species in the ocean such as diatoms, green algae and dinoflagellates (Ryther et al., 1956; Parsons et al., 1984; Sarmiento and Gruber, 2006). The model permits 100% production of organic phosphorus ~~relative photosynthesis~~ for radiation above 50 W m^{-2}. However the availability of phosphate concentration in the model act as an additional limiter for production which indirectly represents the photoinhibition at higher irradiance, for example oligotrophic gyres.

3. **Results and Discussions**

The inclusion of seasonality in Zc by way of parameterizing varZc leads to a remarkable spatio-temporal variability in Zc ~~compensation depth~~ (Figure 3). ~~The~~ Zc ~~compensation depth~~ over the Arabian Sea varies from 10 m to 25 m during December to February (DJF) and deepens ~~up~~ down to 45 m during March to May (MAM) in par with incoming solar radiation. During the monsoon season i.e., June to September (JJAS), ~~the~~ Zc ~~compensation depth~~ again shoals to 10 m-35 m due to the attenuation of solar radiation by the increased biological production (Chl-a). During October to November (OCT-NOV) ~~the~~ Zc slightly deepens as compared to JJAS.

The Bay of Bengal Zc ~~compensation depth~~ deepens from 35 m to 40 m during DJF and further deepens to 50 m during MAM when the solar radiation is maximum and biological production is minimum (Prasannakumar et al., 2002). Further reduction of Zc ~~compensation depth~~ can be seen through JJAS as a result of reduction in solar radiation during monsoon cloud cover. The Zc during OCT-NOV is 35 m on average. ~~However, caution is needed since the Bay of Bengal is dominated by freshwater forcing from rivers and precipitation and temperature inversions occur routinely (Howden and Murtugudde, 2001; Vinayachandran et al., 2013). The impact of these factors on Zc compensation depth variability is not clear and is not addressed here.~~

The equatorial Indian Ocean can be seen as a belt of 40 m - 45 m Zc ~~compensation depths~~ throughout the season except for JJAS. During JJAS, a shallow Zc ~~compensation depth~~ is seen near the coastal Arabian Sea (around 10 m to 35 m) presumably due to the coastal Chl-a blooms. Deep Zc ~~compensation depth~~ off the coast of Sumatra (~ 40 m to 50 m) is found during JJAS. Java-Sumatra coastal upwelling is centered on September to November (Susanto et al., 2001) and upwelling originates at around 100 m deep (Valsala and Maksyutov, 2010; Xing et al., 2012).

Southward of 10°S in the oligotrophic gyre region, the Zc ~~compensation depth~~ varies from 40 m to more than 60 m throughout the year. A conspicuous feature observed while parameterizing the solar radiation and Chl-a dependent Zc is that its maximum value never crosses 75 m especially in the Indian Ocean which is the value specified in OCMIP-II models. The cutoff depth of 75 m in OCMIP-II is obtained from observing the seasonal variance in the oxygen data (Najjar and Keeling, 1997) as an indicator of production zone. However, our results show that parameterizing a production zone based on ~~optimum~~ solar radiation and Chl-a ~~(Parsons et al., 1984)~~ predicts a production zone and its variability that is largely less than 75 m. The relevance of varZc ~~consequence of this~~ in the seasonality of the modeled carbon cycle is illustrated as follows.

3.1. Simulated seasonal cycle of pCO_2 and CO_2 fluxes

The annual mean biases in simulated CO_2 fluxes and pCO_2 were evaluated by comparing with Takahashi et al., (2009) observations (Figure 4). The model biases are significantly reduced with the implementation of varZc compared to that of the constant Zc (hereinafter constZc). A notable reduction in pCO_2 bias (by ~ 10µatm) is observed along the WAS (Figure 4d).

In order to address the role of the new biological parameterization of a variable Zc ~~compensation depth~~, we extended our study by choosing four key regions where the biological production and CO_2 fluxes are prominent in the Indian Ocean with additional sensitivity experiments (see Introduction and references therein). The boxes we considered are, (1) Western Arabian Sea (WAS; 40°E:65°E, 5°S:25°N) (2) Sri Lanka Dome (SLD; 81°E:90°E, 0°:10°N) (3) Seychelles-Chagos Thermocline Ridge (SCTR; 50°E:80°E, 5°S:10°S) and (4) Sumatra Coast

(SC; 90°E:110°E, 0°:10°S; Figure 1). The seasonal variations of Zc over these selected key regions are shown in Figure 5. A detailed analysis of CO_2 fluxes, pCO_2, biological export and new production and the impact of varZc simulations in improving the strength of biological pump and solubility pump for these key regions are presented below.

3.2. Western Arabian Sea (WAS)

The WAS Zc has a double peak pattern over the annual cycle. Over the February-March period Zc deepens ~~up~~ down to a maximum of 43.85 ± 2.3 m into March and then shoals to 25.75 ± 1.5 m (Figure 5) during the monsoon period (uncertainty represents the interannual standard deviations of monthly data from 1990-2010). This shoaling of Zc ~~compensation depth~~ during the monsoon indicates the potential ability of the present biological parameterization to capture the wind-driven upwelling related production in the WAS. During the post monsoon period, the second deepening of Zc ~~compensation depth~~ occurs during November with a maximum depth of 34.91 ± 2.2 m. The ability to represent the seasonality of biological production zone renders a unique improvement in CO_2 flux variability especially in the WAS in comparison to the OCMIP-II experiments (Orr et al, 2003; Figure 6a).

OCMIP –II simulations with a constZc of 75 m underestimate the CO_2 flux when compared to the observations of Takahashi et al. (2009). This underestimation is clearly visible during monsoon period. Our simulations with varZc result in a better seasonality of CO_2 flux when compared with Takahashi et al. (2009) observations (Figure 6a). The improvement due to varZc scheme is able to represent the seasonality of CO_2 flux better especially during the monsoon

period, when wind driven upwelling is dominant. Obviously the relative role of the biological and solubility pumps have to be deciphered in this context.

The CO_2 flux during July from observations, constZc and varZc simulations are 3.09 mol m^{-2} yr^{-1}, 1.82 ± 0.4 mol m^{-2} yr^{-1} and 3.10 ± 0.5 mol m^{-2} yr^{-1}, respectively. Southwesterly wind-driven upwelling over the WAS especially off the Somali coast (Smith and Codispoti, 1980; Schott, 1983; Smith, 1984) and Oman (Bruce, 1974; Smith and Bottero, 1977; Swallow, 1984; Bauer et al., 1991), pulls nutrient-rich subsurface waters closer to the surface while the available turbulent energy due to the strong winds leads to mixed layer entrainment of the nutrients resulting in a strong surface phytoplankton bloom (Krey and Babenerd, 1976; Banse, 1987; Bauer, 1991; Brock et al, 1991). This regional bloom extends over 700 km offshore from the Omani coast due to upward Ekman pumping driven by strong, positive wind-stress curl to the northwest of the low level jet axis and the offshore advection (Bauer et al., 1991; Brock et al., 1991; Brock and McClain, 1992a, b; Murtugudde and Busalacchi, 1999, Valsala, 2009) resulting in strong outgassing of CO_2 flux and an enhanced pCO_2 in the WAS (Valsala and Maksyutov, 2013; Sarma et al., 2002). The seasonal mean CO_2 flux during the southwest monsoon period (JJAS) for constZc and varZc simulations are 1.44 ± 0.2 mol m^{-2} yr^{-1} and 2.31 ± 0.4 mol m^{-2} yr^{-1}, respectively. The biological parameterization of varZc ~~varying compensation depth~~ considerably improves the average CO_2 flux during the monsoon period by 0.86 ± 0.1 mol m^{-2} yr^{-1}. The annual mean CO_2 flux from observations, constZc and varZc simulations are 0.94 mol m^{-2} yr^{-1}, 0.80 ± 0.17 mol m^{-2} yr^{-1} and 1.07 ± 0.2 mol m^{-2} yr^{-1}, respectively. The annual mean CO_2 flux improved by 0.27 ± 0.05 mol m^{-2} yr^{-1}.

Seasonality in pCO_2 also shows a remarkable improvement during the southwest monsoon period (Figure 6b). The pCO_2 with constZc is considerably lower at a value of 385.22 ± 3.5 µatm

during June compared to observational values of 392.83 µatm. However, varZc simulation perform better in terms of pCO_2 variability. The peak value of pCO_2 reaches up to 405.42 ± 5.8 µatm. The seasonal mean pCO_2 during the Southwest monsoon period from observations, constZc and varZc simulations are 397.58 µatm, 389.18 ± 3.6 µatm and 399.95 ± 5.0 µatm, respectively. The improvement in pCO_2 by varZc simulation is 10.76 ± 1.3 µatm when compared with the constZc simulation. This inherently says that constZc simulation fails to capture the pCO_2 driven by upwelling during the Southwest monsoon while varZc simulation is demonstrably better in representing this seasonal increase. The annual mean pCO_2 from observations, constZc and varZc simulations are 394.69 µatm, 389.62 ± 3.9 µatm and 391.19 ± 4.7 µatm, respectively. However it is worth mentioning that there are parts of the year where the constZc performs better compared to varZc. For instance during MAM as well as in November, the constZc simulation yielded a better comparison with the observed pCO_2 whereas varZc simulation yield a reduced magnitude of pCO_2. This may well indicate the biological vs. solubility pump controls on pCO_2 during the intermonsoons. The role of mesoscale variability in the ocean dynamics may also play a role (Valsala and Murtugudde, 2015). Nevertheless during the most important season (JJAS) when the pCO_2, CO_2 fluxes and biological production are found to be dominant in the Arabian Sea, the varZc produces a better simulation.

The improvements shown by the use of varZc ~~implementation of new biological parameterization~~ in the simulation of CO_2 flux and pCO_2 can be elicited by further analysis of the model biological production. Figure 7 shows the comparison of model export production and new production with observational export production from satellite-derived NPP for constZc and varZc simulations. The model export production in the constZc simulation is much weaker when compared to varZc simulation. The varZc simulation has ve improved the model export

436 production. Theoretically, the new and export productions in the model should be in balance with
437 each other (Eppley and Peterson, 1979). The constZc export production is much weaker than
438 new production and it is not in balance. In contrast the varZc simulation yields a nice balance
439 among them.

440 Comparing with the observational export production which peaks in August at a value of
441 154.78 g C m^{-2} yr^{-1}, the varZc simulated export and new productions peak at a value of 160.44 ±
442 20.4 g C m^{-2} yr^{-1} and 167.18 ± 24.0 g C m^{-2} yr^{-1}, respectively, but in July. A similar peak can be
443 observed in constZc simulated new production as well at a value of 178.19 ± 28.0 g C m^{-2} yr^{-1}.
444 This apparent shift of one month during JJAS in the model export production as well as in the
445 new production is noted as a caveat in the present set up which will need further investigation.
446 Arabian Sea production is not just limited by nutrients but also the dust inputs (Wiggert et al.,
447 2006). The dust induced primary production in the WAS, especially over the Oman coast is
448 noted during August (Liao et al., 2016). The mesoscale variability in the circulation and its
449 impact on production and carbon cycle are also a limiting factor in this model as noted above.

450 The seasonal mean export production during the Southwest monsoon period from satellite-
451 derived estimate is 123.57 g C m^{-2} yr^{-1}, whereas for constZc and varZc simulations it is 84.81 ±
452 16.0 g C m^{-2} yr^{-1} and 147.19 ± 23.8 g C m^{-2} yr^{-1}, respectively. The new biological
453 parameterization strengthens the model export production by 62.38 ± 7.8 g C m^{-2} yr^{-1} for the
454 Southwest monsoon period, which is over a 70% increase. This indicates a considerable impact
455 of the biological pump in the model simulated CO_2 flux and pCO_2 over the WAS. For constZc
456 simulation, the computed new production is slightly higher (150.84 ± 27.9 g C m^{-2} yr^{-1}) than that
457 of varZc (133.03 ± 19.5 g C m^{-2} yr^{-1}). The annual mean export production from observations,

constZc and varZc simulations are 94.31 g C m^{-2} yr^{-1}, 77.41 ± 15.1 g C m^{-2} yr^{-1} and 122.54 ± 25.2 g C m^{-2} yr^{-1}, respectively.

To understand how the varZc ~~varying compensation depth~~ parameterization strengthens the export production in the model, we analyzed the phosphate profiles. It appears that the varZc parameterization allows more phosphate concentration (Figure 8a, b) in the production zone and thereby increases the corresponding biological production (Figure 8c, d). The net export production in the model during JJAS is consistent with the satellite data (~~Figure 8d, see also~~ Figure 7b). However, in the constZc case the exports are rather 'flat' throughout the season with imperfect representation of seasonal biological export. The Table 1-4 summarize~~s~~ all the values discussed here.

The impact of varZc in the biological and solubility pumps is computed as per Louanchi et al., (1996, see Appendix A). The varZc parameterization has strengthened ~~s~~ the biological as well as the solubility pump in the model and thereby modifying the phosphate profiles and achieves a seasonal balance in export versus new production (Figure 9a). During the monsoon period the varZc simulation increase the strength of the solubility and biological pumps by 10.43 ± 1.3 g C m^{-2} yr^{-1} and 106.52 ± 9 g C m^{-2} yr^{-1}, respectively (see Table 5 and 6). Similarly, the annual mean strength of solubility pump and biological pump is increased by 3.29 ± 0.6 g C m^{-2} yr^{-1} and 81.18 ± 9.92 g C m^{-2} yr^{-1}, respectively. This supports the fact that the varZc parameterization basically modifies the biological and solubility pumps in the model simulation and thereby improved the seasonal cycle of CO_2 flux and pCO_2.

3.3 Sri Lanka Dome (SLD)

480 The seasonal variation in the Zc ~~compensation depth~~ for the SLD has a similar pattern as that
481 of the WAS. The Zc ~~compensation depth~~ deepens to its maximum during March up to 45.23 ±
482 0.3 m and reaches its minimum during the following monsoon period at 30.79 ± 1.5 m (Figure
483 5). The similarities of varZc between WAS and SLD indicate that they both are under similar
484 cycles of solar influx and biological production. The SLD chl-a dominates only up to July
485 (Vinayachandran et al., 2004) which explains why production with varZc increases earlier
486 compared to the WAS which occurs during August-October.

487 The seasonality in CO_2 flux and pCO_2 were compared with Takahashi et al., (2009)
488 observations (Figure 10). The varZc results in a slight improvement in CO_2 flux when compared
489 with constZc (Figure 10a). However, both constZc and varZc simulations underestimate the
490 magnitude of CO_2 flux when compared with observations. The seasonal mean CO_2 flux during
491 the monsoon period is 1.79 mol m^{-2} yr^{-1} from observations, which means SLD region is a source
492 of CO_2. But the mean values of constZc and varZc simulations yield flux values of -0.008 ± 0.2
493 mol m^{-2} yr^{-1} and 0.24 ± 0.2 mol m^{-2} yr^{-1}, respectively. The constZc simulation misrepresent the
494 SLD region as a sink of CO_2 during monsoon period which is opposite to that of observations.
495 The varZc simulations correct this misrepresentation to a source albeit at a smaller magnitude by
496 0.24 ± 0.09 mol m^{-2} yr^{-1} for the monsoon period. Compared to observations, the varZc case
497 underestimates the magnitude of JJAS mean by 1.55 mol m^{-2} yr^{-1}.

498 The annual mean CO_2 fluxes for constZc and varZc simulations are -0.02 ± 0.1 mol m^{-2} yr^{-1}
499 and 0.10 ± 0.2 mol m^{-2} yr^{-1}, respectively. The varZc parameterization leads to an improvement of
500 0.13 ± 0.1 mol m^{-2} yr^{-1} in the annual mean CO_2 flux when compared with constZc simulation.
501 The observational annual mean of CO_2 flux is 0.80 mol m^{-2} yr^{-1} which is highly underestimated
502 by both simulations. This indicates a regulation of biological production of the region by varZc

503 which makes this region a source of CO_2 during monsoon. The role of the solubility pump may
504 also be underestimated due to the biases in the physical drivers and the lack of mesoscale eddy
505 activities in these simulations (Prasanna Kumar et al., 2002; Valsala and Murtugudde, 2015).

506 The seasonality of pCO_2 (Figure 10b) especially in the monsoon period has significantly
507 improved. The mean pCO_2 during the monsoon season from observation over the SLD region is
508 382.44 µatm. The seasonal mean pCO_2 during monsoon period for constZc and varZc
509 simulations are 371.67 ± 6.04 µatm and 379.24 ± 8.9 µatm, respectively. The annual mean pCO_2
510 from observations, constZc and varZc simulations are 380.21 µatm, 370.76 ± 6.1 µatm and
511 374.94 ± 9.6 µatm, respectively. varZc simulations improve the JJAS mean pCO_2 by 7.56 ± 2.8
512 µatm and the annual mean pCO_2 by 4.18 ± 3.5 µatm, which is reflected in CO_2 flux as well. This
513 is likely due to the impact of new biological parameterization in capturing the episodic upwelling
514 in the SLD region which is further investigated by looking at its biological production.

515 The SLD biological production is highly exaggerated by the model for both constZc and
516 varZc simulations (Figure 11a, b). The seasonal mean biological export for the monsoon period
517 is 51.54 g C m^{-2} yr^{-1} as per satellite-derived estimates. However, the constZc and varZc
518 simulations overestimate it at 167.71 ± 59.04 g C m^{-2} yr^{-1} and 151.51 ± 46.4 g C m^{-2} yr^{-1},
519 respectively. This exaggerated export is visible in climatological annual means where for
520 constZc and varZc simulations they are 144.43 ± 49.8 g C m^{-2} yr^{-1} and 156.08 ± 43.8 g C m^{-2} yr^{-1},
521 respectively.

522 For constZc simulation, new production is overestimated from March to October when
523 compared to observations and the second peak is observed in November (Figure 11a). But the
524 overestimate in new production with varZc is observed only during JJAS period by a value of

525 26.23 g C m^{-2} yr^{-1}. For the SLD region the varZc parameterization overestimates the export
526 production but minimizes the excess new production, especially in the monsoon period by 64.15
527 ± 36.4 g C m^{-2} yr^{-1}. This indicates that the varZc parameterization is somewhat successful in
528 capturing the upwelling episode during monsoon over SLD. All values are summarized in Table
529 1-4.

530 The solubility and biological pumps are modified by the varZc parameterization significantly
531 when compared with the constZc simulation (Figure 9b). Over the monsoon period the strength
532 of the solubility and biological pumps are improved by 2.81 ± 1.1 g C m^{-2} yr^{-1} and 66.68 ± 9.7 g
533 C m^{-2} yr^{-1}, respectively. Similarly the annual mean strength of solubility and biological pump are
534 increased by 0.99 ± 1.2 g C m^{-2} yr^{-1} and 52.5 ± 5.1 g C m^{-2} yr^{-1} respectively. All values are
535 provided in Table 5 and 6.

536

537 **3.4 Sumatra Coast (SC)**

538 The seasonal variation in the Zc ~~compensation depth~~ over the SC region lies between 40 m
539 and 46 m (Figure 5). The seasonal maximum occurs during January to March, especially in
540 March with a depth of 45.5 m. During the monsoon period the Zc ~~compensation depth~~ shoals
541 slightly with a minimum of 41.1 m in July. The variation in Zc is relatively small as compared to
542 the other regions which is consistent with its relatively low production throughout the year.

543 The seasonality of CO_2 flux and pCO_2 captured by constZc and varZc simulations are shown
544 in Figure 12a, b. The varZc simulations overestimate both CO_2 flux and pCO_2, especially during
545 the monsoon. It is found that the constZc simulation is better compared to varZc simulation. The
546 varZc simulation overestimate the seasonal mean CO_2 flux and pCO_2 by 1.19 mol m^{-2} yr^{-1} and

29.61 µatm, respectively, compared to observations (Table 1). However, constZc produces a better estimate compared with observations for CO_2 flux and pCO_2. The constZc simulation deliver a better annual mean than varZc (Table 1, 2). The annual mean bias in constZc and varZc simulations for CO_2 flux is -0.0033 mol m^{-2} yr^{-1} and 0.31 mol m^{-2} yr^{-1}, respectively. Similarly, pCO_2 bias is 1.95 µatm and 9.07 µatm for constZc and varZc simulations.

Biological production simulated by the model along SC explains the overestimation of CO_2 flux and pCO_2 (Figure 13). Both constZc and varZc simulations greatly overestimate export production in the model. But a small enhancement in the new production during JJAS in constZc case is an indicator of upwelling episodes. The seasonal mean new production during the monsoon from constZc and varZc are 63.64 ± 30.9 g C m^{-2} yr^{-1} and 78.11 ± 29.1 g C m^{-2} yr^{-1}, respectively (Table 4). The seasonal mean export production during the monsoon from observations is 58.87 g C m^{-2} yr^{-1} (Table 3). The constZc simulation represent a better new production, which is seen as a relatively small exaggeration of CO_2 flux and pCO_2. The biological response off SC is found to be better with constZc which is in contradiction to a general improvement found with varZc in the other regions examined here. Such discrepancies over the SC could be due to the effect of Indonesian Throughflow (Bates et al., 2006) which is not completely resolved in the model due to coarse spatial resolution (also see Valsala et al., 2010).

The overestimation of export production by varZc simulation is also evident by the increase in strength of the biological and solubility pumps, respectively (Figure 9c). The annual mean and JJAS mean DIC increases in the production zone due to the biological pump is 67.21 ± 1.3 g C m^{-2} yr^{-1} and 83.62 ± 0.5 g C m^{-2} yr^{-1}, respectively. Similarly the increase in DIC due to the effect

of solubility pump during the JJAS period and annual mean are 10.95 ± 5.2 g C m^{-2} yr^{-1} and 3.87 ± 2.2 g C m^{-2} yr^{-1} respectively (see table 5 and 6).

3.5 Seychelles-Chagos Thermocline Ridge (SCTR)

The SCTR is a unique open-ocean upwelling region with a prominent variability in air-sea interactions (Xie et al., 2002). Wind-driven mixing and upwelling of subsurface nutrient rich water play a major role in biological production of this region (Dilmahamod et al., 2016). The seasonal cycle in Zc ~~compensation depth~~ is shown in Figure 5. The maximum Zc ~~compensation depth~~ occurs in November at about 44.94 m and the minimum at 33.2 m in July. The shoaling of Zc ~~compensation depth~~ during the monsoon period shows that the biological parameterization captures the upwelling response over this region.

The seasonality of CO_2 flux and pCO_2 are shown in Figure 14. The Takahashi observations of CO_2 flux shows a peak in June with outgassing of CO_2 during the upwelling episodes. However, both constZc and varZc simulations underestimate this variability. The seasonality of CO_2 flux in varZc shows a significant improvement when compared to constZc simulation, but underestimated when compared to observations. The seasonal mean CO_2 flux during the monsoon from observations, constZc and varZc simulations are 0.82 mol m^{-2} yr^{-1}, -0.32 ± 0.3 mol m^{-2} yr^{-1} and -0.05 ± 0.4 mol m^{-2} yr^{-1}, respectively. This represents a reduction in the seasonal mean sink of CO_2 flux in the SCTR region during the monsoon by 0.27 ± 0.1 mol m^{-2} yr^{-1} bringing it closer to a source region (see Table 1 for details).

The improved CO_2 flux is also supported by the seasonal cycle in pCO_2 . Based on observations, seasonal mean of pCO_2 with constZc during JJAS is underestimated by 11.47

591 µatm, varZc simulation underestimate it by 6.45 µatm. So it is evident that varZc simulation
592 capture the upwelling episodes better, marked by a larger pCO_2 during JJAS period. However,
593 the magnitude of pCO_2 is still underestimated compared to observations (Table 2).

594 Figure 15 shows the biological production of constZc and varZc simulations for SCTR. It is
595 clear that both simulations overestimate the export production and underestimate the new
596 production. The JJAS mean export production from observations, constZc and varZc are 51.08 g
597 C m^{-2} yr^{-1}, 57.39 ± 14.2 g C m^{-2} yr^{-1} and 99.23 ± 29.8 g C m^{-2} yr^{-1}, respectively. The varZc
598 simulations exaggerate the model export production by 48.14 g C m^{-2} yr^{-1}. The varZc simulation
599 improve the JJAS mean new production by 1.14 ± 2.2 g C m^{-2} yr^{-1} (Table 4). The DIC variations
600 due to the biological pump over the monsoon period and the annual mean also support the
601 exaggerated export production. During the monsoon period, the varZc simulation strengthen the
602 biological and solubilitiy pump by 72.64 ± 6.2 g C m^{-2} yr^{-1} and -4.56 ± 1.6 g C m^{-2} yr^{-1},
603 respectively when compared to the constZc simulation (Figure 9d). This is also reflected in the
604 annual mean DIC variations due to the biological and solubility pump effects (see table 5 and 6).
605 This slight improvement in the model new production, especially during the monsoon period
606 signals that the varZc ~~spatially and temporally varying compensation depth~~ better captures the
607 upwelling over SCTR. Considering the annual mean values of model export and new production,
608 constZc simulation are reasonably faithful to observations.

609 The underestimation of CO_2 and pCO_2 as well as the exaggeration of model export
610 production and a slight overestimate in model new production may be due to two reasons. (1)
611 SCTR is a strongly coupled region with remote forcing of the mixed layer – thermocline
612 interactions (Zhou et al., 2008) which can affect the seasonality in biological production that the
613 model may not be resolving reasonably, (2) the bias associated with physical drivers, especially

wind stress may underestimate the CO_2 flux as well biological production. A similar overestimation of biological production was also reported in a coupled biophysical model (Dilmahamod et al., 2016).

Table 1 – 4 shows the entire summary of seasonal and annual mean CO_2 flux, pCO_2 and biological production reported in Section 3.

4. Sensitivity Simulations

From the analysis of four major upwelling regions over Indian Ocean, it is evident that the biological parameterization of varZc ~~spatio-temporally varying compensation depth~~ better captures upwelling episodes and thus it enhances the model export production. This is most clearly visible over the WAS. In order to quantify how much the varZc parameterization contributes to the seasonality of carbon cycle, two additional sensitivity simulations were carried out; (1) with annual mean offline currents and (2) annual mean offline temperatures with the goal of suppressing the dynamical and thermodynamical effects of seasonal upwelling over the WAS (see Section 2 for details). The focus on this region is motivated by its prominence as the most productive zone of the Indian Ocean. Moreover, the improvement in the biological processes in the model by the varZc parameterization is best captured in this region. The results are discussed below.

4.1 Impact of varZc parameterization on seasonality of carbon cycle with annual mean currents.

635 To quantify the impact of varZc parameterization, the model is forced with annual mean
636 currents only over the WAS with unaltered currents in the rest of the ocean. The hypothesis is
637 that the muting of the seasonal variability of Ekman divergence removes the upwelling and the
638 biological pump contribution to production and carbon cycle. The comparison of constZc and
639 varZc then allows us to decipher the impact of varZc on capturing the impacts of upwelling on
640 biological production and the carbon cycle. The smooth blending of currents at the boundary of
641 the WAS domain is achieved by a linear smoothing function as given in Section 2.

642 The model biological responses (inferred by comparing with the control run) in terms of the
643 CO_2 flux shows a flat pattern over the monsoon period for constZc simulation (Figure 16a).
644 While the varZc simulation forced with the annual mean currents shows an enhanced CO_2 flux
645 indicating the outgassing of CO_2 flux in the WAS due to wind-driven upwelling (Figure 16b).
646 This qualitatively shows that the varZc ~~spatially and temporally varying compensation depth~~
647 itself has improved the seasonality in the biological processes (export and new production) and
648 captured the upwelling episodes during the monsoon. The varZc parameterization is responsible
649 for an improvement of 0.48 ± 0.04 mol m^{-2} yr^{-1} and 0.13 ± 0.02 mol m^{-2} yr^{-1} in the JJAS seasonal
650 and annual mean CO_2 fluxes, respectively. This improves the overall model CO_2 flux in the
651 control run especially in July (Figure 16b).

652 Similar improvements are also noticed in pCO_2 (Figure 17). In the constZc simulation
653 with annual mean currents, the pCO_2 dips down during JJAS monsoon period which indicates
654 the inadequacy of constZc in capturing the upwelling enriched pCO_2 difference (Figure 17a, b).
655 The varZc simulation slightly modifies the pCO_2 in the 'right' direction during JJAS despite the
656 annual mean currents.

The export and new productions in the model explain the modification of CO_2 flux and pCO_2 by varZc parameterization. The biological export production is highly underestimated in the constZc simulation forced with annual mean currents while the varZc simulation captures the seasonal upswing in production (Figure 18). The improved JJAS mean and annual mean export production by 43.51 ± 8.6 g C m^{-2} yr^{-1} and 30.28 ± 13.7 g C m^{-2} yr^{-1}, respectively is a clear indication of the positive impacts of a varZc. Similarly the improvement in JJAS mean and annual mean new production (Figure 19) from varZc simulated with annual mean currents are 17.39 ± 0.8 g C m^{-2} yr^{-1} and 14.81 ± 0.1 g C m^{-2} yr^{-1}, respectively. In short the varZc biological parameterization improves the export and new productions in the model. This helps the model to capture the upwelling episodes over the study regions. Table 7 summarizes all the results of biological sensitivity runs.

4.2 Impact of varZc parameterization on seasonality of carbon cyle with annual mean temperatures.

Using the annual mean temperature over the WAS, we are suppressing the cooling effect of temperature due to upwelling and quantifying how much the model seasonality is improved due to varZc parameterization. (see Section 2 for details). The varZc simulations forced with annual mean SST has larger JJAS mean and annual mean CO_2 fluxes by 0.88 ± 0.1 mol m^{-2} yr^{-1} and 0.28 ± 0.07 mol m^{-2} yr^{-1}, respectively (Figure 20 and Table 8). For a given annual mean SST the solubility pump largely controls the CO_2 emission during JJAS if a varZc is prescribed, likely by the enrichment of DIC (inferred from Figure 8b). Similarly the improvement in pCO_2 (Figure 21) with varZc simulation is also remarkable. The JJAS mean and annual mean improvements from

679 the implementation of varZc are 11.05 ± 1.9 µatm and 1.91 ± 1.4 µatm, respectively. The
680 detailed quantification of CO_2 and pCO_2 responses for this experimental setup is given in Table
681 8. The above analysis adds supporting evidence that the varZc simulation strengthen the
682 seasonality of the model compared to the constZc case. This is presumably accomplished by the
683 more accurate Zc ~~compensation depth~~ and production zone implied with a variable Zc.

684

685 **5. Summary and Conclusions**

686 A spatially and temporally varying Zc ~~compensation depth~~ parameterization as a function of
687 solar radiation and Chl-a is implemented in the biological pump model of OCMIP-II for a
688 detailed analysis of biological fluxes in the upwelling zones of the Indian Ocean. The varZc
689 parameterization improves the seasonality of model CO_2 flux and pCO_2 variability, especially
690 during the monsoon period. A significant improvement is observed in WAS where the monsoon
691 wind-driven upwelling dominates biological production. The magnitude of CO_2 flux matches
692 with observations, especially in July when monsoon winds are at their peak. Monsoon triggers
693 upwelling in SLD as well which acts as a source of CO_2 to the atmosphere. The seasonal and
694 annual mean are underestimated with constZc and the SLD is reduced to a sink of CO_2 flux. The
695 varZc simulation modify the seasonal and annual means of CO_2 flux of SLD and depict it as a
696 source of CO_2 especially during the monsoon, but the magnitude is still underestimated
697 compared to Takahashi et al. (2009) observations. The SCTR variability is underestimated by
698 both constZc and varZc simulations, portraying it as a CO_2 sink region whereas observations
699 over the monsoon period indicate that the thermocline ridge driven by the open ocean wind-

700 stress curl is in fact an oceanic source of CO_2. However, the varZc simulation reduces the
701 magnitude of the sink in this region bringing it relatively closer to observations.

702 VarZc biological parameterization strengthens the export and new productions in the model,
703 which allows it to represent a better seasonal cycle of CO_2 flux and pCO_2 over the study regions.
704 The WAS export production is remarkably improved by 62.37 ± 7.8 g C m^{-2} yr^{-1} compared to
705 constZc. This supports our conclusion that the varZc parameterization increases the strength of
706 biological export in the model. Over the SLD, the JJAS seasonal mean export and new
707 productions are underestimated in varZc compared to constZc simulations, but the annual mean
708 export production is improved. Export production at SC and SCTR are highly exaggerated and
709 there is hardly any improvement in new production with a variable Zc especially over the
710 monsoon period. The inability of varZc parameterization to improve the seasonality of SC and
711 SCTR may be due to the interannnual variability of biological production associated with the
712 Indonesian throughflow and remote forcing of the mixed layer-thermocline interactions and the
713 effect of biases in the windstress data used as a physical driver in the model.

714 Sensitivity experiments carried out by prescribing annual mean currents or temperatures over
715 selected subdomains reveal that the varZc retains the seasonality of carbon fluxes, pCO_2, and
716 export and new productions closer to observations. This strongly supports our contention that
717 varZc parameterization improves export and new productions and it is also efficient in capturing
718 upwelling episodes of the study regions. This points out the significant role of having a close
719 balance in seasonal biological export and new production in models to capture the seasonality in
720 carbon cycle. This also confirms the role of biological and solubility pumps in producing the
721 seasonality of carbon cycle in the upwelling zones.

However the underestimation of seasonality of CO_2 flux over the SLD and overestimation over the SC as well as the SCTR are a cautionary flag for the study. This uncertainty poses an important scientific question as to whether the model biology over the SC and SCTR region is not resolving the seasonality in CO_2 flux and pCO_2 properly or whether the seasonality in the Zc ~~compensation depth~~ is not able to fully capture the biological processes.

To address these questions we have used an inverse modeling approach (Bayesian inversion) in order to optimize the spatially and temporally varying Zc ~~compensation depth~~ using surface pCO_2 as the observational constraint and computed the optimized biological production. The results will be reported elsewhere.

Appendix – A

The time evolution equations of the model variables are given by

$$\frac{d[PO_4]}{dt} = L([PO_4]) + J_b PO_4 \qquad (A1)$$

$$\frac{d[DOP]}{dt} = L([DOP]) + J_b DOP \qquad (A2)$$

$$\frac{dDIC}{dt} = L([DIC]) + J_b DIC + J_g DIC + J_v DIC \qquad (A3)$$

$$\frac{d[ALK]}{dt} = L([ALK]) + J_b ALK + J_v ALK \qquad (A4)$$

Where L is the 3D transport operator, which represents the effects of advection, diffusion, and convection. [ ] or square brackets indicate the concentrations in mol m^{-3}. $J_b PO_4$, $J_b DOP$, $J_b DIC$, $J_b ALK$ is the biological source/sink terms and $J_v DIC$, $J_v ALK$ are the virtual source-sink terms representing the changes in surface DIC and ALK, respectively, due to evaporation and precipitation. $J_v DIC$ is the source-sink term due to air-sea exchange of CO_2.

The following equations represent for the biological processes in the model

For Z <Zc,

$$J_{prod} = \frac{1}{\tau}([PO_4] - [PO_4^*]), \qquad [PO_4] > [PO_4^*] \qquad (A5)$$

$$J_{DOP} = \sigma J_{prod} - \kappa[DOP] \qquad (A6)$$

$$J_{PO4} = -J_{prod} + \kappa[DOP] \qquad (A7)$$

$$J_{ca} = Rr_{C:P}(1-\sigma)J_{prod} \qquad (A8)$$

$$J_{DIC} = r_{C:P} J_{PO4} + J_{ca} \quad \text{(A9)}$$

$$J_{ALK} = -r_{N:P} J_{PO4} + 2J_{ca} \quad \text{(A10)}$$

For Z >Zc,

$$J_{prod} = 0, \qquad [PO_4] \leq [PO_4^*] \quad \text{(A11)}$$

$$J_{DOP} = -\kappa[DOP] \quad \text{(A12)}$$

$$J_{PO4} = -\frac{\partial F}{\partial Z} + \kappa[DOP] \quad \text{(A13)}$$

$$F_c = (1-\sigma)\int_0^{Zc} J_{prod}\, dZ \quad \text{(A14)}$$

$$F(Z) = F_c\left(\frac{Z}{Zc}\right)^{-a} \quad \text{(A15)}$$

$$J_{ca} = -\frac{\partial F_{Ca}}{\partial Z} \quad \text{(A16)}$$

$$F_{Ca} = R r_{C:P} F_C e^{-(Z-Zc)/d} \quad \text{(A17)}$$

Where Z is the depth and Zc is the compensation depth in the model. J_{DOP} *and* J_{PO4} are the biogeochemical sources and sinks and J_{prod} , J_{Ca} represents the biogeochemical flows with respect to production and calcification. Within Zc, the production of organic phosphorous in the model J_{prod} is calculated using equation A5. $[PO_4]$ is the model phosphate concentration and $[PO_4^*]$ is observational phosphate. τ is the restoration timescale assumed to be 30 days. Whenever the model phosphate exceeds the observational phosphate, it allows production, below which the production is zero. The observational phosphate data were taken from the World Ocean Atlas (WOA; Garcia et al., 2014). It is assumed that a fixed fraction (σJ_{prod}) of phosphate uptake is

converted into Dissolved Organic Phosphorus (DOP) which is a source for J_{DOP} (equation A6). The phosphate not converted to DOP results in an instantaneous downward flux of particulate organic phosphorus at Zc (equation A14). The decrease of flux with depth due to remineralization is shown by a power law relationship as in equation A15. The values of the constants a, κ, σ are 0.9, 0.2/year to 0.7/year, 0.67, respectively. The rate of production is used to explain the formation of calcium carbonate cycle in surface waters (equation A8) and its export is given by equation A16, where R is the rain ratio, a constant molar ratio of exported particulate organic carbon to the exported calcium carbonate flux at Zc. The exponential decrease of calcium carbonate flux with scale depth d is given by equation A17. The biological source or sink of dissolved inorganic carbon (DIC) and alkalinity (ALK) is explained through equations A9 and A10, respectively. Where the values of rain ratio (R) is taken as 0.07 and the Redfield ratio, $r_{C:P} = 117$, and $r_{N:P} = 16$ and scale depth d is chosen as 3500m.

Biological and Solubility Pump calculations

The biological effect on DIC is calculated from Louanchi et al., (1996). The tendency of DIC due to biomass production and calcite formation in the production zone is expressed as below.

$$\left(\frac{\partial DIC}{\partial t}\right)_b = \left(\frac{\partial PO_4}{\partial t}\right)_b \times R_{C:P} - J_{Ca} \qquad \text{(A18)}$$

The total tendency of DIC in the production zone is:

$$\left(\frac{\partial DIC}{\partial t}\right)_{total} = \left(\frac{\partial DIC}{\partial t}\right)_b + \int_x \int_y \mathrm{F} dx\, dy \qquad \text{(A19)}$$

where $\left(\frac{\partial DIC}{\partial t}\right)_b$ is the evolution of DIC due to the impact of biology (i.e., biological pump). The first term in the R.H.S of Equation A18 is the rate of change of phosphate resulting from photosynthesis and respiration in the model (i.e., J_{po4} in this case) multiplied by the carbon to phosphorous Redfield ratio ($R_{C:P}$ = 117:1) and J_{Ca} represents the calcite formation in the model (see Equation A8 & A16). The solubility pump is calculated as the surface integral of the flux F (Louanchi et al., 1996).

Appendix B

In order to compare our model production of organic phosphorous to the curve of Ryther et al., (1956) we have merely scaled our total production to "relative photosynthesis", which is, according to Ryther et al., (1956) is an index between 0 and 1 indicating the strength of production estimated as $P_l/P_{max.}$ Here P_l is the photosynthesis at each intensity (of light) of different species and P_{max} is the maximum photosynthesis observed in the same control experiment. The curve between relative photosynthesis and light intensity shows the relation between photosynthetic activity and light in marine phytoplankton. Since our method relates biological production to a function of light (limitation) by Chl-a attenuation, it is the best curve to cross-compare our results. In this case we scaled our total biological production within Zc into relative values between 0-1 by $P_l/P_{max.}$ in which P_l is taken as the individual grid cell biological component of organic phosphorus production and P_{max} is the maximum production available in the domain at any given instant. All the grid points are quite similar to the curve of Ryther et al., (1956) as shown in Figure 2.

Acknowledgement

Thanks to two anonymous reviewers and the editor (Marilaure Grégoire) for comments. Sreeush M. G. sincerely acknowledges the fellowship support from Indian Institute of Tropical Meteorology (IITM) to carry out the study. The OCMIP-II routines were taken from (http://ocmip5.ipsl.jussieu.fr/OCMIP/). GFDL data for OTTM is taken from (http://data1.gfdl.noaa.gov/nomads/forms/assimilation.html). Takahashi data is taken from (http://www.ldeo.columbia.edu/res/pi/CO2/) and SeaWiFS data is obtained from the National Aeronautics and Space Administration (NASA) Ocean Color Website (http://oceancolor.gsfc.nasa.gov/). The computations were carried out in High-Performance Computing (HPC) facility of Ministry of Earth Sciences (MoES), IITM.

832 **References**

833 Anderson, L. A., Sarminento, J. L.: Global ocean phosphate and oxygen simulations, Global
834 Biogeochem. Cycles, 9, 621-636, doi:10.1029/95GB01902, 1995.

835 Asselin, R.: Frequency filter for time integrations, Mon. Wea. Rev., 100, 487–490, doi:
836 10.1175/1520-0493, 1972.

837 Banse, K., McClain, C. R.: Winter blooms of phytoplankton in the Arabian Sea as observed by
838 the Coastal Zone Color Scanner, Mar. Ecol. Prog. Ser, 34, 201 – 211, 1986.

839 Banse, K.: Seasonality of phytoplankton chlorophyll in the central and northern Arabian Sea,
840 Deep Sea Res., 34, 713 – 723, doi:10.1016/0198-0149, 1987.

841 Barber, R. T., Marra. J., Bidigare. R. C., Codispoti. L. A., Halpern. D., Johnson. Z., Latasa. M.,
842 Goericke. R., and Smith. S. L.: Primary productivity and its regulation in the Arabian Sea during
843 1995, Deep. Sea. Res. pt. II, 48, 1127 – 1172. doi:10.1016/S0967-0645, 2001.

844 Bates, N. R., Pequignet. A. C., and Sabine. C. L.: Ocean carbon cycling in the Indian Ocean: 2.
845 Estimates of net community production, Global Biogeochem. Cycles., 20, GB3021,
846 doi:10.1029/2005GB002492, 2006.

847 Bauer, S., Hitchcock, G. L., Olson, D. B.: Influence of monsoonally-forced Ekman dynamics
848 upon surface-layer depth and plankton biomass distribution in the Arabian Sea, Deep Sea Res.,
849 38, 531 – 553, doi:10.1016/0198-0149, 1991.

850 Behrenfeld, M. J., Falkowski. P. G.: Photosynthetic rates derived from satellite-based
851 chlorophyll concentration, Limnol. Oceanogr., 42, 1 – 20, doi: 10.4319/lo.1997.42.1.0001, 1997.

852 Boyd, P. W., Rynearson, T. A., Armstrong, E. A., Fu. F., Hayashi. K. and co-authors.: Marine
853 Phytoplankton Temperature versus growth responses from polar to tropical waters – outcome of
854 a scientific community-wide study, PLoS ONE 8(5)., e63091,
855 Doi:10.1371/journal.phone.0063091, 2013.

856 Brock, J C., McClain, C. R.: Interannual variability of the southwest monsoon phytoplankton
857 bloom in the north-western Arabian Sea, J. geophys. Res., 97(C1), 733 – 750,
858 doi/10.1029/91JC02225, 1992.

859 Brock, J. C., McClain, C. R., Hay, W. W.: A southwest monsoon hydrographic climatology for
860 the northwestern Arabian Sea, J. geophys. Res., 97(C6), 9455 – 9465, doi: 10.1029/92JC00813,
861 1992.

862 Brock, J. C., McClain, C. R., Luther, M. E., Hay, W. W.: The phytoplankton bloom in the
863 northwestern Arabian Sea during the southwest monsoon of 1979, J. geophys. Res., 96(C11),
864 623 – 642, doi: 10.1029/91JC01711, 1991.

865 Brock. J., Sathyendranath. S., and Platt. T.: Modelling the seasonality of subsurface light and
866 primary production in the Arabian Sea, Mar. Eco. Prog. Ser., 101, 209 – 221, 1993.

867 Bruce, J. G.: Some details of upwelling off the Somali and Arabian coasts, J. mar. Res., 32, 419
868 – 423, 1974.

869 Bryan. K., Lewis, L. J.: A water mass model of the world ocean, J. Geophys. Res., 84, 2503 –
870 2517, doi: 10.1029/JC084iC05p02503, 1979.

871 Chang, Y. S., Zhang. S., Rosati. A., Delworth. T., Stern. W. F.: An assessment of oceanic
872 variability for 1960-2010 from the GFDL ensemble coupled data assimilation, Clim. Dyn., 40,
873 775 – 803, doi: 10.1007/s00382-012-1412-2, 2012.

874 Christian J. R., Verschall M. A., Murtugudde R., Busalacchi A. J., McClain C. R.:
875 Biogeochemical modelling of the tropical Pacific Ocean. II: Iron biogeochemistry, Deep Sea
876 Res., 49, 545 – 565, doi:10.1016/S0967-0645, 2001.

877 Colwell, R. R.: Global climate and infectious disease: the cholera paradigm, Science., 274(5295),
878 2025 – 2031, doi: 10.1126/science.274.5295.2025, 1996.

879 Dickson, A. G., and F. J. Millero.: A comparison of the equilibrium constants for the dissociation
880 of carbonic acid in seawater media, Deep-Sea Res., 34, 1733 – 1743, 1987.

881 Dilmahamod A. F., Hermes. J. C., Reason C. J. C.: Chlorophyll-a variability in the Seychelles-
882 Chagos Thermocline Ridge: Analysis of a coupled biophysical model, J. of. Mar. Sys., 154, 220
883 – 232, doi:10.1016/j.jmarsys.2015.10.011, 2016.

884 Doney S. C., and co-authors.: Evaluating global ocean carbon models: The importance of
885 realistic physics, Glob. Biogeochem. Cycles, 18, doi:10.1029/2003GB002150, 2004.

886 Eppley, R. W., Peterson. B. J.: Particulate organic matter flux and planktonic new production in
887 the deep ocean, Nature, 282, 677-680, doi:10.1038/282677a0, 1979.

888 Eppley, R. W.: Temperature and phytoplankton growth in the sea, Fish. Bull., 70, 1063 – 1085,
889 1972.

890 Falkowski, P. G., E. A. Laws, R. T. Barber, and J. W. Murray.: phytoplankton and their role in
891 the primary, new and export production, In: Fasham M.J.R (eds) Ocean Biogeochemistry, Global

892 Change – The IGBP series (closed). Springer, Berlin, Heidelberg,
893 doi:https://doi.org/10.1007/978-3-642-55844-3_5, 2003.

894 Feely, R. A., Sabine, C. L., Takahashi, T., Wanninkhof, R.: Uptake and Storage of Carbon
895 Dioxide in the Ocean: The Global CO_2 Survey, Oceanography., 14(4), 18–32,
896 doi:10.5670/oceanog.2001.03, 2001.

897 Friedrichs, M. A. M., and co-authors.: Assessment of skill and portability in regional
898 biogeochemical models: role of multiple planktonic groups, J. GeoPhy. Res., 112, doi:
899 10.1029/2006JC003852, 2007.

900 Friedrichs, M. A. M., Hood, R. R., Wiggert, J. D.: Ecosystem complexity versus physical forcing
901 quantification of their relative impact with assimilated Arabian Sea data, Deep Sea Res., 53, 576-
902 600, doi:10.1016/j.dsr2.2006.01.026, 2006.

903 Garcia, H. E., R. A. Locarnini, T. P. Boyer, J. I. Antonov, O.K. Baranova, M.M. Zweng, J.R.
904 Reagan, D.R. Johnson.: World Ocean Atlas 2013, Volume 4: Dissolved Inorganic Nutrients
905 (phosphate, nitrate, silicate), S. Levitus, Ed., A. Mishonov Technical Ed.; NOAA Atlas NESDIS
906 76, 25 pp, 2014.

907 Gattuso, J. P., B. Gentili, C. M. Duarte, J. A. Kleypas, J. J. Middelburg, and D. Antoine.: Light
908 availability in the coastal ocean: Impact on the distribution of benthic photosynthetic organisms
909 and their contribution to primary production, Biogeosciences, 3, 489 – 513, doi:10.5194/bg-3-
910 489-2006, 2006.

911 Gent, P. R., McWilliams. J. C.: Isopycnal mixing in ocean circulation models, J. Phys.
912 Oceanogr., 20, 150 – 155, doi: 10.1175/15200485, 1990.

913 Harwell, C., Kim, K., Burkholder, J., Colwell, R., Epstein, P. R., Grimes, D., Hofmann, E. E.,
914 Lipp, E. K., Osterhaus, A., and Overshreet, R. M.: Emerging marine diseases-climate links and
915 anthropogenic factors, Science., 285(5433), 1505 – 1510, doi: 10.1126/science.285.5433.1505,
916 1999.

917 Howden, S., Murtugudde, R.: Effects of river inputs into the Bay of Bengal, J. Geophys. Res.,
918 106, 19,825-19,843. doi: 10.1029/2000JC000656, 2001.

919 Jerlov N. G.: Marine optics, Second ed., Elsevier, pp 231, 1976.

920 Jung, E., and Kirtman. B. P.: ENSO modulation of tropical Indian ocean subseasonal variability,
921 Geophy. Res. Lett., 43, doi: 10.1002/2016GL071899, 2016.

922 Keeling, C. D., Whorf, T. P., Wahlen, M., and van der plicht, J.: Interannual extremes in the rate
923 of rise of atmospheric carbon dioxide since 1980, Nature, 375, 666 – 670, 1995.

924 Key, R. M., et al,.: A global ocean carbon climatology: Results from Global Data Analysis
925 Project (GLODAP), Global Biogeochem. Cycles, 18, GB4031, doi:10.1029/2004GB002247,
926 2004

927 Krey, J., Bahenerd, B.: Phytoplankton production atlas of the international Indian Ocean
928 expedition, Institut fur Meereskundeander Universitat Kiel, Kiel, German, 1976.

929 Laws, E. A., P. G. Falkowski, W.O. Smith, Jr., H. Ducklow and J. J. McCarthy: Temperature
930 effects on export production in the open ocean, Global Biogeochem. Cycles, 14, 1231 – 1246.

931 Large, W. G., McWilliams, J. C., Doney, S. C.: Oceanic vertical mixing: A review and a model
932 with a nonlocal boundary layer parameterization, Rev. Geophys., 32, 363 – 403, doi:
933 10.1029/94RG01872, 1994.

934 Le Quere, C., Orr, J. C., Monfray, P., Aumont, O.: Interannual variability of the oceanic sink of
935 CO_2 from 1979 through 1997, Global Biogeochem. Cycles., 14, p1247 – 1265, doi:
936 10.1029/1999GB900049, 2000.

937 Lee, P. F., Chen, I. C., Tzeng. W. N.: Spatial and Temporal distributions patterns of bigeye tuna
938 (Thunnusobsesus) in the Indian Ocean, Zoological studies-Taipei-, 44(2), 260, 2005.

939 Lehodey .P., Senina I., Sibert. J., Bopp. L., Calmettes B., Hampton .J., Murtugudde. R.:
940 Preliminary forecasts of Pacific bigeye tuna population trends under the A2 IPCC scenario, Prog
941 in Oceanography., 86, 302 – 315, doi:10.1016/j.pocean.2010.04.021, 2010.

942 Liao, X., Zhan, H., Du, Y.: Potential new production in two upwelling regions of the Western
943 Arabian Sea: Estimation and comparison, J. Geophy. Res. Oceans., 121,
944 doi:10.1002/2016JC011707, 2016.

945 Lopez-Urrutia, A., E. San Martin, R. P. Harris, and X. Irigoien.: Scaling the metabolic balance of
946 the oceans, Proc. Natl. Acad. Sci. U.S.A., 103, 8739-8744,doi:10.1073/pnas.0601137103, 2006.

947 Louanchi. F., N. Metzl., and Alain Poisson.: Modelling the monthly sea surface f_{CO2} fields in the
948 Indian Ocean, Marine Chemistry, 55, 265 – 279, 1996.

949 Marra, J. F., Veronica P. Lance, Robert D. Vaillancourt, Bruce R. Hargreaves.: Resolving the
950 ocean's euphotic zone, Deep Sea. Res. pt. I., 83, 45 -50, doi:10.1016/j.dsr.2013.09.005, 2014.

951 Matsumoto K., Tokos. K. S., Price., A. R., Cox. S. J.: First description of the Minnesota Earth
952 System Model for Ocean biogeochemistry (MESMO 1.0), Geosci. Model Dev., 1, 1-15,
953 doi:10.5194/gmd-1-1-2008, 2008.

McCreary, J., Murtugude, R., Vialard, J., Vinayachandran, P., Wiggert, J. D., Hood, R. R., Shankar, D., Shetye, S.: Biophysical processes in the Indian Ocean, Indian Ocean Biogeochemical Processes and Ecological Variability., 9 – 32, doi: 10.1029/GM185, 2009.

Mehrbach, C., C. H. Culberson, J. E. Hawley, and R. M. Pytkowicz.: Measurement of the apparent dissociation constants of carbonic acid in seawater at atmospheric pressure, Limnol. Oceanogr., 18, 897 – 907, 1973.

Moisan, J. R., Moisan, A. T., Abbott, M. R.: Modelling the effect of temperature on the maximum growth rates of phytoplankton populations, Eco. Modelling., 153, 197-215, doi:10.1016/S0304-3800(02)00008, 2002.

Morel, A.: Optical modeling of the upper ocean in relation to its biogenous matter content (Case 1 Waters), J. Geophys. Res., 93, 10479-10, 768, doi: 10.1029/JC093iC09p10749, 1988.

Murtugudde R., McCreary J. P., Busalacchi, A. J.: Oceanic processes associated with anomalous events in the Indian Ocean with relevance to 1997-1998, J. Geophy. Res., 105, 3295-3306, doi: 10.1029/1999JC900294, 2000.

Murtugudde, R., Busalacchi, A. J.: Interannual variability of the dynamics and thermodynamics of the tropical Indian Ocean, J. Clim. 12, 2300-2326, doi:10.1175/1520-0442, 1999.

Murtugudde, R., Seager, R., Thoppil, P.: Arabian Sea response to monsoon variations, Paleoceanography., 22, PA4217, doi:10.1029/2007PA001467, 2007.

Najjar, R. G., Keeling, R. F.: Analysis of the mean annual cycle of the dissolved oxygen anomaly in the world ocean, J. Mar. Res., 55, 117 – 151, doi:10.1357/0022240973224481, 1997.

974 Najjar, R. G., Orr, J. C.: Design of OCMIP-2 simulations of chlorofluorocarbons, the solubility
975 pump and common biogeochemistry, http://www.ipsl.jussieu.fr/OCMIP/., 1998.

976 Najjar, R. G., Sarmiento, J. L., Toggweiler, J. R.: Downward transport and fate of organic matter
977 in the ocean: simulations with a general circulation model, Global biogeochem. Cycles., 6, 45-
978 76, doi/10.1029/91GB02718, 1992.

979 Naqvi, S. W. A., Moffett, J. W., Gauns, M. U., Narvekar, P. V., Pratihary, A. K., Naik, H.,
980 Shenoy, D. M., Jayakumar, D. A., Goepfert, T. J., Patra, P. K., Al-Azri, A., and Ahmed, S. I.:
981 The Arabian Sea as a high-nutrient, low-chlorophyll region during the late Southwest Monsoon,
982 Biogeosciences., 7, 2091-2100, doi:10.5194/bg-7-2091-2010, 2010.

983 Naqvi, S., Naik, H., Narvekar, P.: The Arabian Sea, in Biogeochemistry, edited by K. Black and
984 G. Shimmield, pp. 156 – 206, Blackwell, Oxford, 2003.

985 Orr, J. C., and co-authors.: Anthropogenic ocean acidification over the twenty-first century and
986 its impact on calcifying organisms, Nature, 437, 681 – 686, doi:10.1038/nature04095, 2005.

987 Orr, J. C. and co-authors.: Estimates of anthropogenic carbon uptake from four three-
988 dimensional global ocean models, Glob. Biogeochem. Cycles., 15, p43 – 60, doi:
989 10.1029/2000GB001273, 2001.

990 Orr, J. C., Aumont, O., Bopp, L., Calderia, K., Taylor, K., et. al.: Evaluation of seasonal air-sea
991 CO2 fluxes in the global carbon cycle models, International open Science conference (Paris, 7-
992 10 Jan. 2003), 2003.

993 Osawa, T., Julimantoro, S.: Study of fishery ground around Indonesia archipelago using remote
994 sensing data, International archives of the Photogrammetry, Remote sensing and spatial
995 information science., vol XXXVIII, part-8, 2010.

996 Parsons, T. R., Takahashi, M., Habgrave, B.: In Biological Oceanographic Processes, 3rd ed.,
997 330pp., Pergamon Press, New York, doi: 10.1002/iroh.19890740411, 1984.

998 Prasanna Kumar, .S., Muraleedharan, P. M., Prasad, T. G., Gauns, M., Ramaiah, N., de Souza, S.
999 N., Sardesai, S., Madhupratap, M.: Why is the Bay of Bengal less productive during summer
1000 monsoon compared to the Arabian Sea?, Geophys. Res. Lett., 29(24), 2235,
1001 doi:10.1029/2002GL016013, 2002.

1002 Prasanna Kumar, S., Roshin, P. R., Narvekar, J., Dinesh Kumar, P., Vivekanandan, E.: What
1003 drives the increased phytoplankton biomass in the Arabian Sea?, Current Science, 99(I), 101 –
1004 106, 2010.

1005 Prassana Kumar. S, Ramaiah. N, Gauns. M., Sarma V. V. S. S., Muraleedharan. P. M.,
1006 RaghuKumar. S., Dileep Kumar., Madhupratap. M.: Physical forcing of biological productivity
1007 in the Northern Arabian Sea during the Northeast Monsoon, Deep Sea Res. Pt. II., 48, 1115-
1008 1126, doi:10.1016/S0967-0645(00)00133-8, 2001.

1009 Praveen, V., Ajayamohan**,** R. S., Valsala**,** V., Sandeep, S.: Intensification of upwelling along
1010 Oman coast in a warming scenario, Geophys. Res. Lett., 43, doi:10.1002/2016GL069638, 2016.

1011 Qasim, S. Z.: Biological productivity of the Indian Ocean, J. mar. Sci., 6, 122 – 137, 1977.

1012 Qasim, S. Z.: Oceanography of Northern Arabian Sea, Deep Sea Res., 29(9A), 1041 – 1068,
1013 doi:10.1016/0198-0149(82)90027-9, 1982.

1014 Redi, M.: Oceanic isopycnal mixing by coordinate rotation, J. Phys. Oceanogr., 12, 1154 – 1158,
1015 doi: 10.1175/1520-0485, 1982.

1016 Regaudie-de-Gioux, A., and C. M. Duarte.: Compensation irradiance for planktonic community
1017 metabolism in the ocean, Global Biogeochem. Cycles, 24, GB4013,
1018 doi:10.1029/2009GB003639, 2010.

1019 Roxy, M. K., Modi, A., Murtugudde, R., Valsala, V., Panickal, S., Prasanna Kumar, S.,
1020 Ravichandran, M., Vichi, M., Levy, M.: A reduction in marine primary productivity driven by
1021 rapid warming over the tropical Indian Ocean, 43, 826 – 833, J. Geophy. Res. Letters.,
1022 doi:10.1002/2015GL066979, 2015.

1023 Ryther, J., Menzel, D.: On the production, composition, and distribution of organic matter in the
1024 Western Arabian Sea, Deep Sea Research and Oceanographic Abstracts., 12(2), 199 -209.
1025 doi:10.1016/0011-7471(65)90025-2, 1965.

1026 Ryther, J.: Photosynthesis in the ocean as function of light Intensity, Limnol. Oceanogr., vol 1,
1027 issue 1, doi: 10.4319/lo.1956.1.1.0061, 1956.

1028 Sarma V. V. S. S.: Net plankton community production in the Arabian Sea based on O_2 mass
1029 balance model, Glob. biogeochem. Cycles., 18, GB4001, doi:10.1029/2003GB002198, 2004.

1030 Sarma, V. V. S. S.: An evaluation of physical and biogeochemical processes regulating the
1031 perennial suboxic conditions in the water column of the Arabian Sea, Global Biogeochem.
1032 Cycles., 16, doi:10.1029/2001GB001461, 2002.

1033 Sarmiento, J. L., and Gruber, N.: Ocean Biogeochemical Dynamics, Princeton University Press,
1034 New Jersey, 2006.

1035 Sarmiento, J. L., Monfray. P., Maier-Reimer., Aumont, O., Murnane, R. J., Orr, J. C.: Sea-air
1036 CO_2 fluxes and carbon transport: A comparison of three ocean general circulation models,
1037 Global Biogeochem. Cycles., 14, p1267 – 1281. doi: 10.1029/1999GB900062, 2000.

1038 Schott, F.: Monsoon response of the Somali current and associated upwelling, Prog.Oceanogr.,
1039 12, 357 – 381, doi:10.1016/0079-6611(83)90014-9, 1983.

1040 Smetacek, V., and Passow, U.: Spring bloom initiation and Sverdrup's critical depth model,
1041 Limnol. Oceanogr., 35, 228 – 234, doi: 10.4319/lo.1990.35.1.0228, 1990.

1042 Smith, L. S.: Understanding the Arabian Sea: Reflections on the 1994-1996 Arabian Sea
1043 Expedition, Deep Sea Res. Pt. II., 48, 1385-1402, doi:10.1016/S0967-0645(00)00144-2, 2001.

1044 Smith, R. L., Bottero, L. S.: On upwelling in the Arabian Sea. In Angel, M (ed) A voyage of
1045 Discovery. Pergammon Press, New York, p. 291 – 304, 1977.

1046 Smith, S. L., Codistpoti, L. A.: Southwest monsoon of 1979: chemical and biological response of
1047 Somali coastal waters. Science, 209, 597 – 600. doi:10.1126/science.209.4456.597, 1980.

1048 Smith, S. L.: Biological indications of active upwelling in the northwestern Indian Ocean in 1964
1049 and 1979, a comparison with peru and northwest Africa, Deep Sea Res., 31, 951 – 967,
1050 doi:10.1016/0198-0149(84)90050-5, 1984.

1051 Susanto. R., Gordon, A. L., Zheng. Q.: Upwelling along the coasts of Java and Sumatra and its
1052 relation to ENSO, J. Geophy. Res. Lett., 28, 1599-1602, doi: 10.1029/2000GL011844, 2001.

1053 Swallow, J. C.: Some aspects of the physical oceanography of the Indian Ocean, Deep Sea Res.,
1054 31, 639 – 650, doi:10.1016/0198-0149(84)90032-3, 1984.

1055 Takahashi, T., Sutherland, S. C., Wanninkhof, R., Sweeney, C., Feely, R. A., Chipman, D. W.,
1056 Hales, B., Friederich, G., Chavez, F., Sabine, C., et al.: Climatological mean and decadal
1057 changes in surface ocean pCO_2 and net sea-air CO_2 flux over the global oceans. Deep Sea Res.,
1058 Pt. II., 56, 554 – 557, doi:10.1016/j.dsr2.2008.12.009, 2009.

1059 Valsala V., Maksyutov, S.: A short surface pathway of the subsurface Indonesian Throughflow
1060 water from the Java Coast associated with upwelling, Ekman Transport, and Subduction. Int. J.
1061 Oceanogr., 15, doi: 10.1155/2010/540743, 2010.

1062 Valsala V., Maksyutov, S.: Interannual variability of air-sea CO_2 flux in the north Indian Ocean,
1063 Ocean Dynamics., 1 – 14, doi 10.1007/s10236-012-0588-7, 2013.

1064 Valsala, K. V., Maksyutov, S., Ikeda, M.: Design and Validation of an offline oceanic tracer
1065 transport model for a carbon cycle study, J. clim., 21, doi: 10.1175/2007JCLI2018.1, 2008.

1066 Valsala, V.**,** Maksyutov, S., Murtugudde, R.: Interannual to Interdecadal Variabilities of the
1067 Indonesian Throughflow Source Water Pathways in the Pacific Ocean, J. Phys. Oceanogr., 41,
1068 1921–1940, doi: 10.1175/2011JPO4561.1, 2011.

1069 Valsala, V., Maksyutov, S.: Simulation and assimilation of global **oc**ean pCO_2 and air-sea CO_2
1070 fluxes using ship observations of surface ocean pCO_2 in a simplified biogeochemical model,
1071 Tellus., 62B, doi: 10.1111/j.1600-0889.2010.00495, 2010.

1072 Valsala, V**.,** Murtugudde, R.: Mesoscale and Intraseasonal Air-Sea CO_2 Exchanges in the
1073 Western Arabian Sea during Boreal Summer, Deep Sea Res. Pt. I, 103, 103-113,
1074 doi:10.1016/j.dsr.2015.06.001, 2015.

1075 Valsala, V., Roxy, M., Ashok, K., Murtugudde, R.: Spatio-temporal characteristics of seasonal to
1076 multidecadal variability of pCO_2 and air-sea CO_2 fluxes in the equatorial Pacific Ocean, J.
1077 Geophys. Res., 119, 8987 – 9012, doi:10.1002/2014JC010212, 2014.

1078 Valsala, V.: Different spreading of Somali and Arabian coastal upwelled waters in the northern
1079 Indian Ocean: A case study. J. Phy. Oceanogr., 803 – 816, doi: https://doi.org/10.1007/s10872-
1080 009-0067-z, 2009.

1081 Vialard,. J. P. and co-authors.: Air-Sea Interactions in the Seychelles-Chagos Thermocline Ridge
1082 Region, BAMS, doi:10.1175/2008BAMS2499.1, 2009.

1083 Vinayachandran P. N., Shankar D., S. Vernekar, K. K. Sandeep, P. Amol, C. P. Neema and A.
1084 Chatterjee.: A summer monsoon pump to keep the bay of Bengal salty, Geophys. Res. Lett., 40,
1085 1777 – 1782, doi:10.1002/grl.50274, 2013.

1086 Vinayachandran P. N., Yamagata, T.: Monsoon Response of the Sea around Sri Lanka:
1087 Generation of Thermal Domes and Anticyclonic Vortices, J. Phy. Oceano., 28, 1946 – 1960, doi:
1088 10.1175/1520-0485, 1998.

1089 Vinayachandran, P. N., Chauhan, P., Mohan, M., Nayak, S.: Biological response of the sea
1090 around Sri Lanka to summer monsoon, Geophys. Res. Lett., 31, L0I302,
1091 doi:10.1029/2003GL018533, 2004.

1092 Wang .X. J., Behrenfeld. M., Le Borgne .R., Murtugudde .R., and Boss. E.: Regulation of
1093 phytoplankton carbon to chlorophyll ratio by light, nutrients and temperature in the equatorial
1094 Pacific Ocean: a basin-scale model. Biogeosciences., 6, 391 – 404, doi:10.5194/bg-6-391-2009,
1095 2009.

Weiss, R. F.: Carbon dioxide in water and seawater: The solubility of a non-ideal gas, Mar. Chem., 2, 203-215, 1974.

Wiggert J. D., Jones. B. H., Dickey .T D., Brink .K. H., Weller .R .A., Marra. J., Codispoti. L. A.: The Northeast Monsoon's impact on mixing, phytoplankton biomass and nutrient cycling in the Arabian Sea, Deep Sea Res. Pt. II, 47, 1353-1385, doi:10.1016/S0967-0645(99)00147-2, 2000.

Wiggert, J. D., Hood, R. R., Banse, K., Kindle, J. C.: Monsoon-driven biogeochemical processes in the Arabian Sea, Progr. Oceanogr., 65, 176-213, doi:10.1016/j.pocean.2005.03.008, 2005.

Wiggert. J. D., Murtugudde, R. G., Christian J. R.: Annual ecosystem variability in the tropical Indian Ocean: results of a coupled bio-physical ocean general circulation model, Deep Sea Res. Pt. II., 53, 644-676, doi:10.1016/j.dsr2.2006.01.027, 2006.

Xie, S. P., Annamalai, H., Schott, F. A., McCreary Jr. J. P.: Structure and mechanism of south Indian ocean climate variability, J. clim., 15, 864 – 878, doi: 10.1175/1520-0442, 2002.

Xing W., Xiaomei. L., Haigang Z., Hailong. L.: Estimates of potential new production in the Java-Sumatra upwelling system, Chinese Journal of Oceanology and Limnology., 30, 1063-1067, doi:10.1007/s00343-012-1281, 2012.

Yamanaka, Y., Yoshie, N, MasahikoFujii, Maka .N. Aita and Kishi. M. J.: An Ecosystem coupled with Nitrogen-Silicon-Carbon cycles applied to station A7 in the Northwestern Pacific, J. of Oceanogr., 60, p227-241, doi: 10.1023/B:JOCE.0000038329.91976.7d, 2004.

1115 Zhou X., Weng. E., Luo., Y.: Modelling patterns of nonlinearity in the ecosystem responses to
1116 temperature, CO_2 and precipitation changes, Eco. Appli., 18, 453 – 466, doi: 10.1890/07-0626.1,
1117 2008.

1118

1119

Table: 1 WAS = Western Arabian Sea, SLD = Sri Lanka Dome, SC = Sumatra Coast, SCTR = Seychelles-Chagos Thermocline Ridge. JJAS mean and climatological annual mean of CO_2 flux from Takahashi observations, constZc and varZc simulations. Units are mol m^{-2} yr^{-1}.

Regions	CO_2 flux (mol m^{-2} yr^{-1})					
	JJAS Mean			Annual Mean		
	OBS	constZc	varZc	OBS	constZc	varZc
WAS	1.99	1.44 ± 0.2	2.31 ± 0.4	0.94	0.80 ± 0.1	1.07 ± 0.2
SLD	1.79	-0.008 ± 0.2	0.24 ± 0.09	0.80	-0.02 ± 0.1	0.10 ± 0.2
SC	0.31	0.60 ± 0.5	1.51 ± 1.01	0.21	0.21 ± 0.3	0.53 ± 0.5
SCTR	0.82	-0.32 ± 0.3	-0.05 ± 0.4	0.55	-0.02 ± 0.1	-0.07 ± 0.2

Table: 2 Same as Table 1, but for pCO_2. Units are µatm.

Regions	pCO_2 (µatm)					
	JJAS Mean			Annual Mean		
	OBS	constZc	varZc	OBS	constZc	varZc
WAS	397.58	389.18 ± 3.7	399.95 ± 5.01	394.69	389.62 ± 3.9	391.19 ± 4.7
SLD	382.44	371.67 ± 6.04	379.24 ± 8.9	380.21	370.76 ± 6.1	374.94 ± 9.6
SC	372.52	382.36 ± 12.7	402.14 ± 21.8	372.69	374.65 ± 9.3	381.76 ± 13.6
SCTR	377.18	365.71 ± 5.08	370.72 ± 7.4	379.89	372.69 ± 4.7	369.00 ± 5.4

Table: 3 JJAS mean and climatological annual mean of export production from satellite derived Net Primary Production data, constZc and varZc simulations. Units are g C m^{-2} yr^{-1}.

Regions	Export Production (g C m^{-2} yr^{-1})					
	JJAS Mean			Annual Mean		
	OBS	constZc	varZc	OBS	constZc	varZc
WAS	123.57	84.81 ± 16.04	147.19 ± 23.8	94.31	77.41 ± 15.1	122.54 ± 25.2
SLD	51.54	167.71 ± 59.04	151.51 ± 46.4	43.25	144.43 ± 49.8	156.08 ± 43.8
SC	58.87	260.11 ± 104.7	310.03 ± 99.5	54.53	172.52 ± 72.4	215.52 ± 70.8
SCTR	51.08	57.39 ± 14.2	99.23 ± 21.8	40.45	55.15 ± 17.9	80.35 ± 26.04

Table: 4 JJAS mean and climatological annual mean for New production derived from the model.

Regions	New Production (g C m^{-2} yr^{-1})					
	JJAS Mean			Annual Mean		
	OBS	constZc	varZc	OBS	constZc	varZc
WAS	--	150.84 ± 27.9	133.03 ± 19.5	--	108.43 ± 23.4	81.47 ± 15.7
SLD	--	141.93 ± 64.1	77.78 ± 27.6	--	111.05 ± 71.1	50.37 ± 26.3
SC	--	63.64 ± 30.9	78.11 ± 29.1	--	56.69 ± 43.3	54.58 ± 23.3
SCTR	--	12.17 ± 16.3	13.32 ± 18.6	--	13.74 ± 15.5	12.94 ± 13

Table 5: Biological pump impact over DIC in the model due to constZc and varZc simulations for JJAS and annual mean.

Biological Pump ($gC\ m^{-2}\ yr^{-1}$)	**constZc**		**varZc**	
	JJAS Mean	**Annual Mean**	**JJAS Mean**	**Annual Mean**
WAS	45.18 ± 14.8	45.49 ± 14.38	151.7 ± 23.8	126.67 ± 24.3
SLD	89.39 ± 58.1	108.65 ± 48.6	156.07 ± 48.4	161.15 ± 43.5
SC	235.54 ± 95.4	155.21 ± 67.4	319.16 ± 94.9	222.92 ± 68.7
SCTR	30.49 ± 13.4	26.81 ± 16.8	103.13 ± 19.6	83.98 ± 23.6

Table 6: Same as Table 5, But for Solubility pump.

Solubility Pump ($gC\ m^{-2}\ yr^{-1}$)	**constZc**		**varZc**	
	JJAS Mean	**Annual Mean**	**JJAS Mean**	**Annual Mean**
WAS	17.29 ± 3.5	9.63 ± 2.1	27.72 ± 4.8	12.92 ± 2.7
SLD	-0.09 ± 2.4	-0.32 ± 2.3	2.9 ± 3.5	1.31 ± 3.5
SC	7.22 ± 6.9	2.56 ± 3.8	18.17 ± 12.1	6.43 ± 6.0
SCTR	-3.95 ± 3.7	-0.35 ± 2.3	-0.61 ± 5.3	-0.86 ± 2.8

Table 7: JJAS mean and climatological annual mean response from the model forced with annual mean currents.

WAS region forced with Annual mean currents	JJAS mean		Improvement	Climatological annual mean		Improvement
	constZc	varZc		constZc	varZc	
CO_2 flux (mol m^{-2} yr^{-1})	0.80 ± 0.2	1.29 ± 0.2	0.48 ± 0.04	0.65 ± 0.1	0.79 ± 0.1	0.13 ± 0.02
pCO_2 (µatm)	381.81 ± 3.4	387.24 ± 3.9	5.43 ± 0.5	388.68 ± 3.4	388.40 ± 3.6	-0.28 ± 0.1
Export production (g C m^{-2} yr^{-1})	60.71 ± 4.7	104.22 ± 13.4	43.51 ± 8.6	74.30 ± 4.5	104.58 ± 18.3	30.28 ± 13.7
New Production (g C m^{-2} yr^{-1})	34.76 ± 2.3	52.16 ± 1.51	17.39 ± 0.8	29.91 ± 1.7	44.72 ± 1.6	14.81 ± 0.1

Table 8 Same as Table 7 but from annual mean temperature simulation.

WAS region forced with Annual mean temperature	JJAS mean		Improvement	Climatological annual mean		Improvement
	constZc	varZc		constZc	varZc	
CO_2 flux (mol m^{-2} yr^{-1})	1.85 ± 0.2	2.74 ± 0.4	0.88 ± 0.1	0.81 ± 0.1	1.10 ± 0.2	0.28 ± 0.07
pCO_2 (µatm)	393.20 ± 3.01	404.26 ± 4.9	11.05 ± 1.9	384.61 ± 3.3	386.52 ± 4.8	1.91 ± 1.4

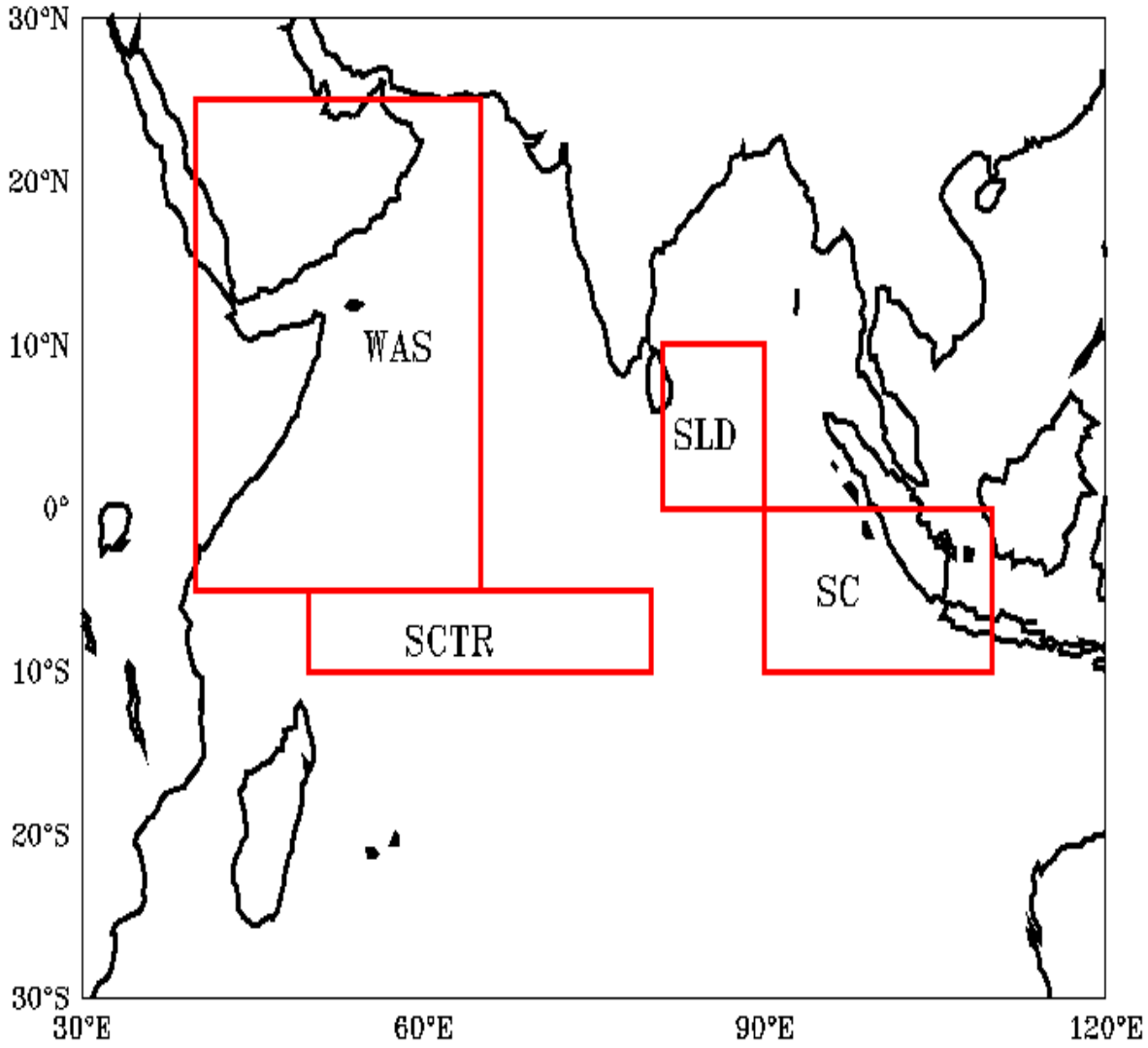

Figure 1: Red boxes shows the study regions (1) WAS (Western Arabian Sea, 40°E:65°E, 5°S:25°N) (2) SLD (Sri Lanka Dome, 81°E:90°E, 0°:10°N) (3) SCTR (Seychelles-Chagos Thermocline Ridge, 50°E:80°E, 5°S:10°S) and (4) SC (Sumatra Coast, 90°E:110°E, 0°:10°S).

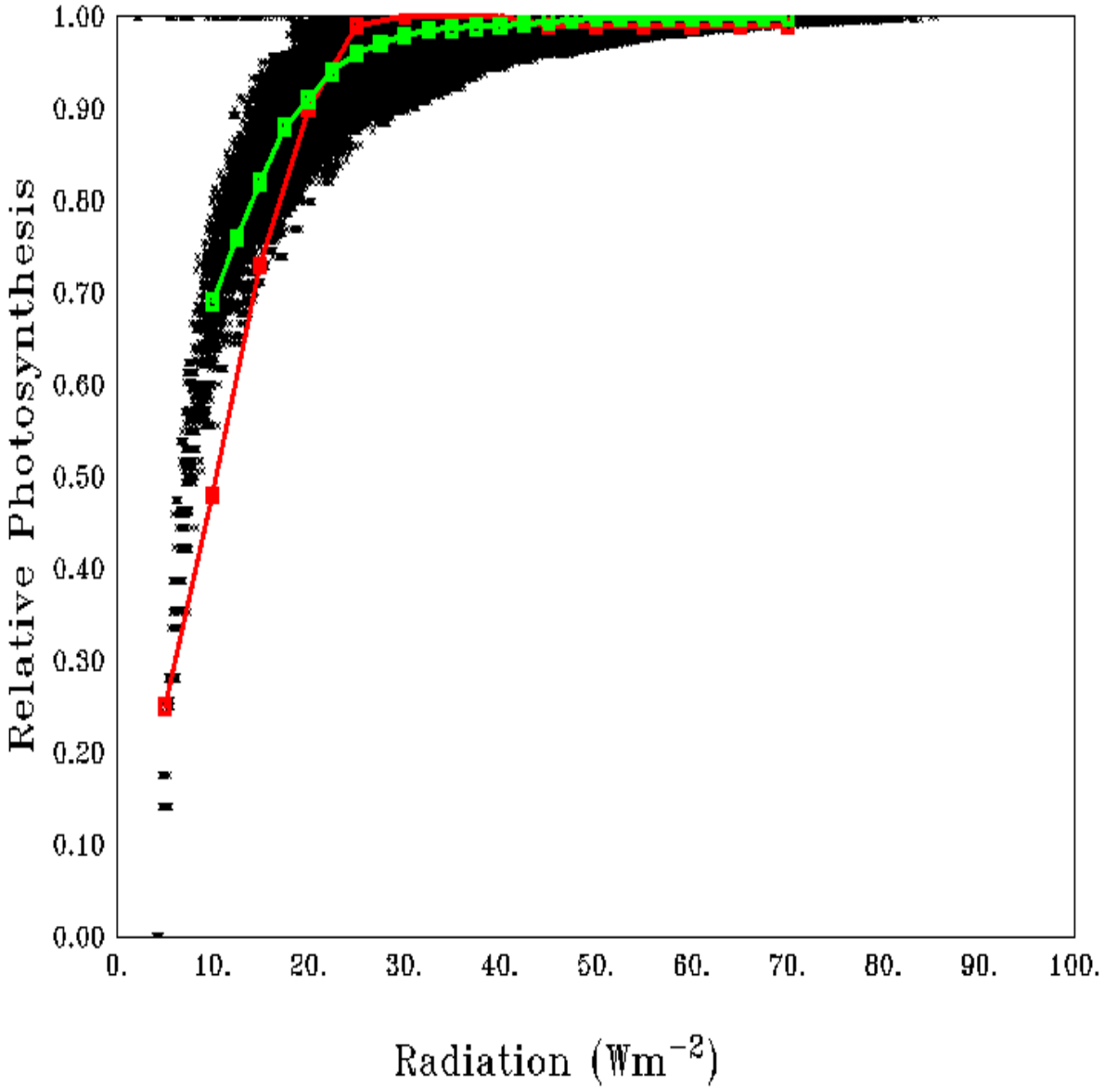

Figure 2: Scatter of average relative photosynthesis versus different light intensities in the model (black dots) and its mean (green curve). Red curve shows the theoretical P – I curve from Parsons et al., (1984).

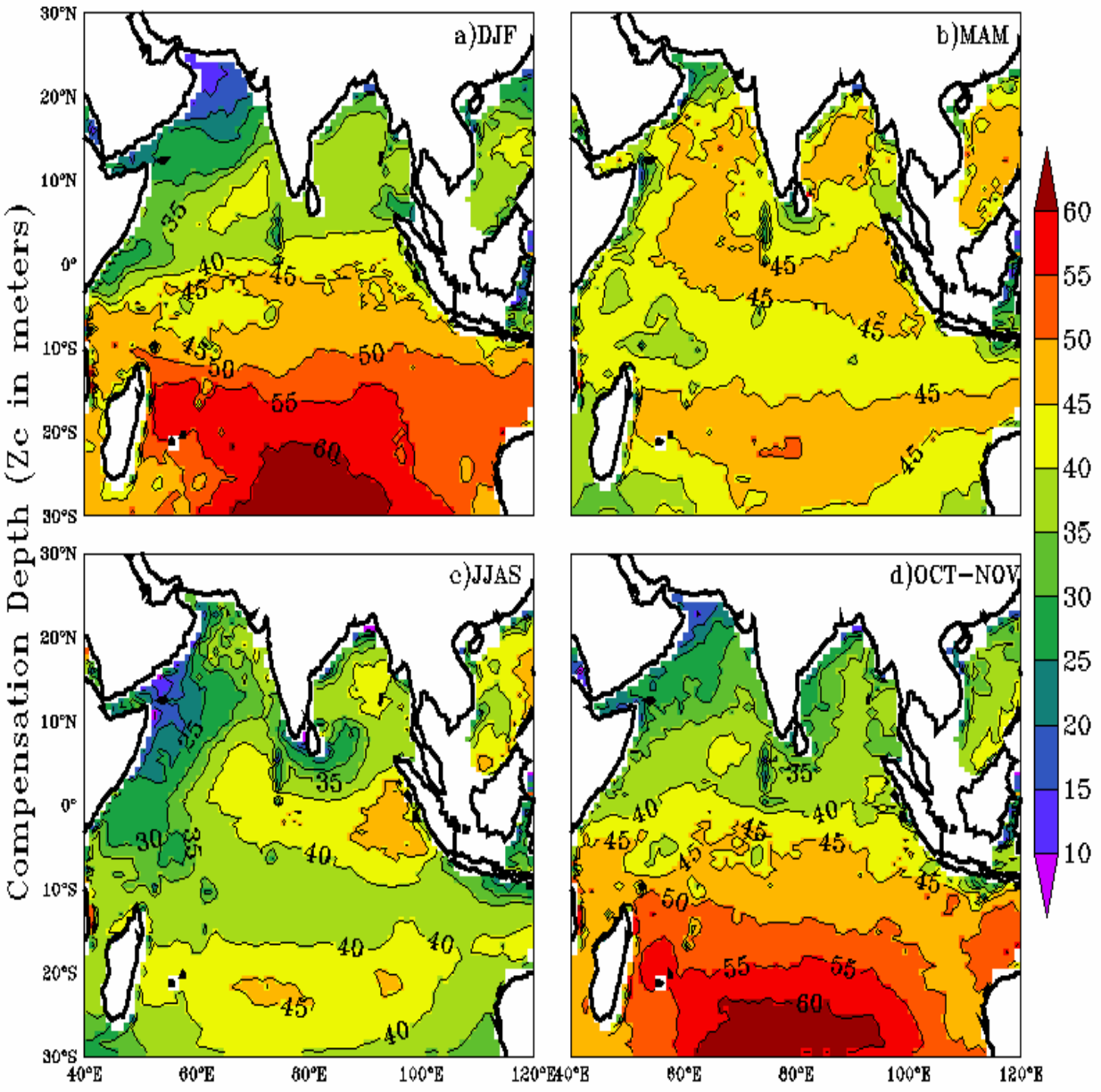

Figure 3: Seasonal mean maps of varying compensation depth (varZc), (a) December to February (DJF), (b) March to May (MAM), (c) June to September (JJAS), (d) October to November (OCT-NOV). Units are meters.

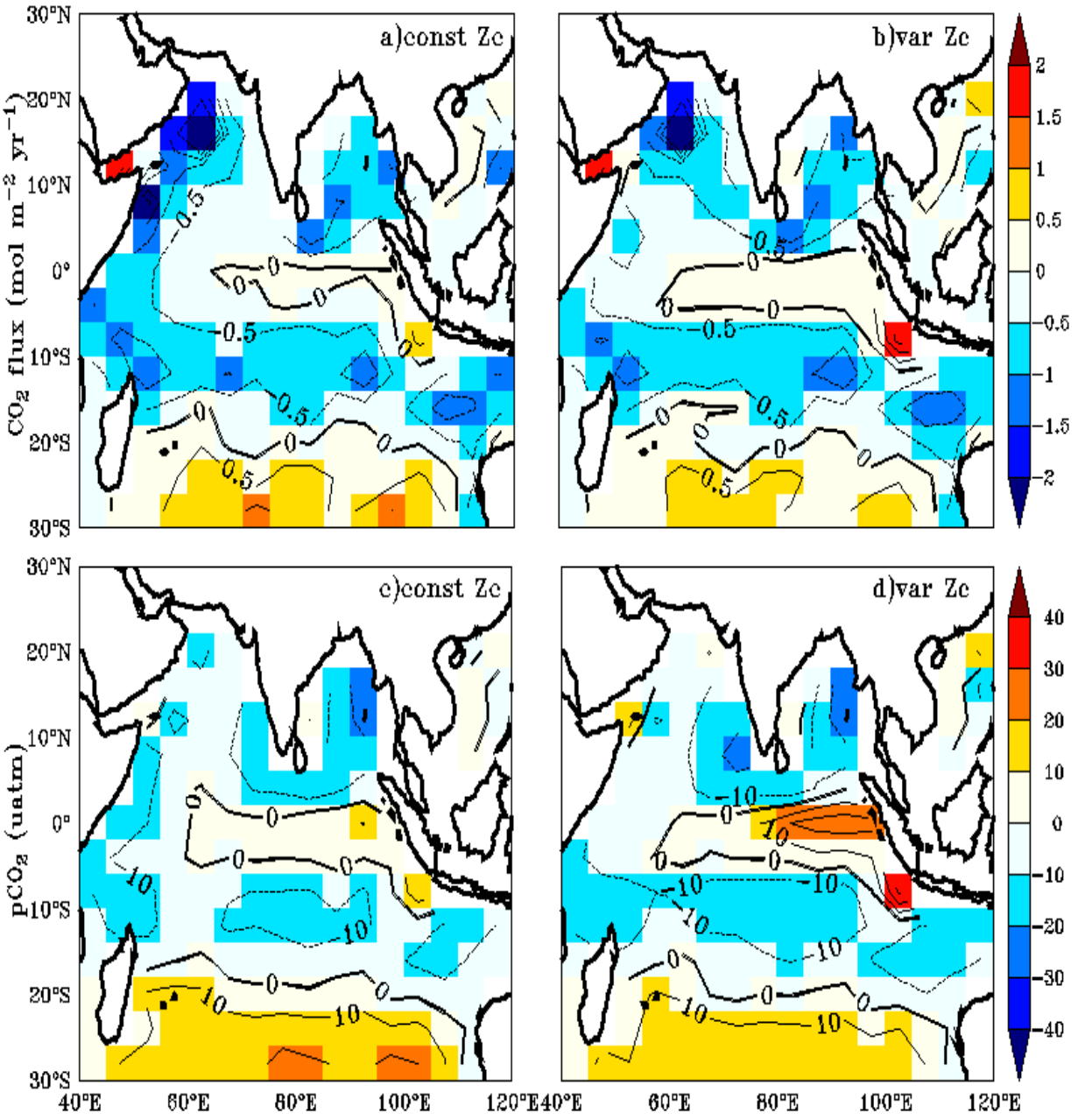

Figure 4: Annual mean biases in the model evaluated against Takahashi et al. (2009) observations for CO_2 flux (a, b) and pCO_2 (c, d) with constant Zc (constZc) and varying Zc (varZc). Units of CO_2 flux and pCO_2 are mol m^{-2} yr^{-1} and µatm, respectively.

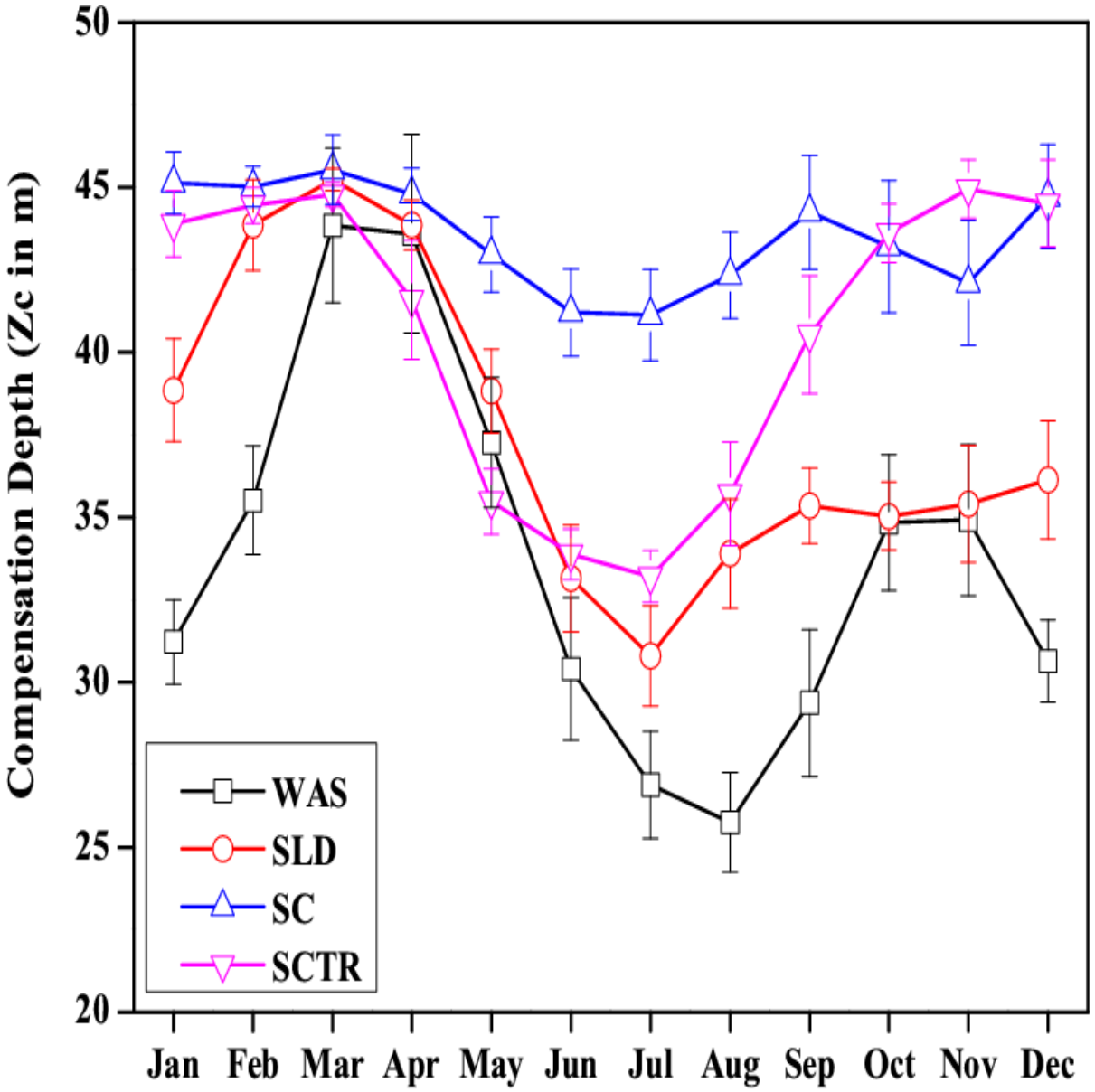

Figure 5: Seasonal variations in varZc over the study regions shown as climatology computed over 1990-2010. Error bar shows standard deviations of individual months over these years. Units are meters.

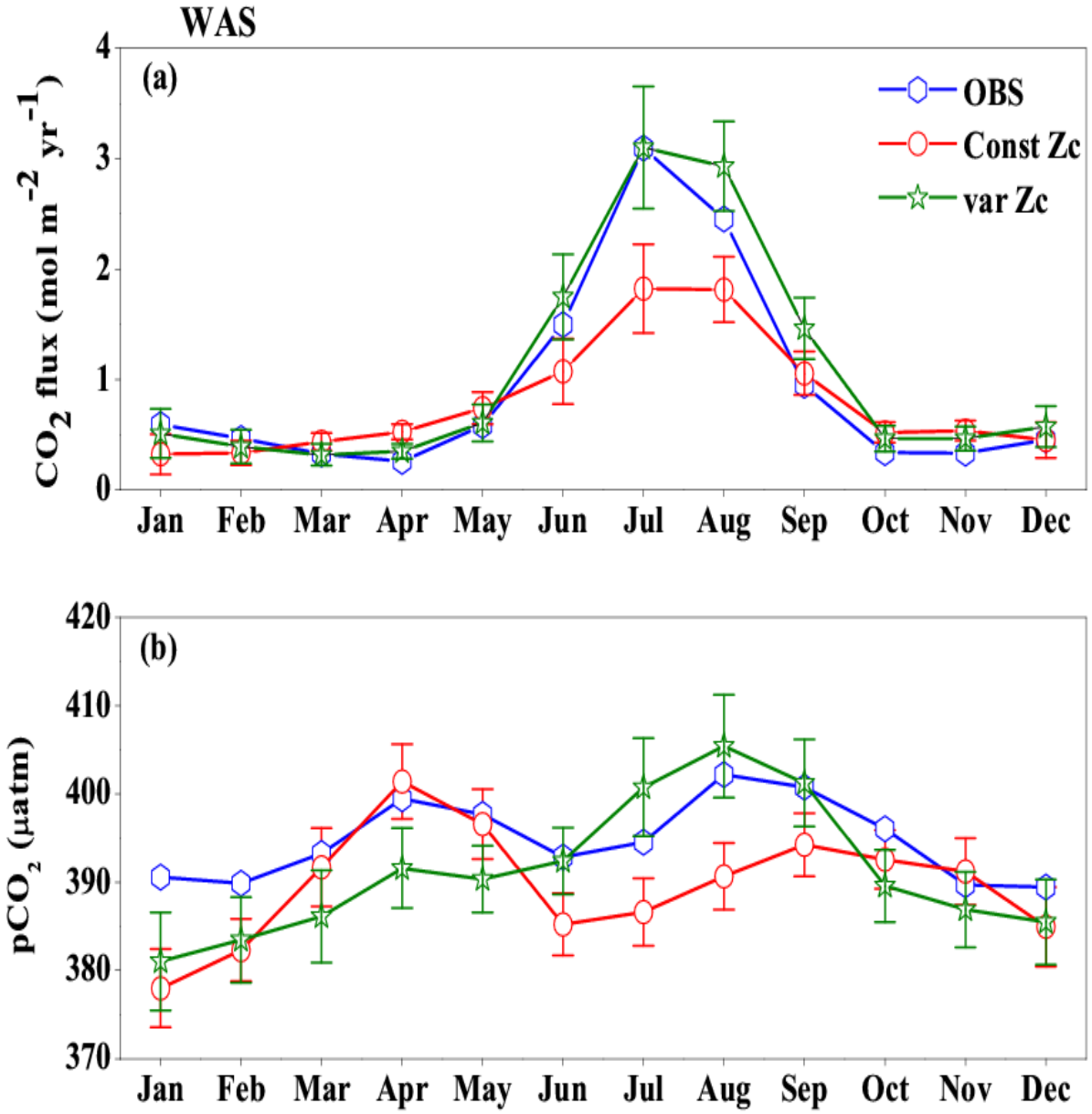

Figure 6: Comparison of model (a) CO_2 flux and (b) pCO_2 simulated with constZc and varZc with that of Takahashi et al. (2009) observations (OBS) over WAS as climatology computed over 1990-2010. Error bar shows standard deviations of individual months over these years. Units of CO_2 flux and pCO_2 are mol m^{-2} yr^{-1} and µatm, respectively. Legend is common for both graphs.

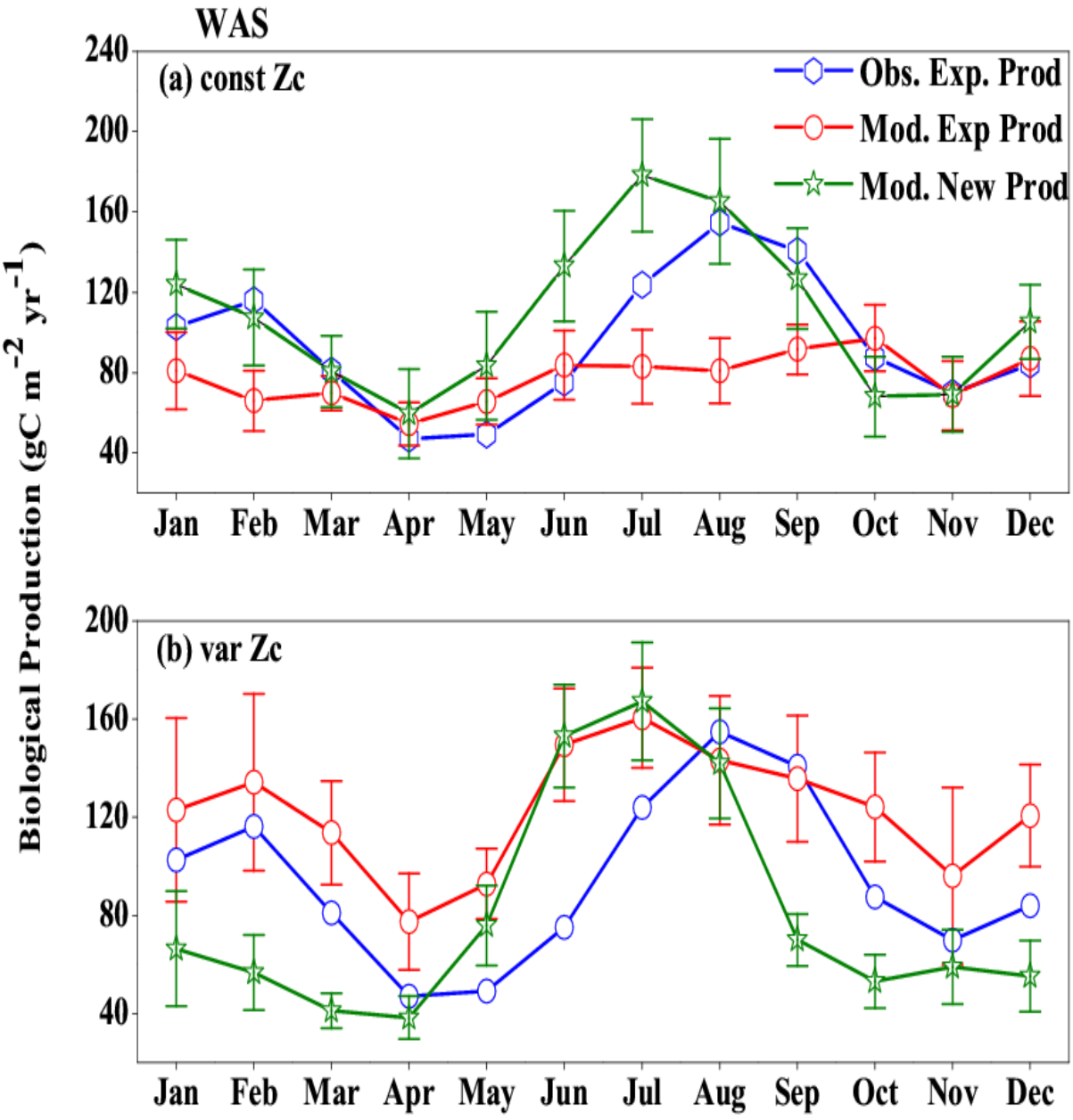

Figure 7: Comparison of model export production (Mod. Exp. Prod) and new production (Mod. New Prod) with satellite derived export production (Obs. Exp. Prod) for (a) ConstZc and (b) varZc simulations for WAS. Units are g C m^{-2} yr^{-1}. Legends are common for both graphs.

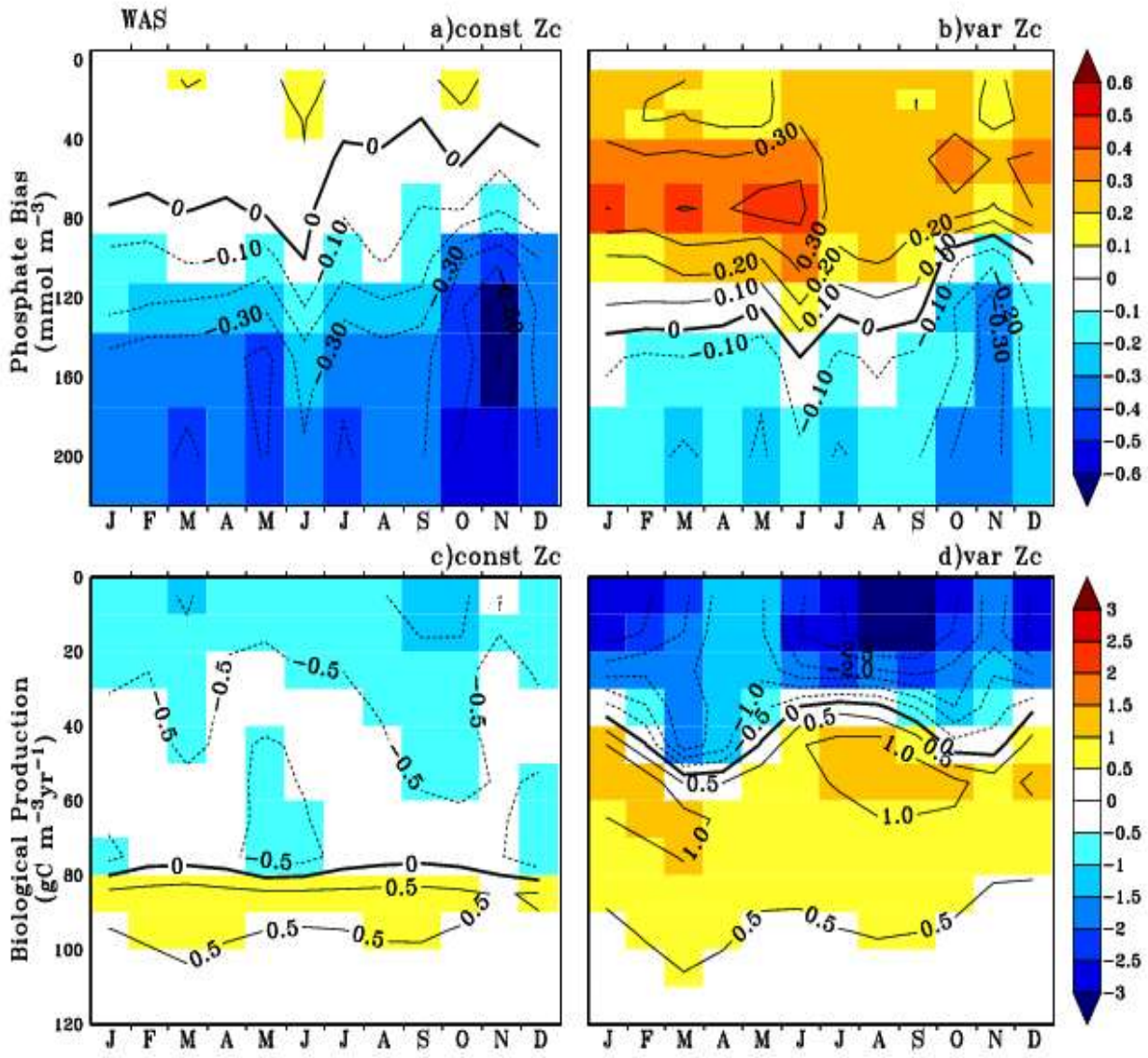

Figure 8: Annual mean bias of model phosphate when compared with climatological observational data (a) for constZc and (b) for varZc simulations. Corresponding annual mean biological source/sink profiles (c, d) in the model for WAS. Unit of phosphate is mmol m^{-3} and biological production is g C m^{-3} yr^{-1}.

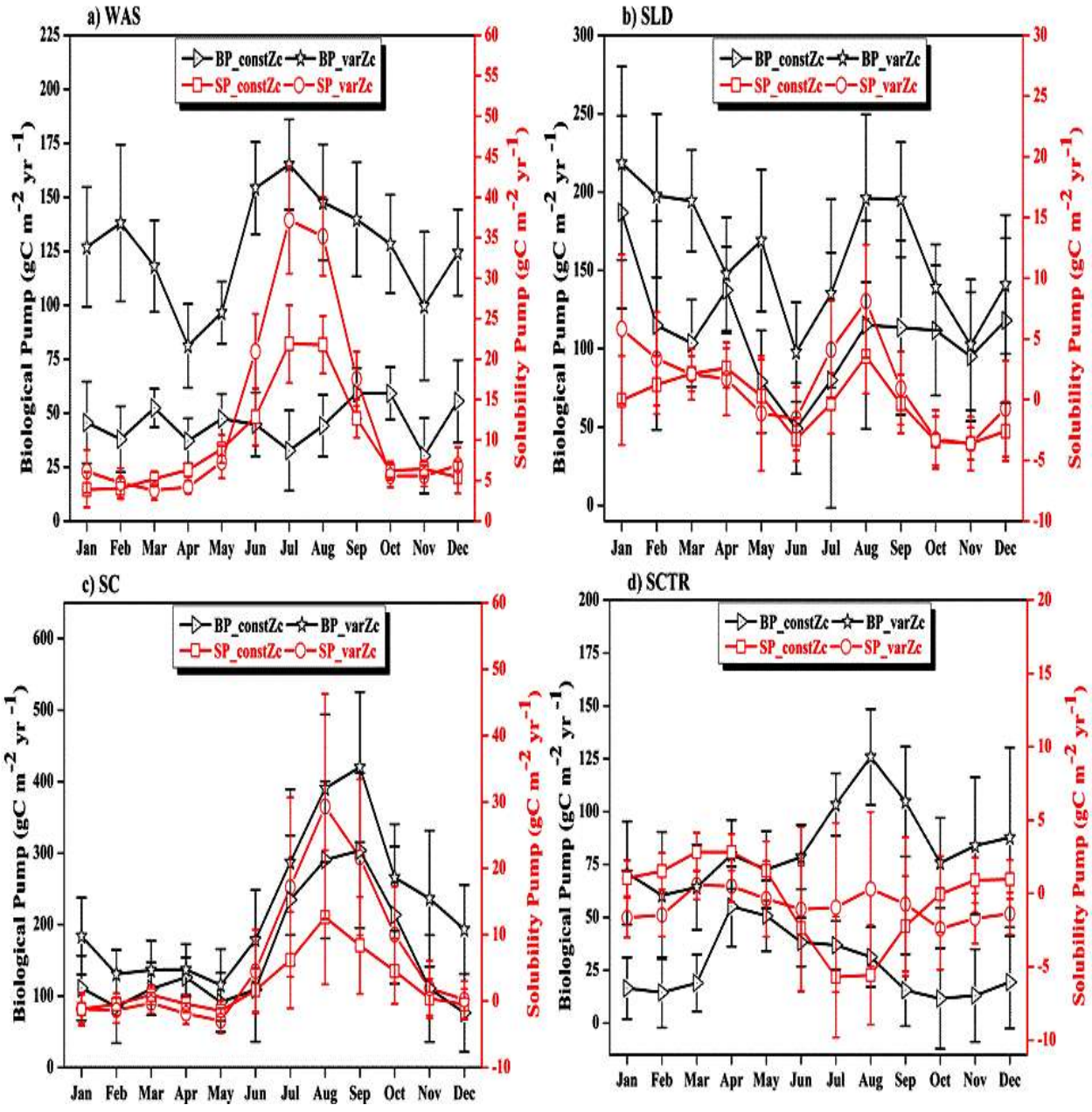

Figure 9: The strength of the biological pump (BP, black lines) and solubility pump (SP, red lines) from constZc and varZc simulations for (a) WAS (b) SLD (c) SC and (d) SCTR. The left axis shows the biological pump and the right axis shows the solubility pump. Error bar shows standard deviations of individual months over the years 1990 - 2010. Units are g C m^{-2} yr^{-1}.

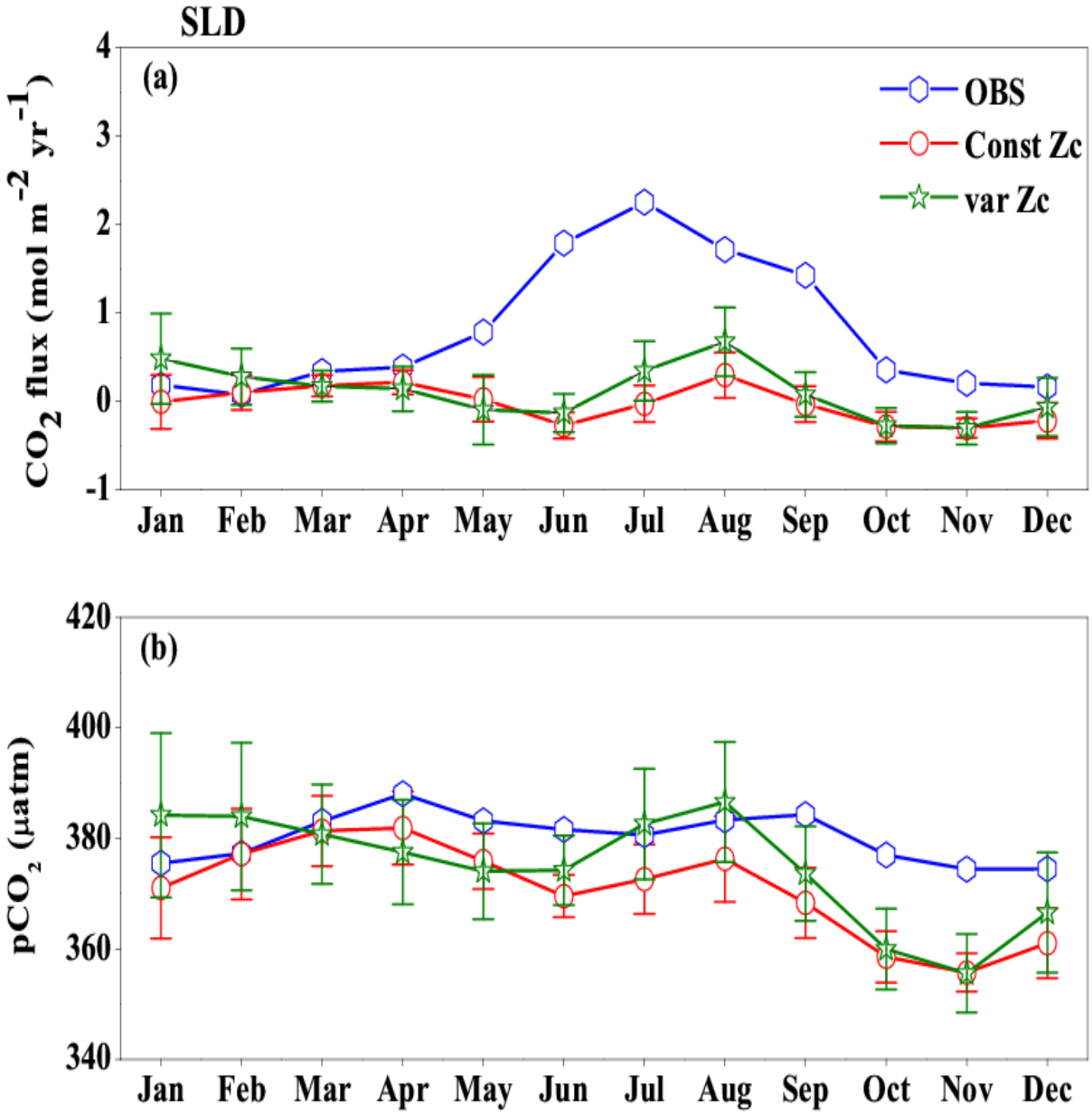

Figure 10: Same as Figure (6), but for SLD.

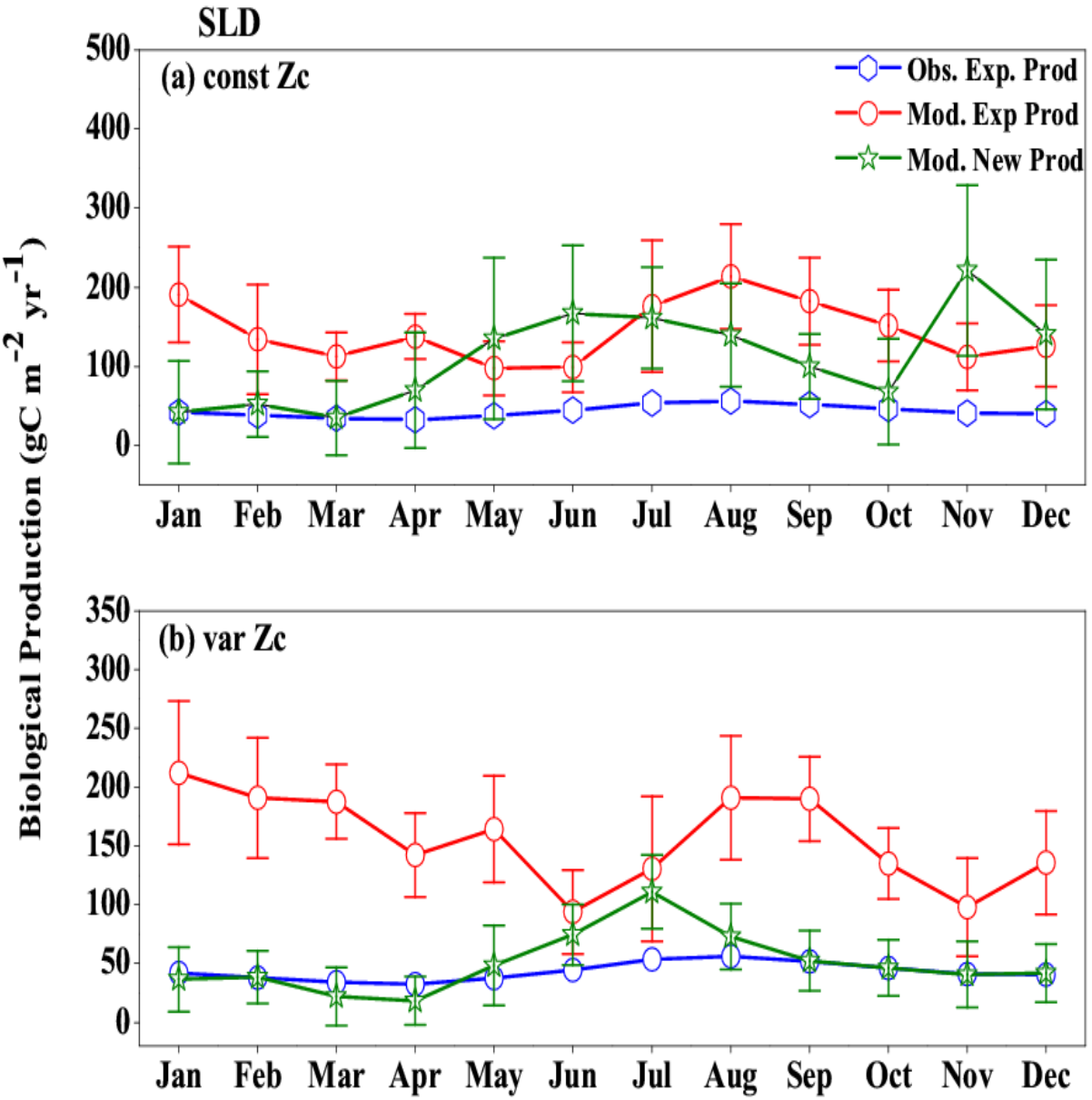

Figure 11: Same as Figure (7), but for SLD.

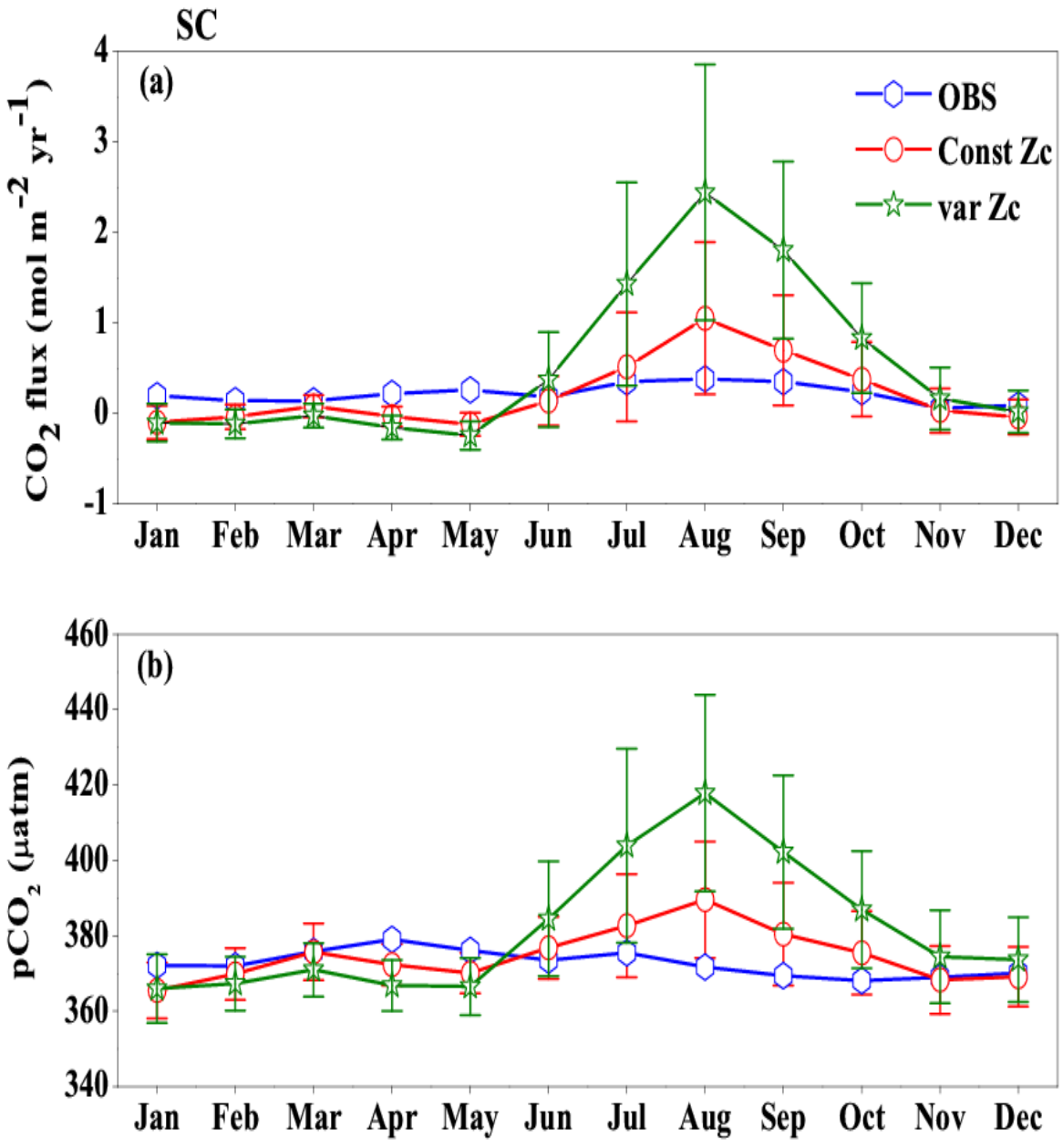

Figure 12: Same as Figure (6), but for SC.

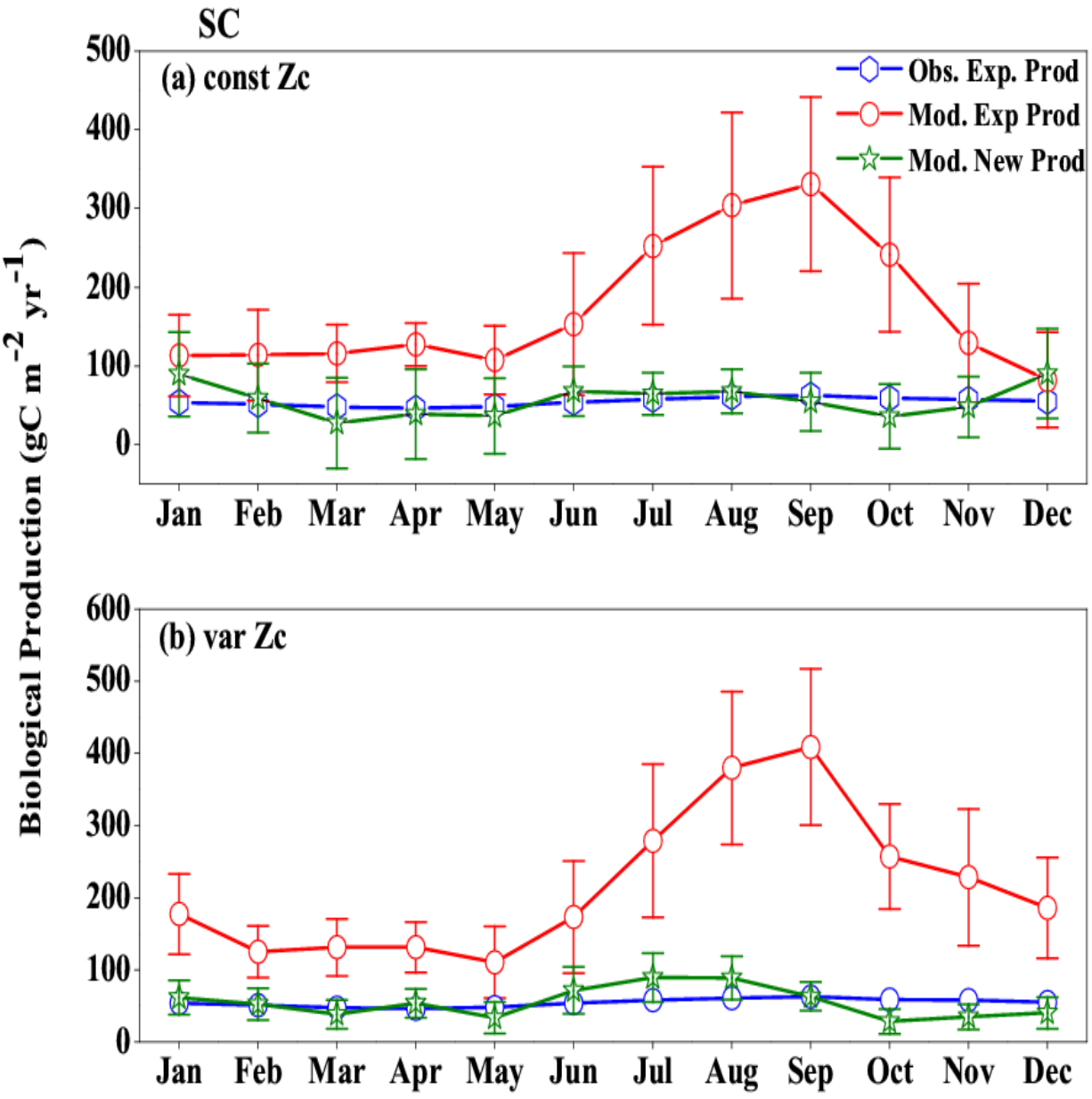

Figure 13: Same as Figure (7), but for SC.

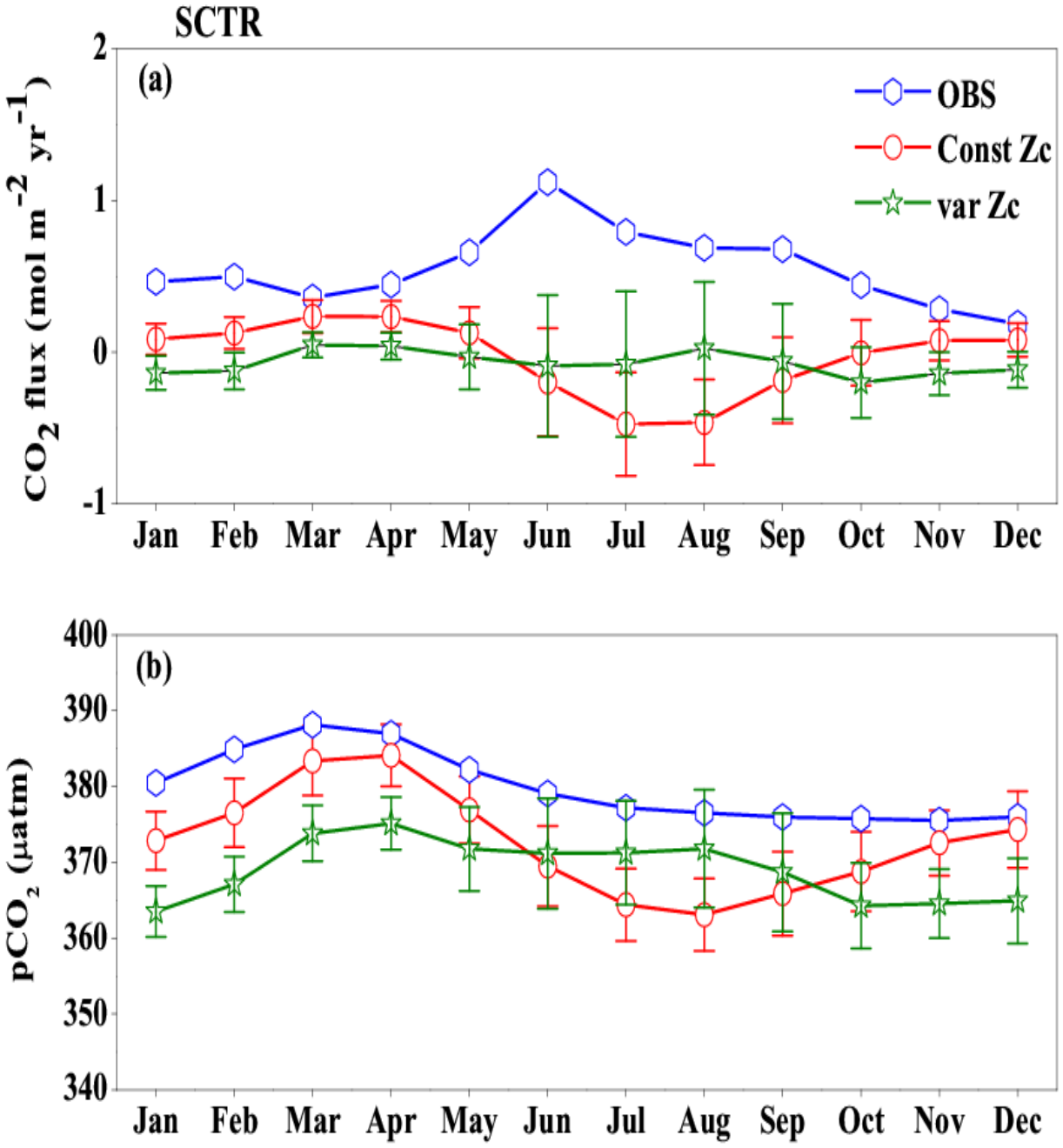

Figure 14: Same as Figure (6), but for SCTR.

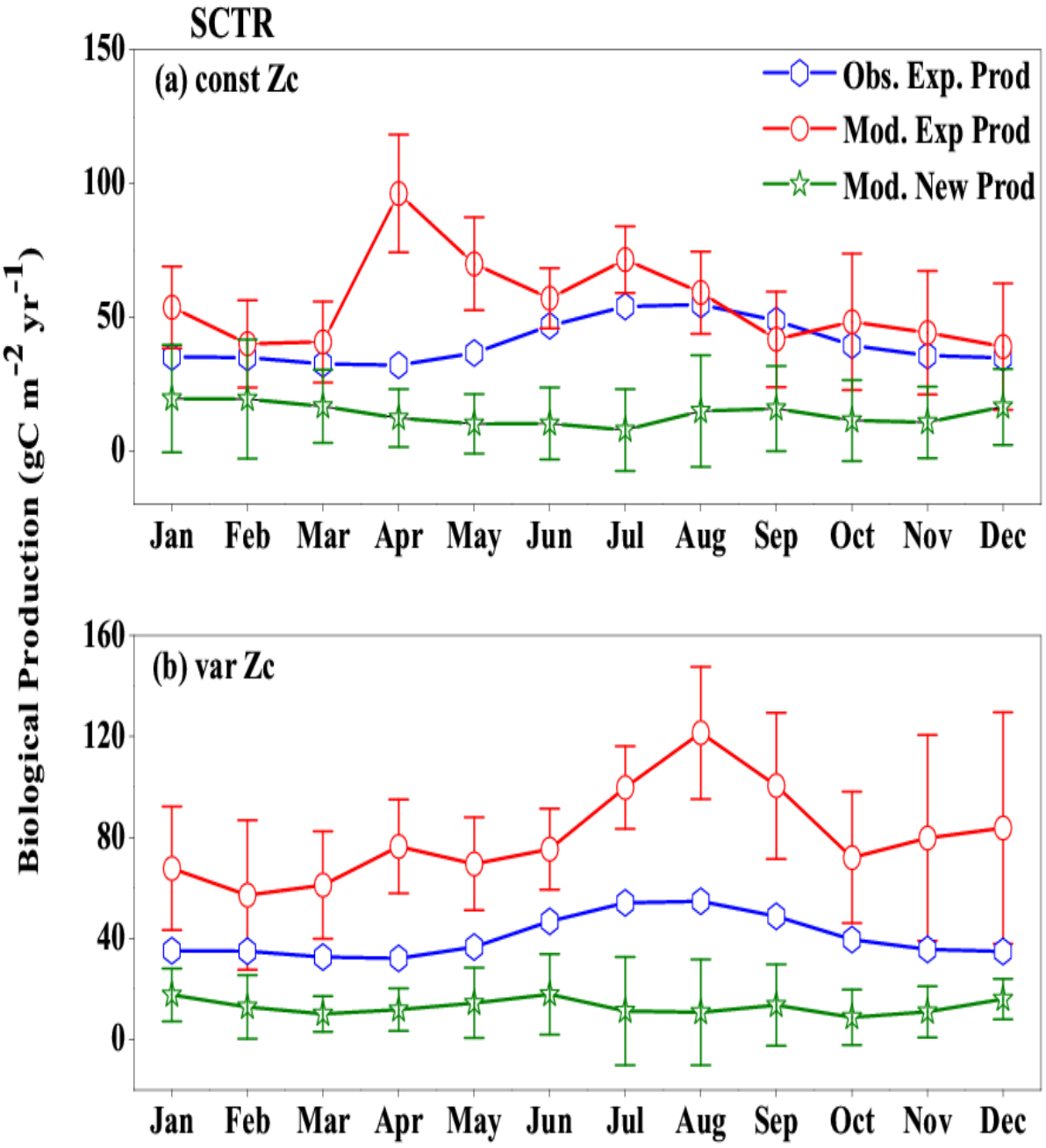

Figure 15: Same as Figure (7), but for SCTR.

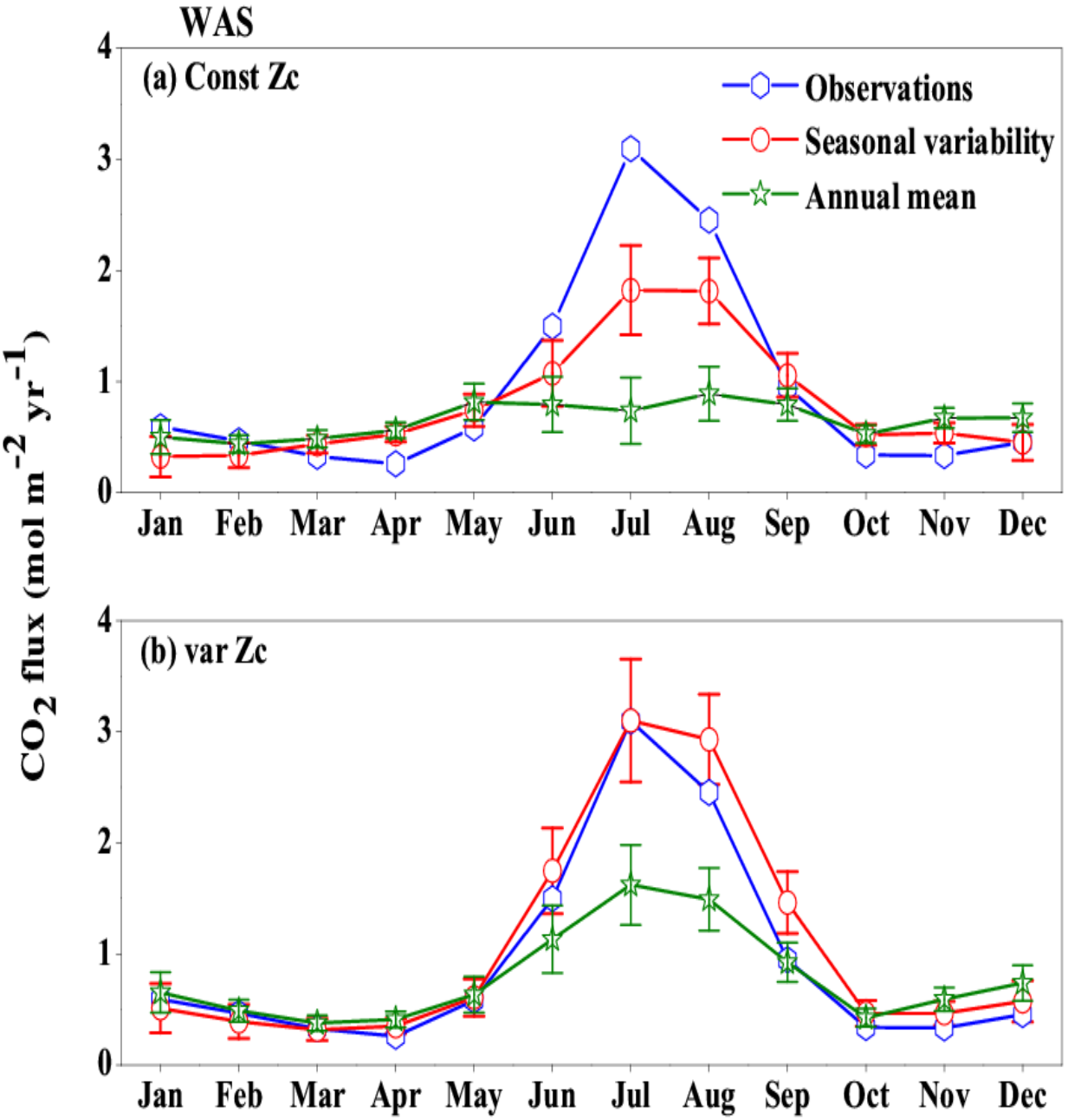

Figure 16: Response of CO_2 flux from the model forced with annual mean currents over the WAS as climatology computed over 1990-2010. Error bar shows standard deviations of individual months over these years. (a) constZc and (b) varZc. Units are mol m^{-2} yr^{-1}. Legends are same for both graphs.

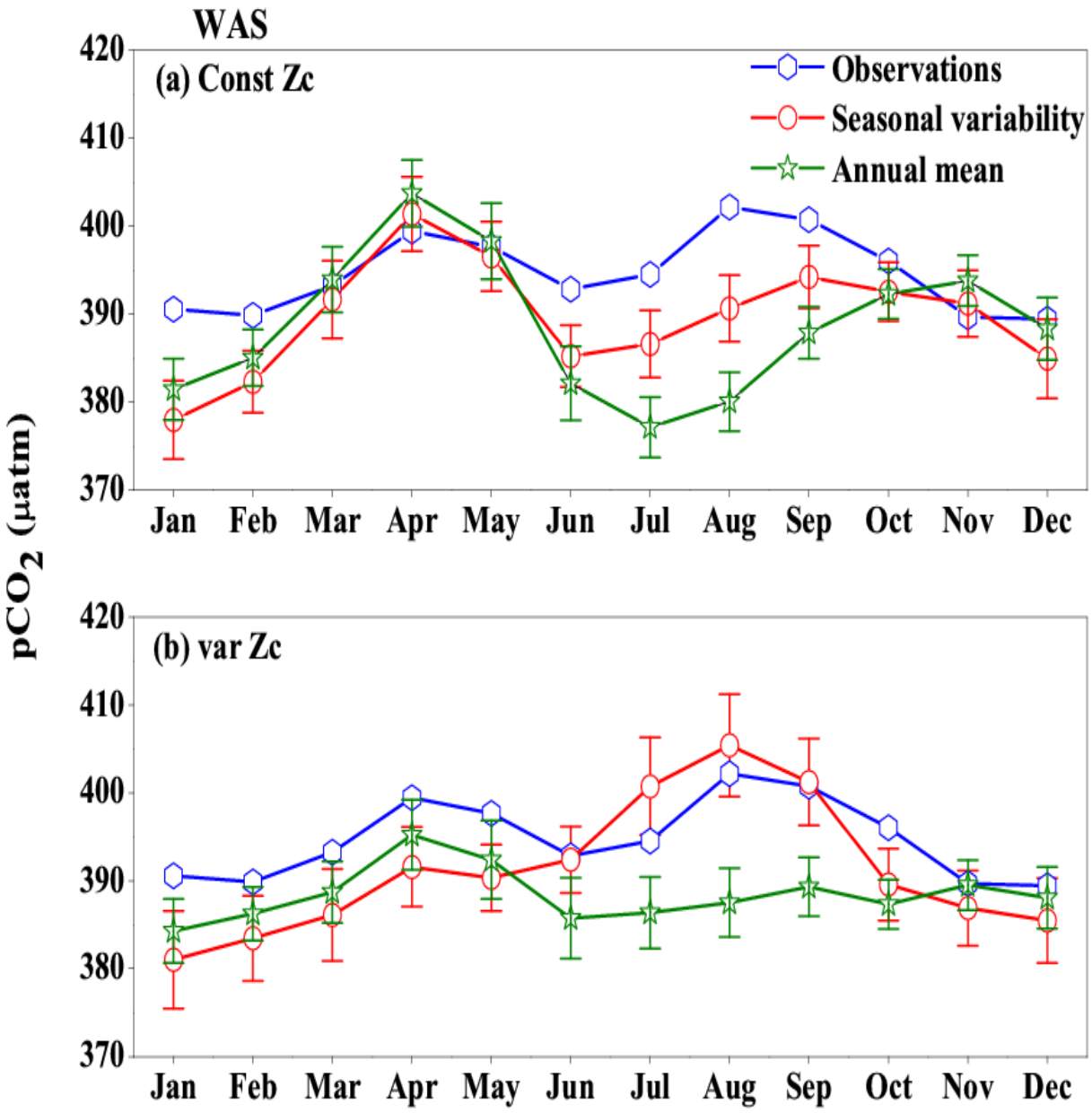

Figure 17: Same as Figure (16), but for pCO_2. Units are µatm.

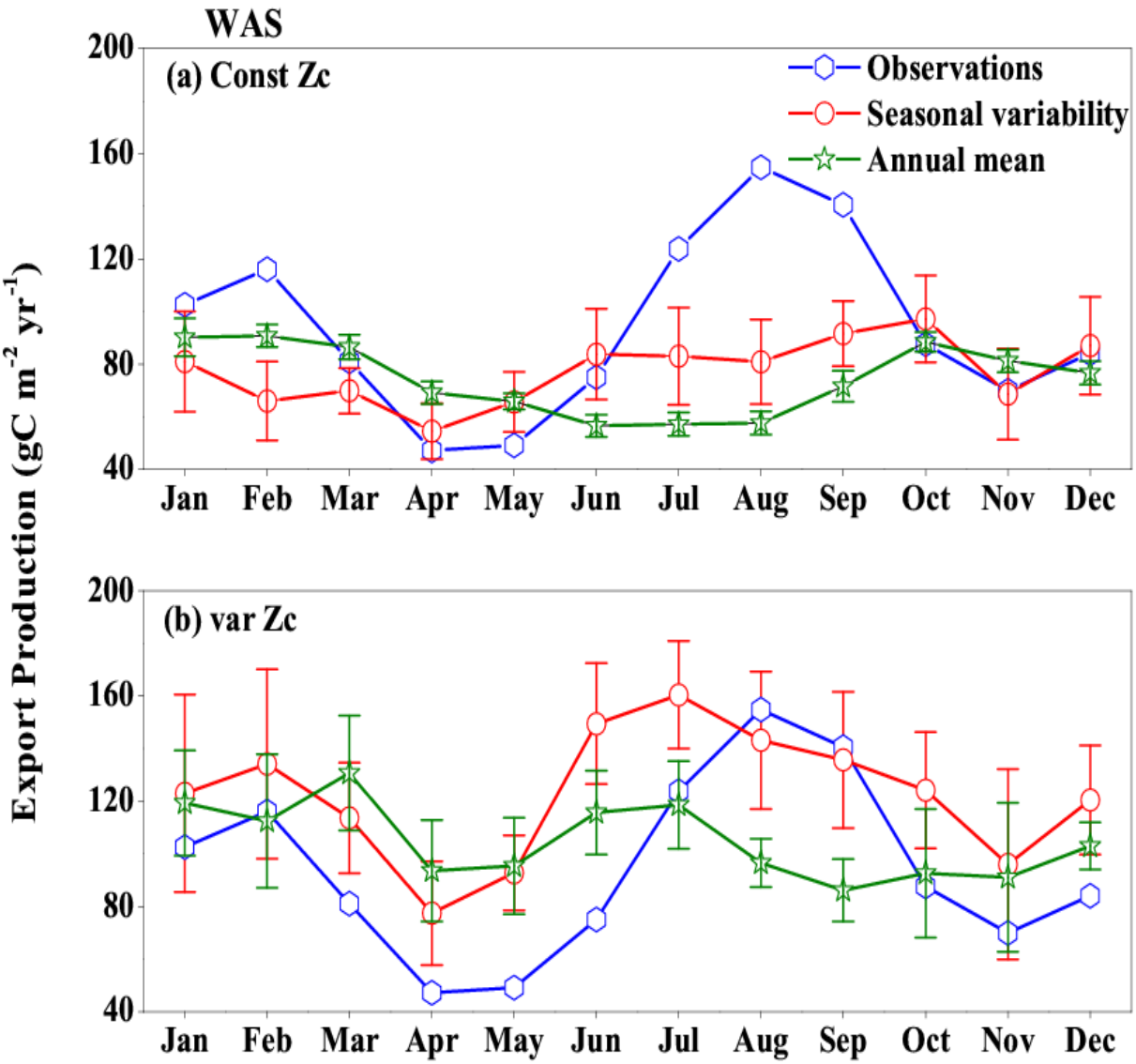

Figure 18: Response in export production of the model forced with annual mean currents in the WAS as climatology computed over 1990-2010. Error bar shows standard deviations of individual months over these years. (a) constZc (b) varZc. Units are g C m^{-2} yr^{-1}. Legends are same for both graphs.

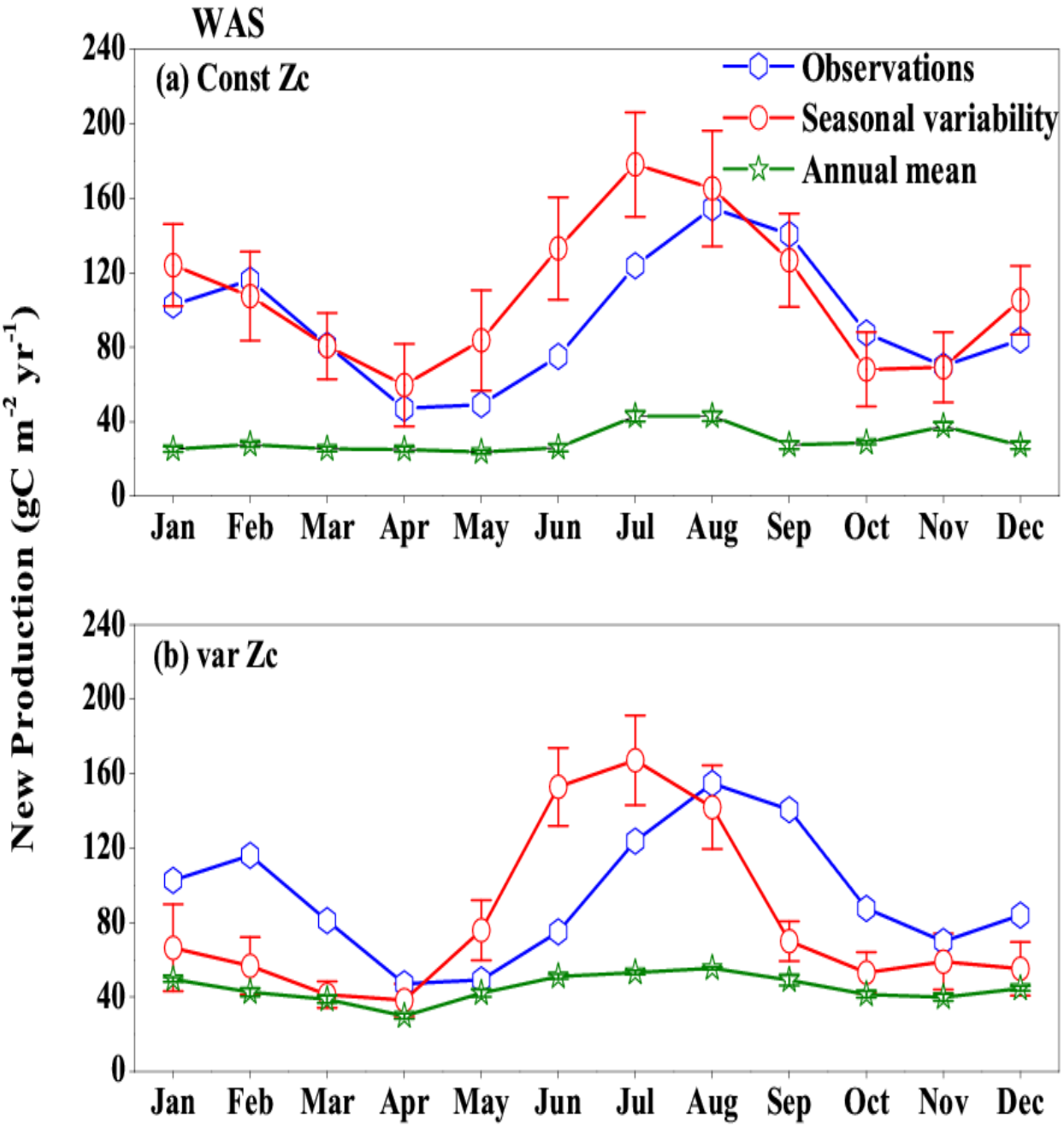

Figure 19: Same as Figure (18), but for New Production. Units are g C m^{-2} yr^{-1}.

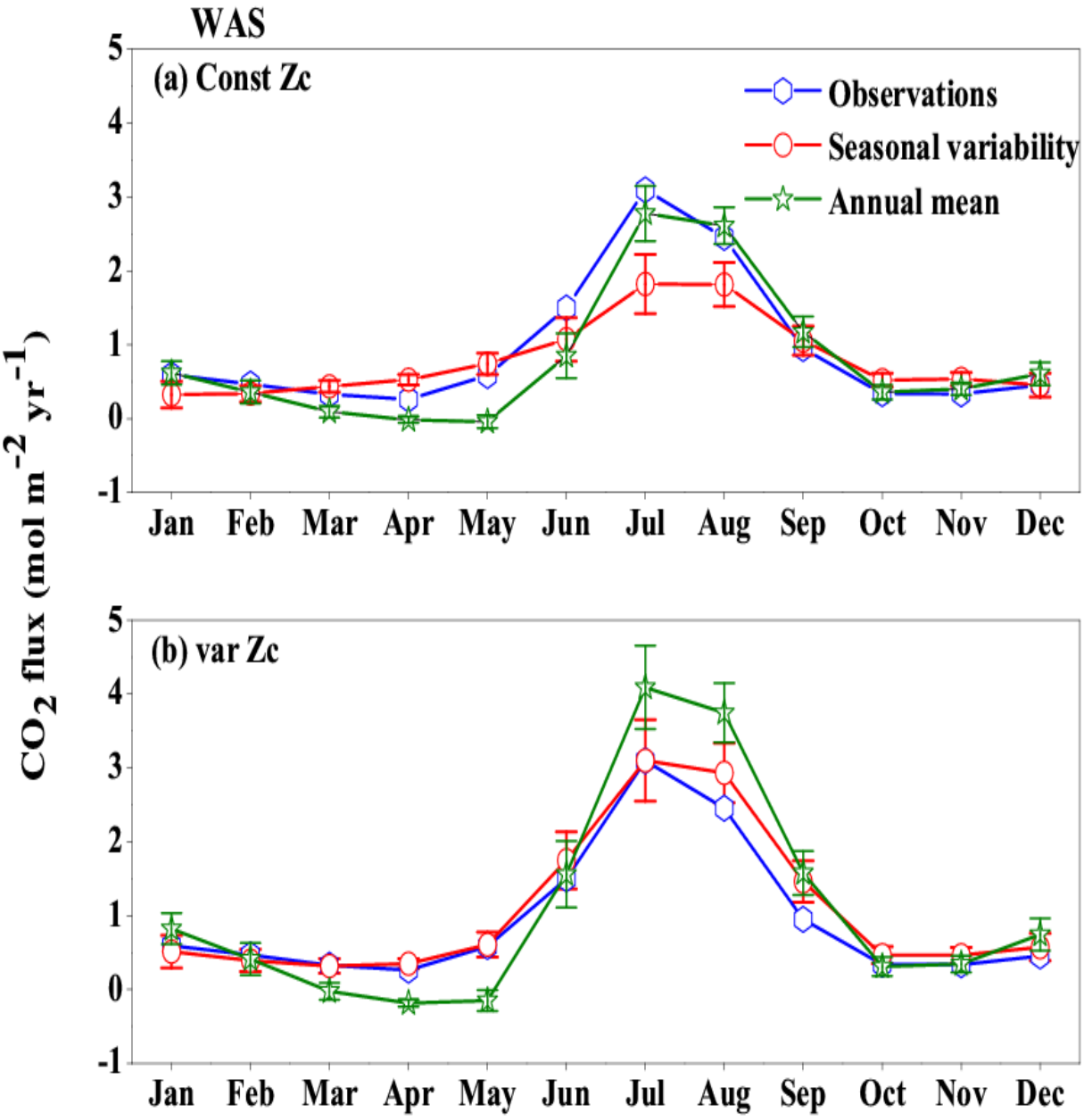

Figure 20: Response of CO_2 flux from the model forced with annual mean SST over the WAS as climatology computed over 1990-2010. Error bar shows standard deviations of individual months over these years. (a) constZc and (b) varZc. Units are mol m^{-2} yr^{-1}. Legends are same for both graphs.

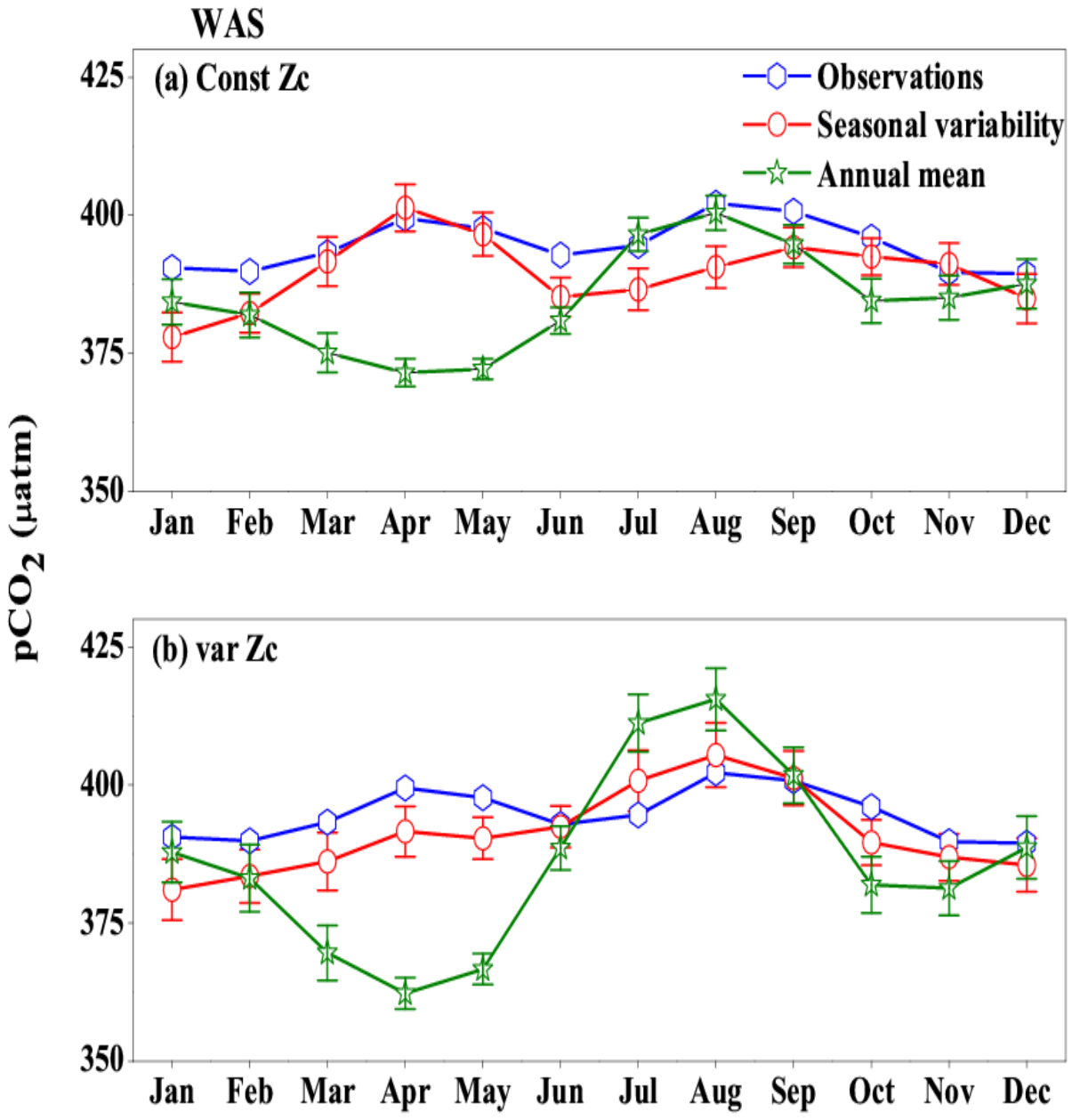

Figure 21: Same as Figure (20), But for pCO_2. Units are µatm.